ALADIN-HIRLAM Newsletter

No 6, February 2016

Around ALADIN&HIRLAM in 130 pages

ALADIN Programme, c/o P. Termonia, IRM, Avenue Circulaire 3, 1180 Bruxelles, Belgium

HIRLAM-B Programme, c/o J. Onvlee, KNMI, P.O. Box 201, 3730 AE De Bilt, The Netherlands

CONTENTS

Introduction

I am happy to provide you with the sixth edition of the combined Newsletter of the HIRLAM and ALADIN consortia.
This edition is mainly dedicated to a "Tour d'ALADIN et d'HIRLAM", with contributions describing the main achievements at our meteorological services in 2015.
Besides these scientific and technical articles, you will find in this Newsletter an "Interview" and an overview of operational configurations.
Information about new regular group video meetings has also been included in the list of events planned for 2016.
The "Publications"page will be back in the seventh edition of the Newsletter.

I hope you enjoy reading the sixth ALADIN-HIRLAM Newsletter, thank the authors for their contributions and hand it off first to the ALADIN and HIRLAM Programme Managers who will update you with the last important news at the consortia level.

Patricia

For additional information, please visit the ALADIN and HIRLAM websites, or just ask the authors of the articles.

Signing of the 5th ALADIN MoU in Budapest

Editorial

Jeanette Onvlee and Piet Termonia

We are pleased to announce the ALADIN and HIRLAM signed their two new MoUs, starting a new phase of five years of NWP activities of both consortia.

The new ALADIN MoU5 was signed on 9 February in the conference room of the OMSZ in Budapest. In this MoU the scopes of the different types of activities are better articulated. This will particularly help to facilitate collective efforts that are complementary to the core activities of the ALADIN consortium, for instance endorsing the unique position of the RC LACE consortium. The new ALADIN MoU also contains a few innovations in the scientific coordination of the ALADIN consortium. A notion of a special type of configurations, the so-called Canonical Model Configurations is introduced and there will be a new funded scientific position called the Code Architect. The aim of this is to increase our much needed efforts on the design and the definitions of our NWP codes. This will lay the foundations for the next steps in a closer collaboration between the two consortia.

Within HIRLAM, an external review was held of the HIRLAM-B programme (2011-2015). The reviewers expressed their satisfaction with the achievements and progress made in the past five years, and provided many useful recommendations for HIRLAM management regarding the activities that will need to be undertaken jointly with ALADIN to achieve the goal of forming one single consortium by the end of the 2016- 2020 MoU's. The main high-level strategic objectives for the period of HIRLAM-C (2016-2020) were set by the HIRLAM Council in June; the path to achieve them will be detailed in a scientific strategy, to be finalized in the first half of 2016. The new HIRLAM-C MoU was signed last December in Reading, and the new management group (HMG) was appointed. The new HMG has started up its activities in a first, fruitful and inspiring, meeting last January.

Preliminary list of 2016 planned events

1 Meetings

- 20th ALADIN General Assembly, **9-10 February 2016, Budapest, Hungary**
- 21st ALADIN Workshop & HIRLAM All Staff Meeting 2016 (& 20th ALADIN LTM meeting), **4-7 April 2016, Lisbon, Portugal**
- Coordination meeting between ALADIN CSSI and HIRLAM MG, **8 April 2016, Lisbon, Portugal**
- 13th ALADIN PAC meeting, **23 May 2016** morning, **Ankara** (Tk) t.b.c.,
- 4th joint HAC/PAC meeting, **23 May 2016** afternoon, **Ankara** (Tk) t;b;c.,
- HAC meeting, **24 May 2016**, **Ankara** (Tk) t.b.c. ,
- 38th EWGLAM and 23rd SRNWP meetings, **3-6 October 2015, Rome, Italy**

2 Working Weeks / Working Days

- HIRLAM WW on EPS, De Bilt, 29 Feb – 4 March, and another meeting during fall
- HIRLAM WW on Surface Data Assimilation, Oslo, 11-14 April,
- HIRLAM WW on Observations: fall
- HIRLAM WW on Radiation: 2 meetings
- HIRLAM WW on Cloud working group: 1 meeting
- HIRLAM WW on System: spring, fall
- HARP Verification: 1 meeting (late spring?)
- Aladin/LACE working days on Surface ?
- Aladin/LACE working days on ALARO-1, Brussels, 12-14 September
- Aladin/LACE working days on Data assimilation, Budapest, 3rd week of September (t.b.c.)
- more information on-line

3 Regular video meetings

Roger Randriamiampianina took the initiative to organize regular group video meetings on atmospheric Data Assimilation via google hangouts, for DA staff from both ALADIN and HIRLAM.

First technical tests with google hangouts showed very good quality communication. First video meeting on 18 February.

Tour d'ALADIN & d'HIRLAM

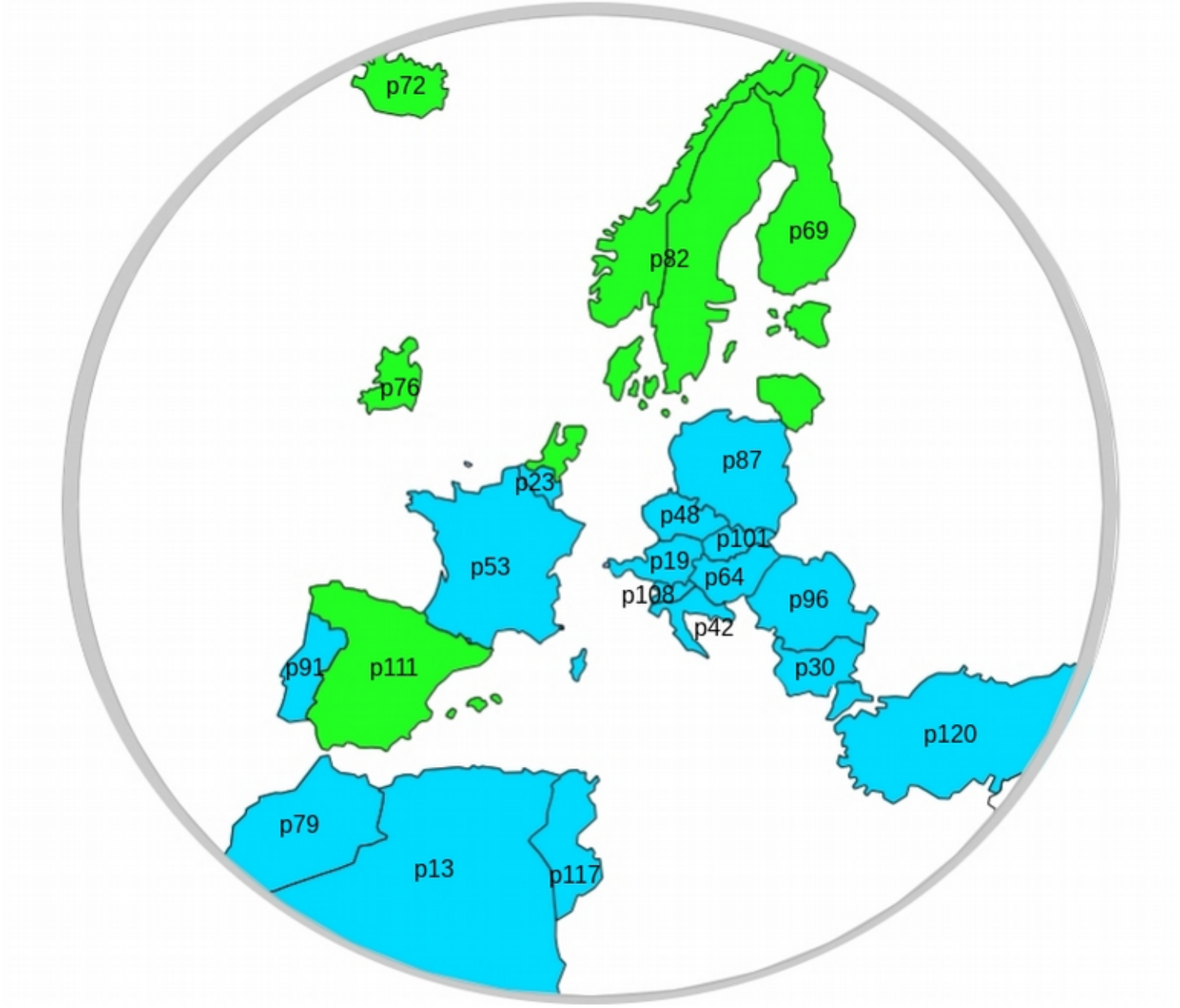

Click on the page number to go directly to the article proposed by each NMS

Control of ALADIN-Algeria model

Sara Rouidja, Nasser Kessali

1 Introduction

This study presents the scores of the ALADIN model established during the months of April, May and June for the temperature at two meters and months (May and June) for the wind 10 meters. The ALADIN model control maturities 12 hours, 24 hours was made with respect to the analysis fields (12 and 24), in fact forecast maturities 12 hours and 24 hours are controlled relative to the 12Z analysis, while the forecast maturities 24 hours relative to the 00Z analysis.

2 Controlled parameters and methods

We chose two parameters to control surfaces, the temperature at 2 meters and wind at 10 meters.
The calculation of the scores of numerical models of weather forecasting is based mainly on statistical methods, we used two indicators of differences essentially the square root of the mean square error (RMSE) and the bias.

The check is done with respect to the analysis (initial state) model, BIAS and RMSE were calculated on the same timescales.

$$(1)\ BIAIS = \frac{1}{n}\sum F_i - A_i \qquad (2)\ RMSE = \sqrt{\frac{1}{n}\sum \left(F_i - A_i\right)^2}$$

n: number checkpoint, F: forecasting fields, A: field analysis

3 Results and analysis

3.1 Temperature at 2 meters

The analysis of figures from the monthly evolution through maps and monthly average temperature parameter at two meters during the day suggests that :

- Average monthly given by the model is often negative with a maximum value (absolute value) of about -1 ° C (Fig1-2, 12h maturity).
- Through maps show the presence of negative bias of about -0.5 to -2.5 ° C on the continent and from -0.5 to 0.5 ° C over the ocean.
- The biggest negative bias is registered in the Tindouf area.
- Overnight (Fig 3-4, 24h maturity) biases are positive.

3.2 Wind at 10 meters

The graphs analysis of the monthly evolution of bias and the maps Monthly Average of the wind at 10 meters during the day (Fig 5-6, maturities 12h) suggests that:

- Bias is more pronounced compared with those recorded during night.
- During the day, the maximum bias reachs 6 m/s and increases during June month.
- Overnight (Fig 7-8, maturities 24h) biases are less important.

3.3 Results

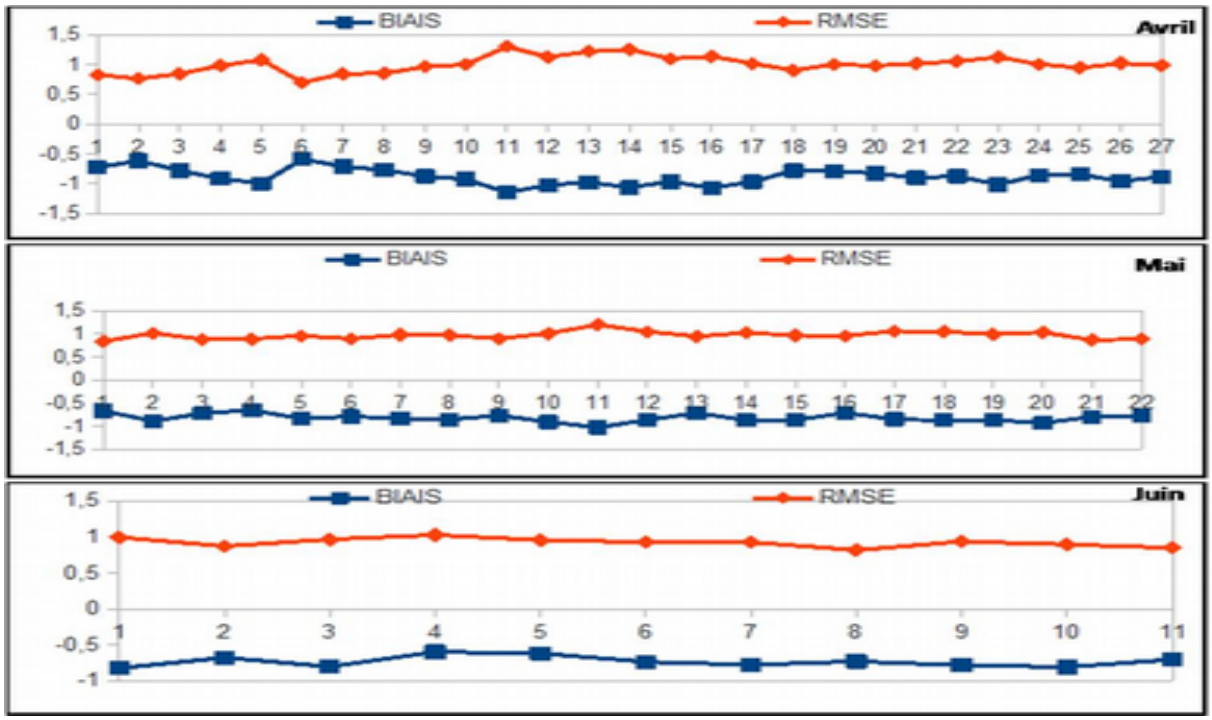

Figure 1: Monthly evolution of the mean square error (RMSE) (given in red) and bias (given blue) for the 2m temperature in degrees Celsius (° C).

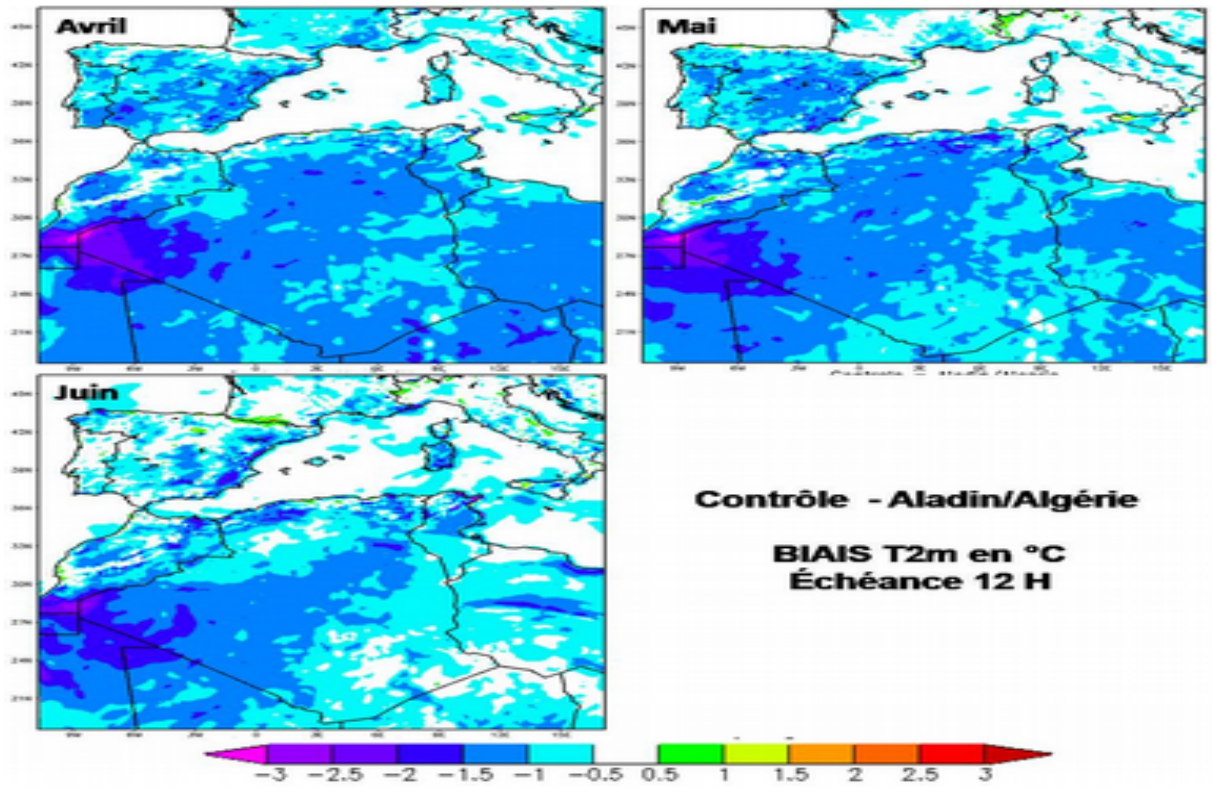

Figure 2: Monthly average temperatures bias recorded at 12 hours obtained with the ALADIN model compared to the analysis.

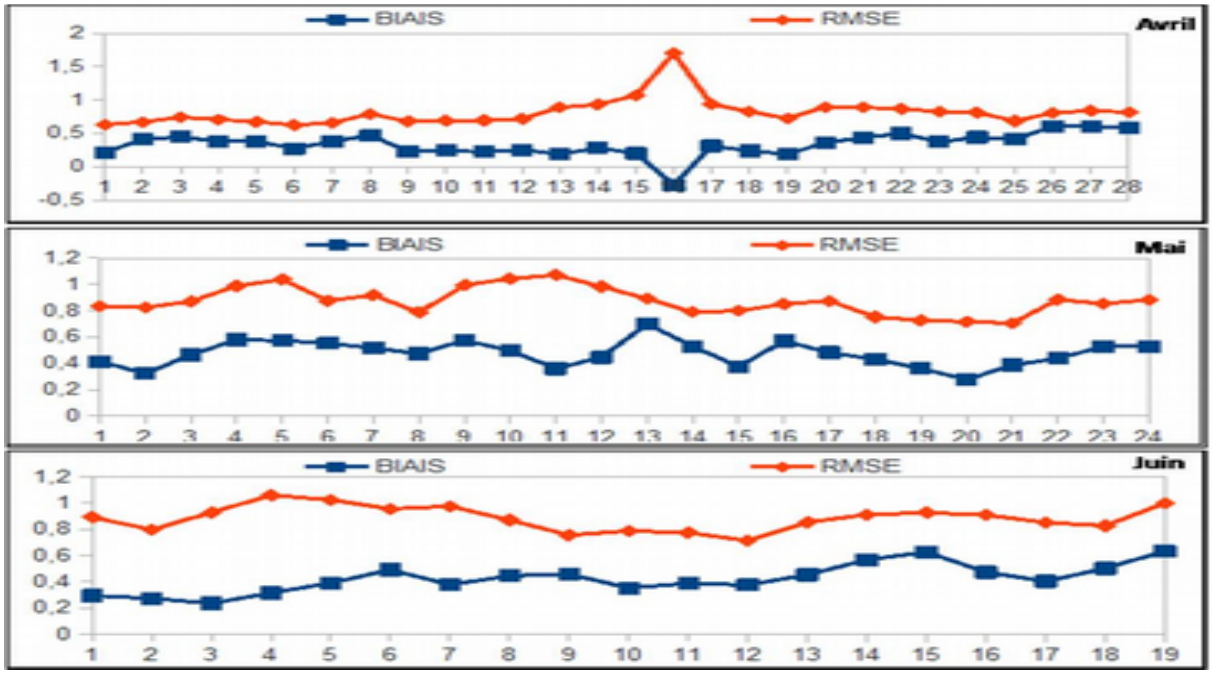

Fig. 3 : Monthly evolution of the mean square error (RMSE) (given in red) and bias (given in blue) for the 2m temperature in degrees Celsius (° C).

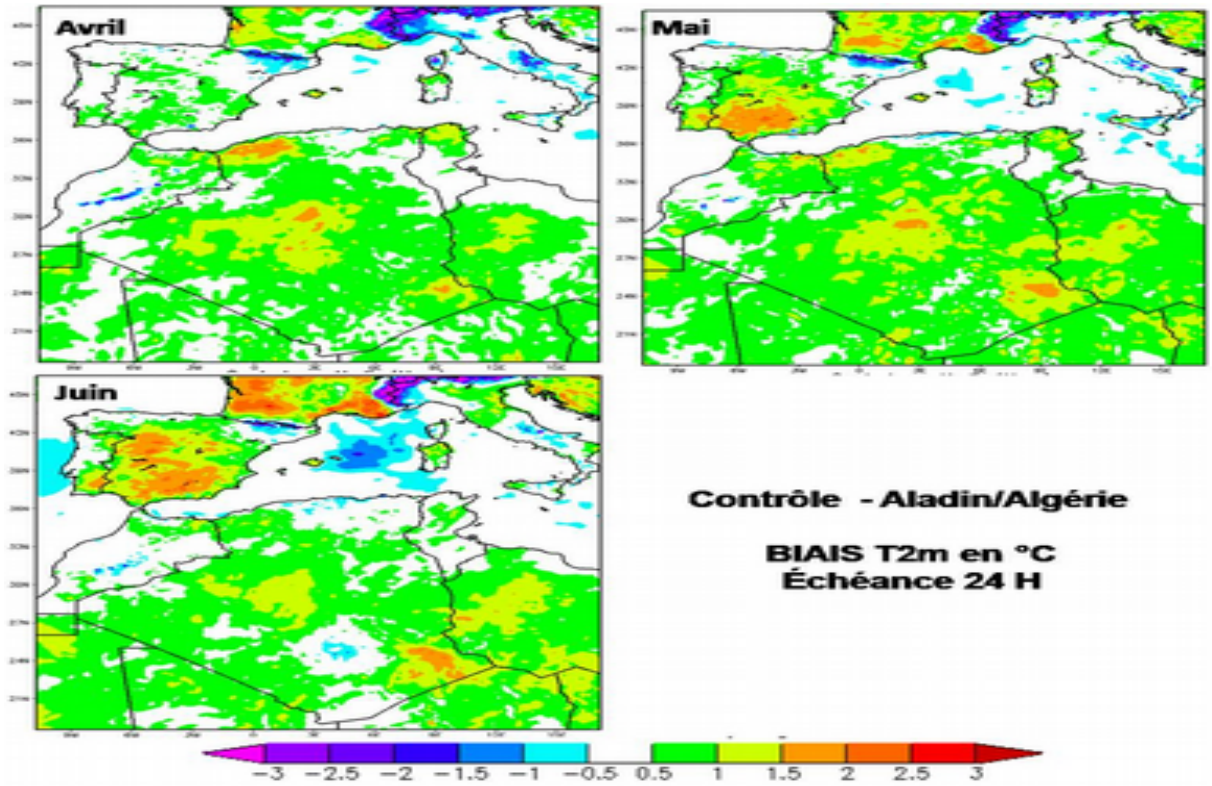

Fig. 4 : Monthly average temperatures at 2 meters recorded at 24 hours obtained with the ALADIN model compared to the analysis.

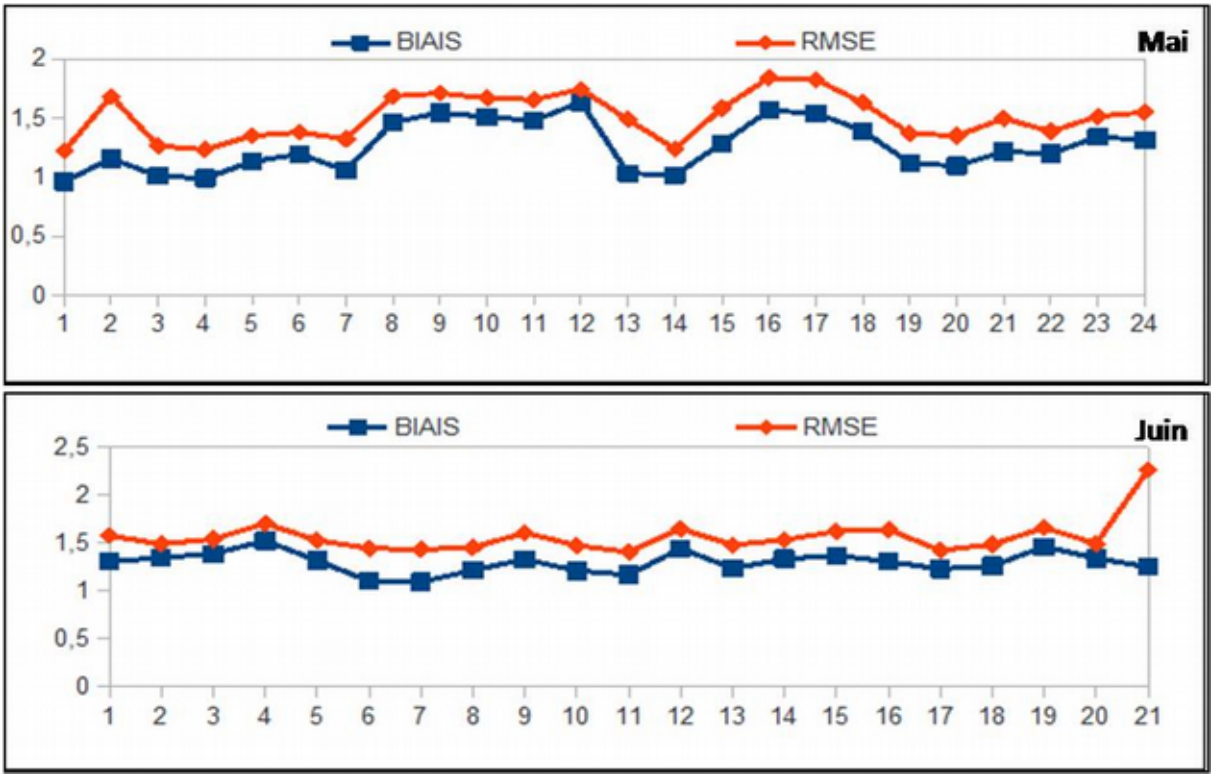

Fig. 5 : Monthly evolution of the mean square error (RMSE) (given in red) and bias (given in blue) for wind speed at 10 meters averaged over the period May and June expressed in (m / s). Calculations are made on the field of study of the ALADIN model in relation to the analysis to maturity 12:00

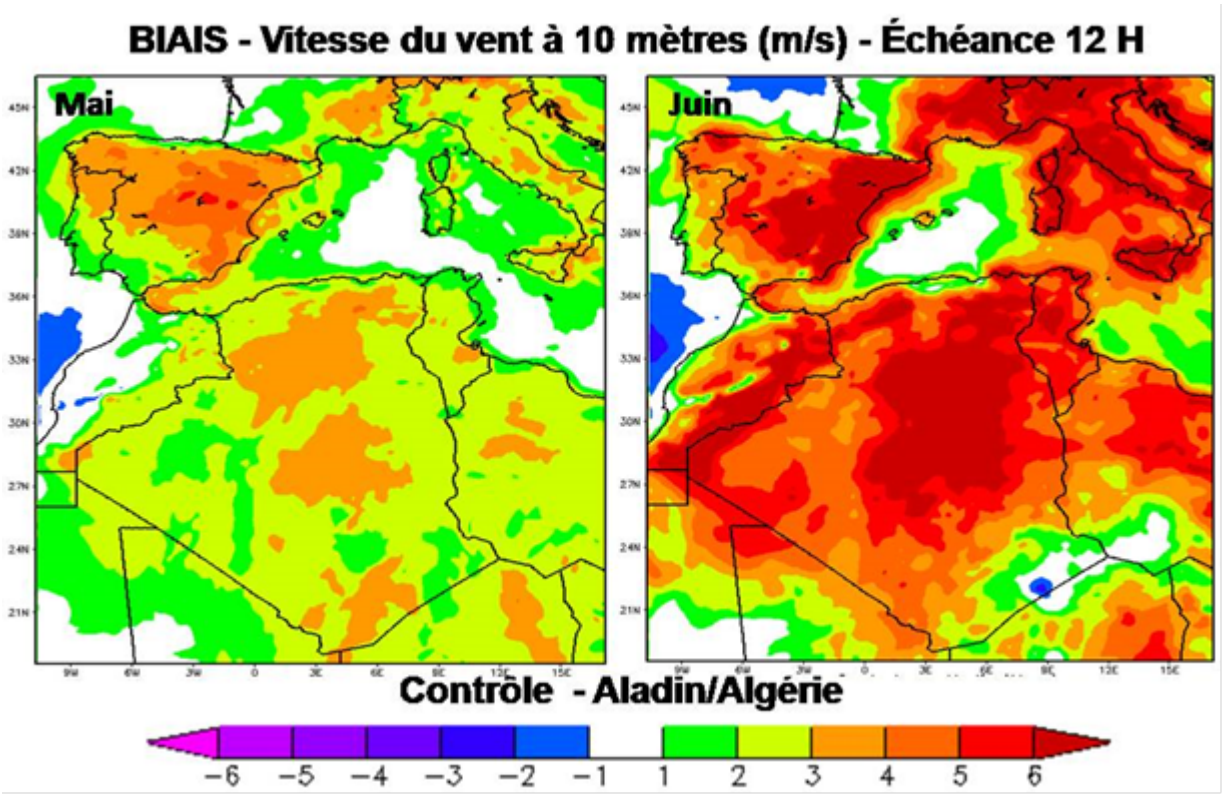

Fig. 6 : Monthly averages bias of wind speeds at 10 meters at maturity recorded 12 hours obtained with the ALADIN model compared to the analysis.

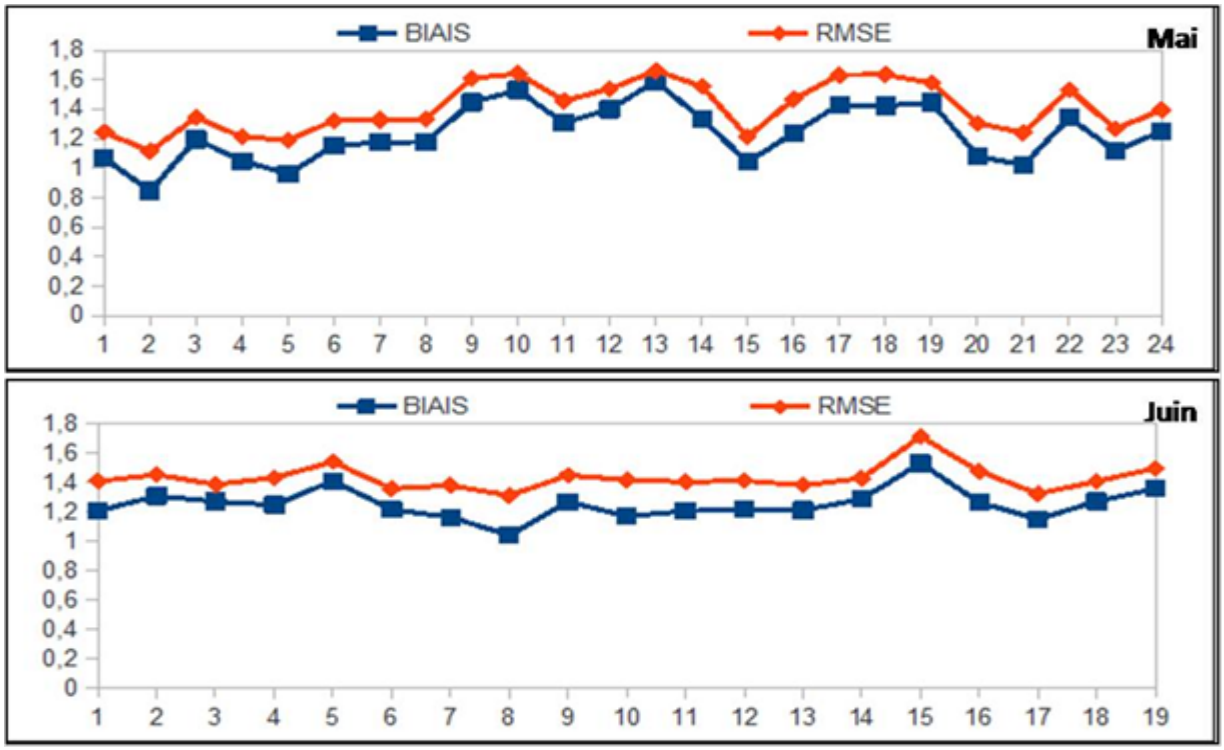

Fig. 7 Monthly evolution of the mean square error (RMSE) (given in red) and bias (given in blue) for the wind to 10 meters averaged over the period May and June expressed in (m / s). Calculations are made on field of study of the ALADIN model in relation to the analysis to maturity 24 hours.

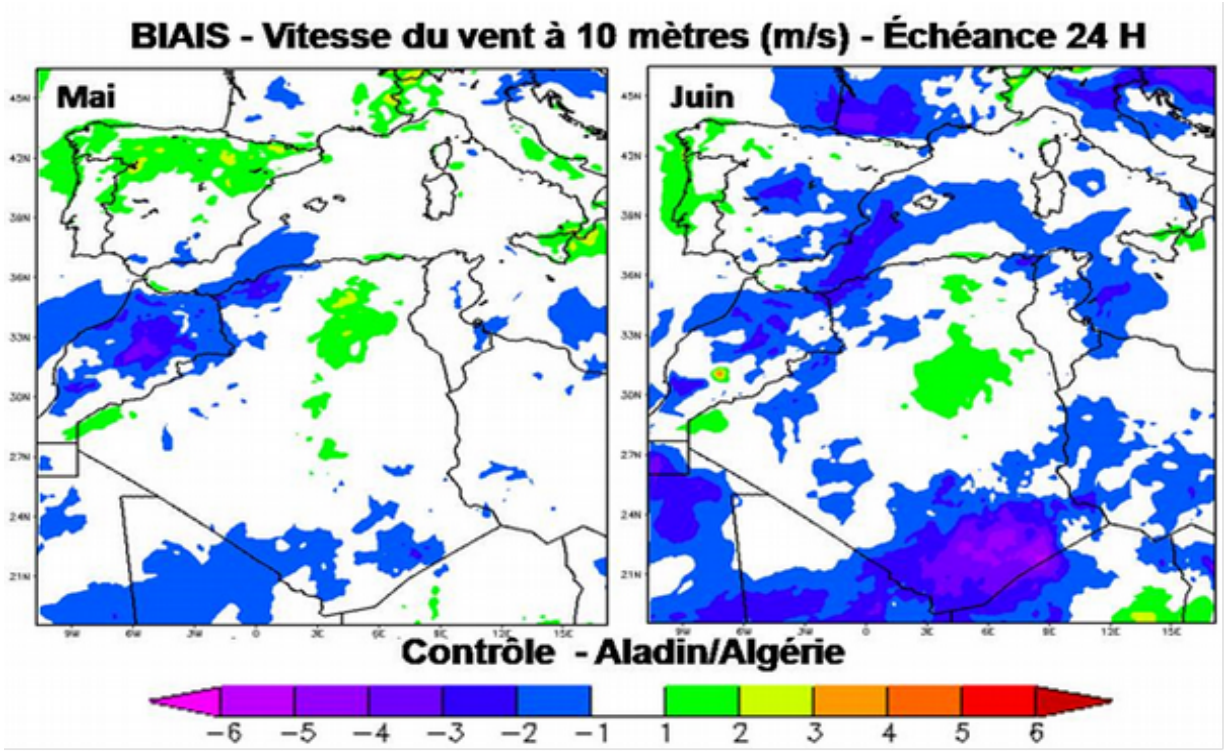

Fig. 8 Monthly averages bias of wind speeds at 10 meters at maturity recorded 24 hours obtained with the ALADIN model compared to the analysis.

4 Conclusion

The study of the ALADIN model scores per rapport to the analysis (12h and 24h) showed that for temperatures to two meters the results show the presence of a negative bias during the day and overnight positive, particularly au over the continent and relatively low on the sea surface.
Also, for the wind at 10 meters bias is often positive, with very marked values during the day.

Nowcasting with AROME

Christoph Wittmann and Florian Meier

1 Introduction

Nowcasting has been one of the main focal points in the ZAMG NWP team for quite some time. The current operational nowcasting system is INCA (Integrated Nowcasting through Comprehensive Analysis; Haiden et al. 2011). The system is well established and widely used for various applications (automatic warning system, road maintenance, hydrological modelling, energy related forecasts, etc.). However, by design INCA has deficiencies in predicting the dynamical evolution of convection as just kinematic translation of existing cells can be captured. In 2015 first steps have been undertaken to introduce an AROME Nowcasting version which should, in combination with INCA, help to allow some significant improvements in the nowcasting range, especially for deep convection. The experiences of Météo-France with their AROME-PI system could serve as an excellent motivation to start with this work.

2 Design of the AROME Nowcasting system

An AROME nowcasting (AROME-NC) version is implemented in its first test version since spring 2015 in addition to the operational AROME system (AROME-OPER) in Austria (see also table 1 for details). Every hour a short cutoff (0.5 hour) 2.5km 3D-VAR is run on the AROME-OPER domain including all available observations and in addition radar data (Doppler wind, reflectivities). The forecast from the last AROME-OPER run is used as the first guess (open loop, no closed assimilation cycle). The resulting analysis is interpolated to the slightly smaller AROME-NC domain (but same 2.5km resolution) and used to initialize the AROME nowcasting run. The main reason for running AROME-NC on a slightly smaller domain is limited computational resources of the current HPC system at ZAMG.

Table 1: Main settings for operational AROME system and coupled AROME nowcasting version

	AROME-OPER	AROME-NC
horiz. resolution	2.5km	2.5km
grid points	600 x 432	432 x 270
vertical levels	90	90
runs / day	8	24
forecast range (h)	60	12
time step	60s	60s
init 3D	3D VAR *)	3D VAR **)
init soil	CANARI	DOWNSCALING
coupling model	IFS	AROME-OPER

*) 3 hourly, closed cycle

**) 1 hourly, open cycle

The observation data set entering 3DVAR for AROME-OPER and AROME-NC is identical with one major exception: Radar Doppler wind and reflectivity data is only entering the nowcasting system at the time of writing. A beneficial usage of radar data within the assimilation suite requires a comprehensive quality control of the incoming raw data. Certain effort has therefore been invested in the remote sensing team at ZAMG to develop a radar quality software using algorithms from two different sources: INCA and BALTRAD. In addition a de-aliasing algorithm for radial wind has been implemented (He et al. 2012). AROME-NC has been run for a three month test period in summer 2015 and since November 2015 a regular test mode has been set up. The first results are summarized in the following section.

3 First results

The new AROME-NC has been evaluated during a three months period in summer 2015. Although all relevant forecast parameters have been included into the evaluation process, main focus was put on precipitation. Figure 1 compares hourly precipitation forecasts up to 12 hours lead time using the A amplitude component of the SAL scores and INCA precipitation analysis as the reference. It is evident that AROME-NC shows a better performance (i.e. A closer to 0) than AROME-OPER during the first forecast hours. AROME-OPER (blue) is overestimating precipitation activity significantly during the afternoon (just 12 UTC runs included) before a period of underestimation can be observed in the evening (and night). This diurnal cycle in terms of the A score can usually be explained by a slight shift of convective activity in the model: Too early triggering during the day resulting further in a too early decay in the evening and night compared to reality. However, AROME-NC (red) is in better correspondence with observation, particularly during the first hours. The improvement can be mainly associated with the additional assimilation of radar data. During the first forecast hour a slight underestimation of AROME-NC can be observed. This behaviour was somehow surprising in the beginning and was therefore part of further analysis. Part of this “dry spin-up” could be solved by changing initialization and coupling strategy for 3D hydrometeor fields in AROME-NC. At least for case studies this seems to be the case while there is still need for confirmation by long term verification.

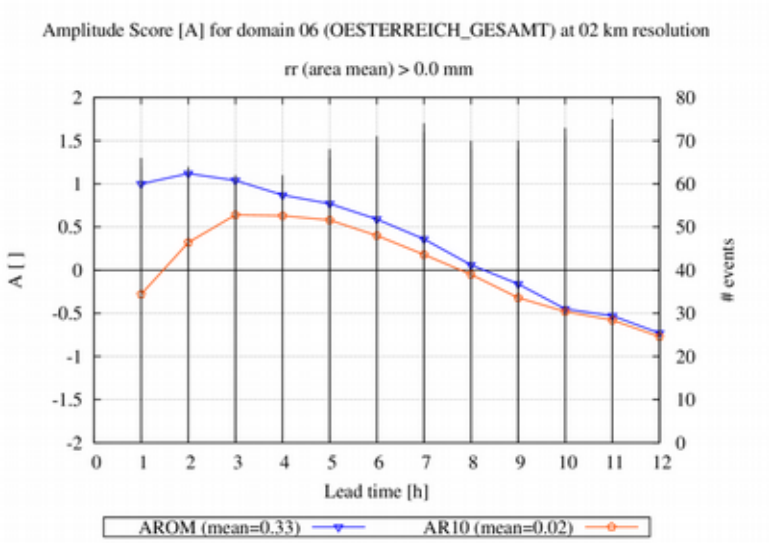

Figure 1: A component of SAL scores evaluating hourly areal mean precipitation for AROME-OPER (blue) and AROME-NC (red) for a 3month period using INCA precipitation analysis as observation reference. A=0 indicates perfect correspondence with observation, A>0 overestimation, A<0 underestimation

In addition, experiments using in latent heat nudging (LNH) were carried out. In case studies it could be shown using LNH in addition to 3DVAR might be beneficial in the nowcasting range. Figure 2 shows a case where a significant precipitation signal seen in the INCA precipitation analysis (Figure 2, top) is more or less missed by the AROME-NC 1h forecast run using radar data in 3DVAR (bottom left). The AROME-NC version using in addition LNH (bottom right) is in much better correspondence with the analysis. A test run with LNH over a longer period will show whether this benefit can be confirmed or not.

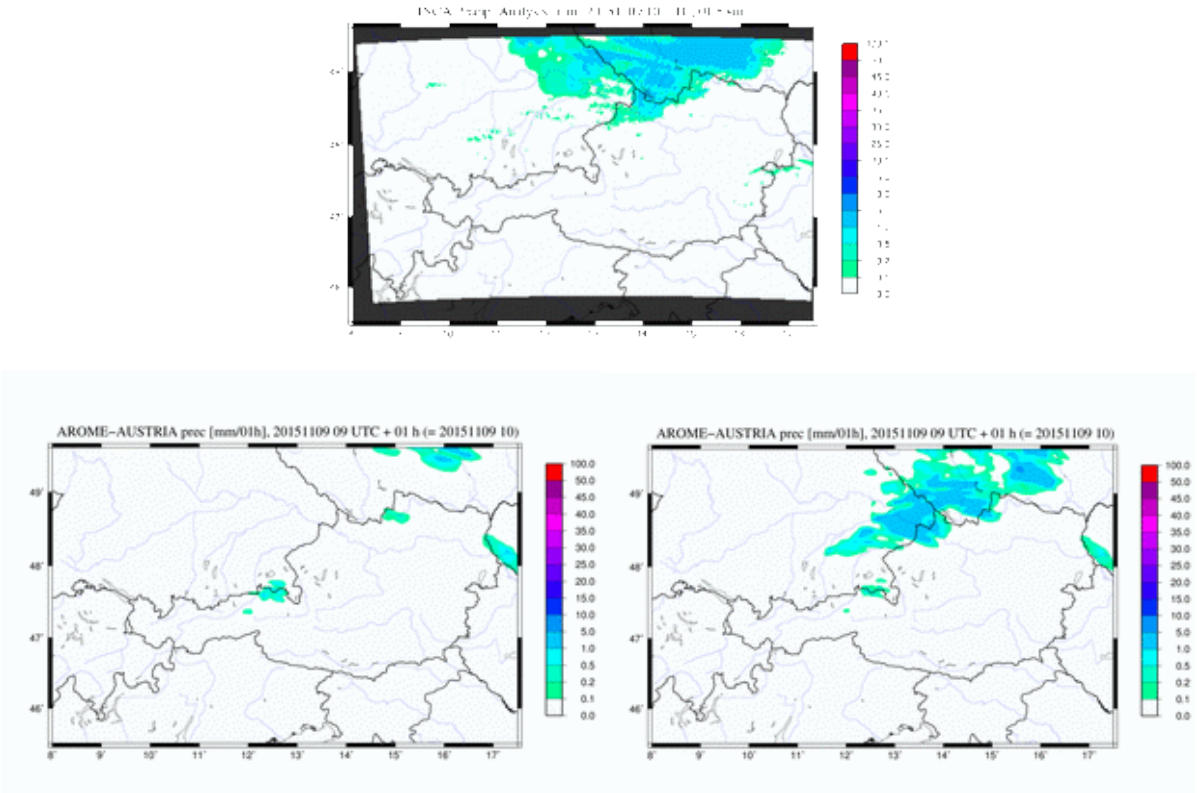

Figure 2: Case study showing +1h hour precipitation forecast of AROME-NC (bottom left) using radar assimilation in 3DVAR and another version with radar assimilation + LHN (bottom right) and the corresponding INCA precipitation analysis (top)

4 Summary and Outlook

The development of a nowcating version of AROME has been started in 2015 and will stay a main focus at ZAMG in the near future. In its final and operational development phase AROME-NC should help to improve quality of the forecasts in the very short forecasting for various applications. At the moment, the AROME-NC system is run with 2.5km grid point spacing 24 times per day covering a forecast range of 12 hours. First results in summer 2015 are rather encouraging. The main part of the improvement can be associated to the assimilation of radar data. Additional observational data (like ModeS, GNSS based ZTD from Austrian network) will be investigated. An increase of the horizontal resolution to approximately 1km is foreseen at a later stage and is dependent on the available computational resources at ZAMG.

5 References

Haiden, T., A. Kann, C. Wittmann, G. Pistotnik, B. Bica, and C. Gruber, 2011: The Integrated Nowcasting through Comprehensive Analysis (INCA) System and Its Validation over the Eastern Alpine Region. Wea. Forecasting, ***26****, 166-183.*

Guangxin He, Gang Li, Xiaolei Zou, and Peter Sawin Ray, 2012: Applications of a Velocity Dealiasing Scheme to Data from the China New Generation Weather Radar System (CINRAD). Wea. Forecasting, 27, 218–230. doi: http://dx.doi.org/10.1175/WAF-D-11-00054.1

Application and impact of the flux-conservative physics-dynamics interface in AROME

Daan Degrauwe, Yann Seity, François Bouyssel, Piet Termonia

1 Introduction

The physics-dynamics interface is the part of the model that is responsible for updating the prognostic dynamical variables with the contributions from the physics parameterizations. Due to historic reasons, the different physics packages in the ALADIN system use different physics-dynamics interfaces: the ARPEGE, ALADIN and ALARO physics are called in the routine APLPAR, and are interfaced through the routines CPTEND_NEW and CPUTQY, while the AROME physics are called in the routine APL_AROME, and are interfaced with the routine CPUTQY_AROME. Figure 1 gives a schematic illustration of the current situation.

This situation is unfortunate for several reasons. First, from a maintenance point of view, efforts are wasted when supporting two interfaces which essentially have the same task. Second and more importantly, this situation also obstructs the spill-over of scientific advances between both physics packages: either one uses this package, or (s)he uses the other one. Combining parts of both packages is problematic.

A third inconvenience with having two physics dynamics interfaces is the following. In fact, it would be a mistake to consider the physics-dynamics interface as a purely technical (i.e. code-related) issue. Indeed, given its central place in the code, i.e. the place where all contributions of the different physics parameterizations come together, the physics-dynamics interface is the exquisite spot to diagnose budgets, or to impose constraints such as conservation of energy and mass, or consistency in the thermodynamic assumptions. As is explained below, it is also in this aspect that the two physics-dynamics interfaces of the ALADIN system differ.

The interface of ARPEGE/ALADIN/ALARO is based on the paper by Catry *et al.* (2007). It is shown in that paper how a flux-based formulation leads to a system that is intrinsically energy- and mass-conservative. However, the current implementation in CPTEND_NEW is quite unflexible in the sense that it is written for 4 prognostic hydrometeors (cloud droplets, cloud ice crystals, rain and snow) and a limited number of interactions between them.

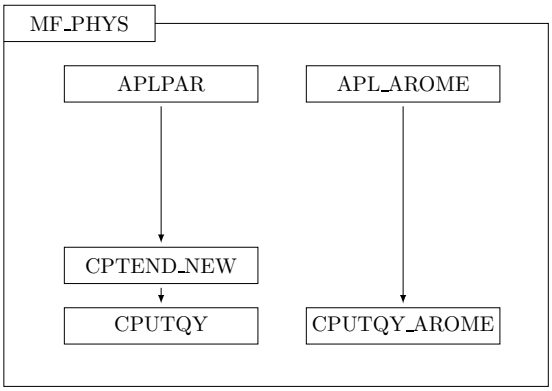

Figure 1: Two physics-dynamics interfaces existing in the ALADIN system

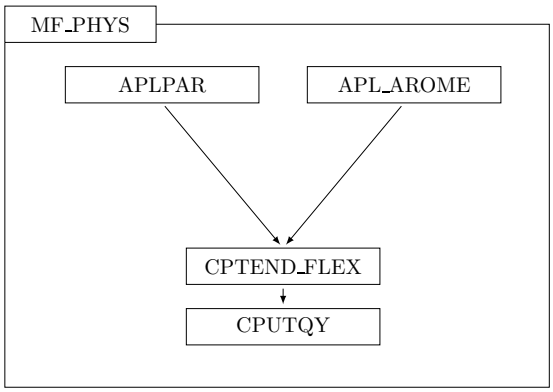

Figure 2: The unified, flexible physics-dynamics interface

The AROME interface, on the other hand, is more general in the sense that it deals with an arbitrary number of prognostic hydrometeors, including graupel and hail. However, as it is based on adding temperature tendencies, it does not guarantee conservation of energy, nor are the involved thermodynamic computations entirely consistent.

The work presented in this contribution is part of a paper that is to be submitted (Degrauwe *et al.*, 2015). A more extensive literature review and theoretical foundation of this work can be found in that paper.

2 The flexible physics-dynamics interface: CPTEND_FLEX

To remedy the situation of the two physics dynamics interfaces, a flexible interface (CPTEND_FLEX) has been developed that combines the advantages of both existing interfaces. Since it is based on the same flux-conservative formulation as the ARPEGE/ALADIN/ALARO interface, it inherits the intrinsic conservation of energy and mass. On the other hand, it is formulated in the most general way, allowing for an arbitrary number of hydrometeors (including graupel, hail, or any future hydrometeors), as well as an arbitrary number of interactions between them. This flexible interface can thus be used for both physics packages, as is schematically illustrated in figure 2. It should be noted that a similar action has been undertaken regarding the diagnostics of both physics packages, resulting in the DDHFLEX development[1].

The flexible physics-dynamics interface makes it possible to get rid of some of the approximations that are made currently when running AROME:

- the heat transport by precipitation is neglected;
- the effect of moisture transport on the total specific heat capacity is neglected in the energy budget of diffusive processes (shallow convection and turbulence);
- the radiation scheme uses the dry-air heat capacity, instead of the moist (including hydrometeors) air heat capacity;
- the total effect of the different parameterizations is obtained by adding temperature tendencies. This approach does not guarantee conservation of energy.

[1] A difference in implementation being that DDHFLEX is for the time being not threadsafe, while CPTEND_FLEX is.

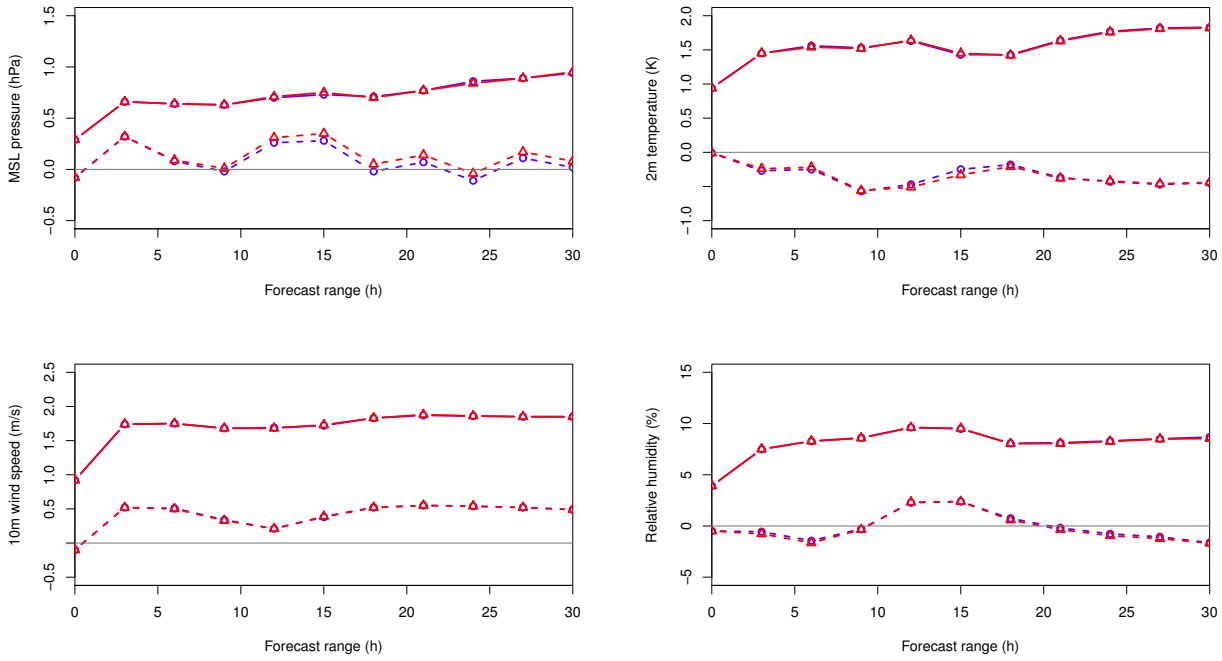

Figure 3: RMSE (solid line) and bias (dashed line) over the period 1 November 2014 – 30 November 2014, for REF (blue circles) and FCI (red triangles).

3 Impact on operational scores

To evaluate the meteorological impact of the flux-conservative physics-dynamics interface, AROME has been run in its operational Météo-France configuration during two months: 1–30 November 2014, and 6 January–6 February 2015. The first month is characterized by exceptionally mild weather, with numerous episodes of heavy precipitation in the South-West of France. The second month was characterized by strong winds and episodes of heavy snowfall.

Figures 3 and 4 show bias and rmse for several meteorologic variables for the two periods, respectively. These scores are calculated by comparing the AROME forecasts with observations throughout the French territory.

Figures 5 and 6 compare the forecasted precipitation over the two periods. To avoid the problem of the double penalty, the precipitation is verified with the neighbourhood observation Brier skill score (Amodei and Stein, 2009). This score is determined by calculating the probability that a precipitation threshold is exceeded in the vicinity of an observation. By choosing the threshold, one focuses the verification more on light or heavy precipitation.

The scores indicate that the impact of using the flux-conservative set of equations appears quite limited when considering time- and space-averaged scores such as the ones considered here. It should be stressed that no retuning has been done for the experiments with the flux-conservative equations. As a result, no significant improvement of the scores could be expected anyway. The fact that the scores do not change substantially, merely indicates that the approximations that are made in the current temperature-tendency based interface are indeed small on a domain-wide scale. However, as is shown in the next section, some significant differences are observed under specific circumstances.

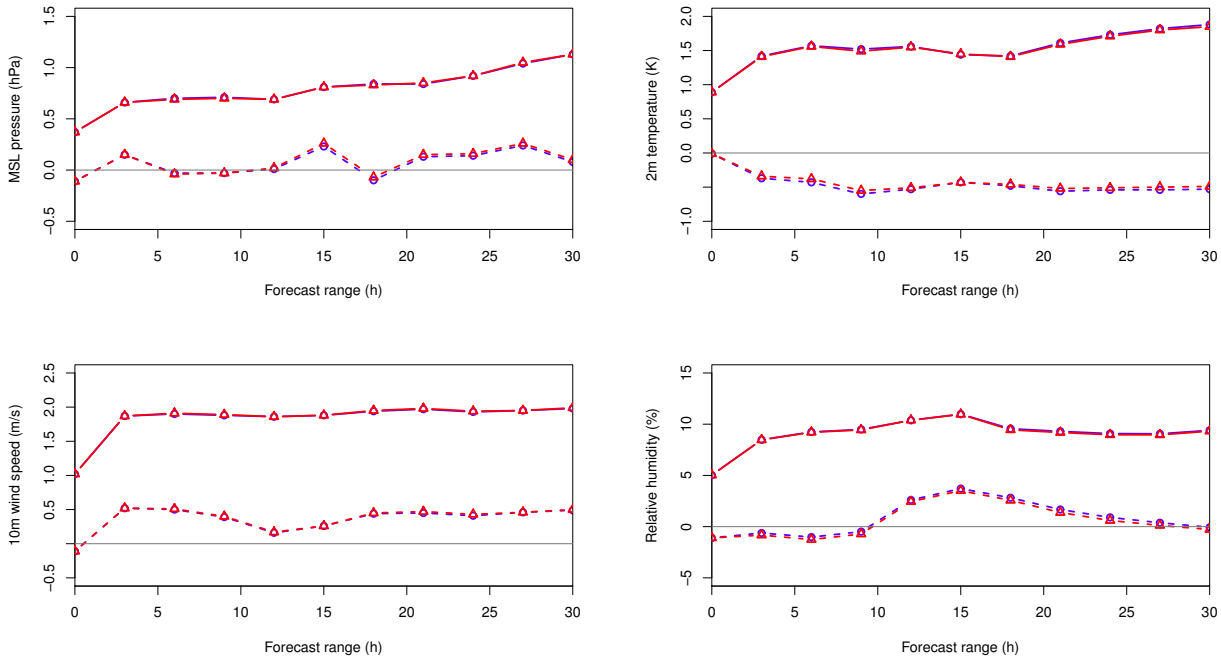

Figure 4: RMSE (solid line) and bias (dashed line) over the period 6 January 2015 – 6 February 2015, for REF (blue circles) and FCI (red triangles).

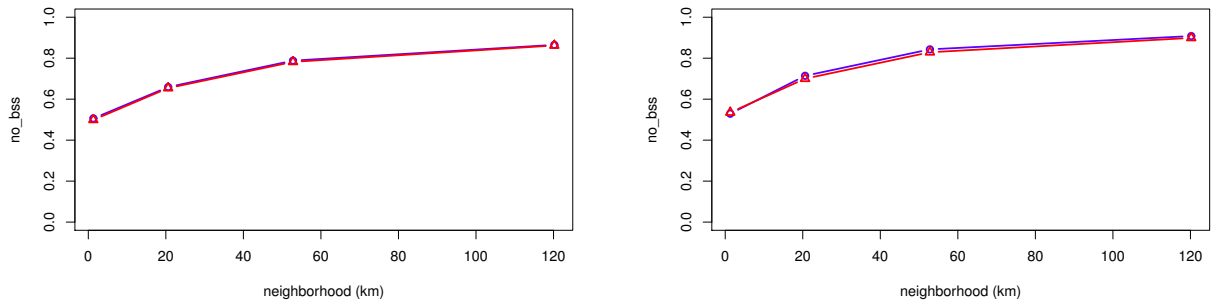

(a) threshold 2mm (b) threshold 10mm

Figure 5: Neighbourhood observation Brier skill score for precipitation between 1200UTC and 1800UTC over the period 1 November 2014 – 30 November 2014, for REF (blue circles) and FCI (red triangles).

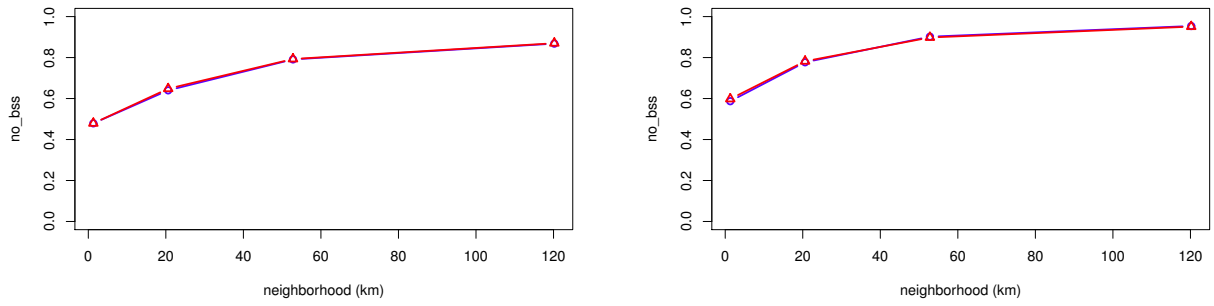

(a) threshold 2mm (b) threshold 10mm

Figure 6: Neighbourhood observation Brier skill score for precipitation between 1200UTC and 1800UTC over the period 6 January 2015 – 6 February 2015, for REF (blue circles) and FCI (red triangles).

4 Case study of a cold pool originating from heavy precipitation

When precipitation evaporates while falling through unsaturated air, it cools its environment. As such, a region of relatively cool air, the so-called cold pool, originates when heavy, localized precipitation occurs, for instance in precipitating convective systems. It has been shown that the cold pool is in fact a key element in the lifecycle of a such systems. On the one side, new convective cells originate at the border of the cold pool and its warmer surroundings, but on the other hand, if the cold pool becomes too strong, it may cut off the supply of warm air to the updraft (Engerer *et al.*, 2008). The cold pool is also accompanied by a meso-scale high pressure area, which plays a crucial role in the wind gusts that go with heavy precipitation. For these reasons, it is no surprise that the representation of the cold pool is also crucial in a NWP model (Engerer *et al.*, 2008; De Meutter *et al.*, 2014).

Although evaporative cooling is the main cause for a cold pool, a second mechanism may enhance it. As precipitation falls from colder layers aloft to hotter layers below, it will be heated by the surrounding air, which in response will cool down. This secondary thermodynamic effect (the advection of sensible heat) of precipitation is neglected in the current AROME physics-dynamics interface, while it is correctly accounted for with the flux-conservative interface CPTEND_FLEX. One can thus expect that the depth of a forecasted cold pool depends on which interface is used.

This is confirmed when looking at the AROME forecasts over the Balearic islands on 15 January 2015. This case is characterized by convection developing ahead of an active cold front coming from the south. Figures 7a and 7b show the forecasted 1200 UTC–1800 UTC accumulated precipitation with the current AROME interface (REF) and with the flux-conservative interface (FCI). It is observed that the overall structure of the precipitation is very similar with both interfaces, but the heaviest precipitation occurs in a somewhat smaller area with FCI. Also the maximum precipitation is a bit larger (26mm/6h with REF versus 32mm/6h with FCI). The difference between REF and FCI becomes even more clear when comparing the 2m temperature and the surface pressure in Figures 7c and 7d, respectively. The temperature is significantly lower with FCI (up to 5 K cooler), and the surface pressure is higher (up to 1.4 hPa).

To further illustrate the impact of the heat transport by precipitation on the cold pool, the vertical profiles in the point with the maximal precipitation as marked in figure 7b are studied. The vertical profile of the precipitation fluxes (figure 8a) shows how snow and graupel originate aloft, they melt to form rain at around 850 hPa, and the rain starts to evaporate below 930 hPa. Figure 8b shows the vertical profile of the two phenomena that are responsible for the development of the cold pool: the latent heat effects from conversions between water vapour and hydrometeors (solid line), and the falling of cold hydrometeors into warmer air layers (dashed line). It is clear that the second effect is orders of magnitude smaller than the first effect, at least when considering the full vertical extent of the model. However, as shown in figure 8c, the heat transport by hydrometeors is not entirely negligible in the range between the surface and 900 hPa, and thus contributes to the formation of the cold pool.

This case shows that even small terms in the energy budget can have a significant impact under certain conditions, and that it is better to properly account for them.

5 Conclusions and future work

This contribution shows how the flexible physics-dynamics interface that entered cy40t1 has multiple advantages. First, it makes code maintenance easier. Second, it allows to get rid of some of the thermodynamic approximations that are currently made by the AROME physics-dynamics interface. Although the tests show that the impact on monthly scores is quite limited, a case study of a heavy precipitation case shows that under certain conditions, the approximations do have a noticeable impact on the result.

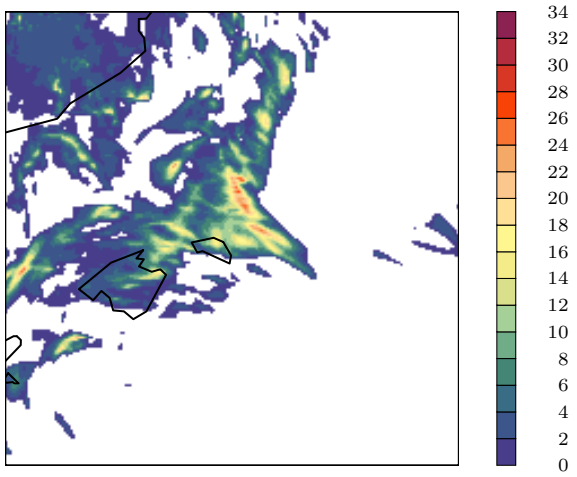

(a) REF precipitation (mm) between 1200UTC and 1800UTC

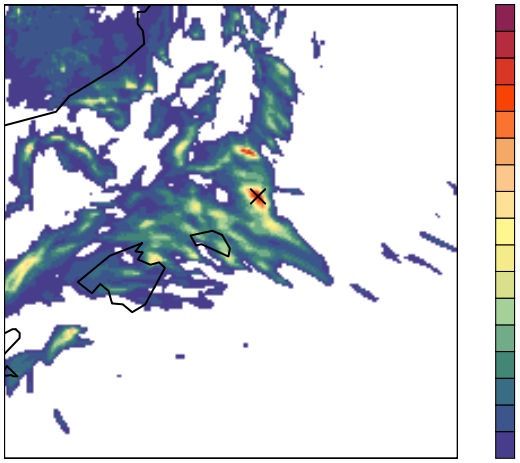

(b) FCI precipitation (mm) between 1200UTC and 1800UTC

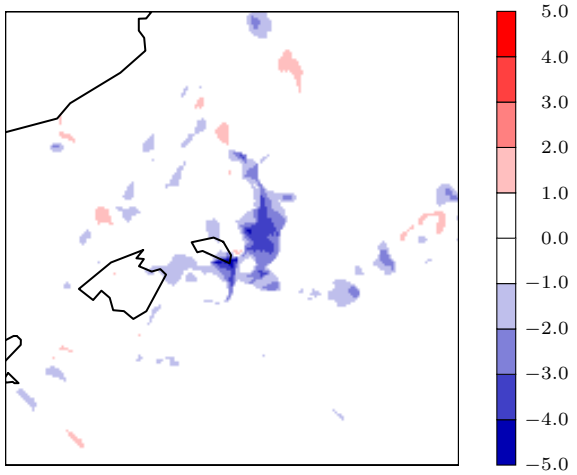

(c) 2m temperature difference (K) between FCI and REF at 1800UTC

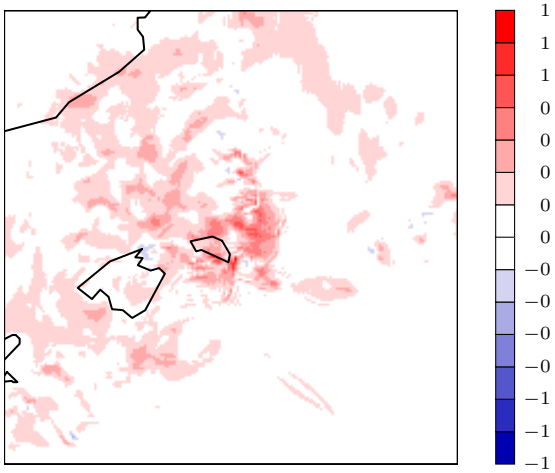

(d) Surface pressure difference (hPa) between FCI and REF at 1800UTC

Figure 7: Case of heavy precipitation on 15 January 2015.

A third advantage of a unified physics-dynamics interface for all physics packages in the ALADIN system is that it allows for an exchange of parameterizations between ARPEGE/ALADIN/ALARO and AROME. Indeed, for radiation, this work has already been done, with the new ACRANEB2 radiation scheme now being available in both physics packages. A uniform physics-dynamics interface guarantees a consistent treatment of radiation in both environments. The longer-term goal should be to move in a similar direction for the other parameterizations. As such, the strict distinction between both physics packages can fade away, and they turn into canonical configurations of a single NWP model.

6 References

Amodei, M. J. and Stein, Deterministic and fuzzy verification methods for a hierarchy of numerical models, Meteorological Applications, 16, 191-203, 2009.

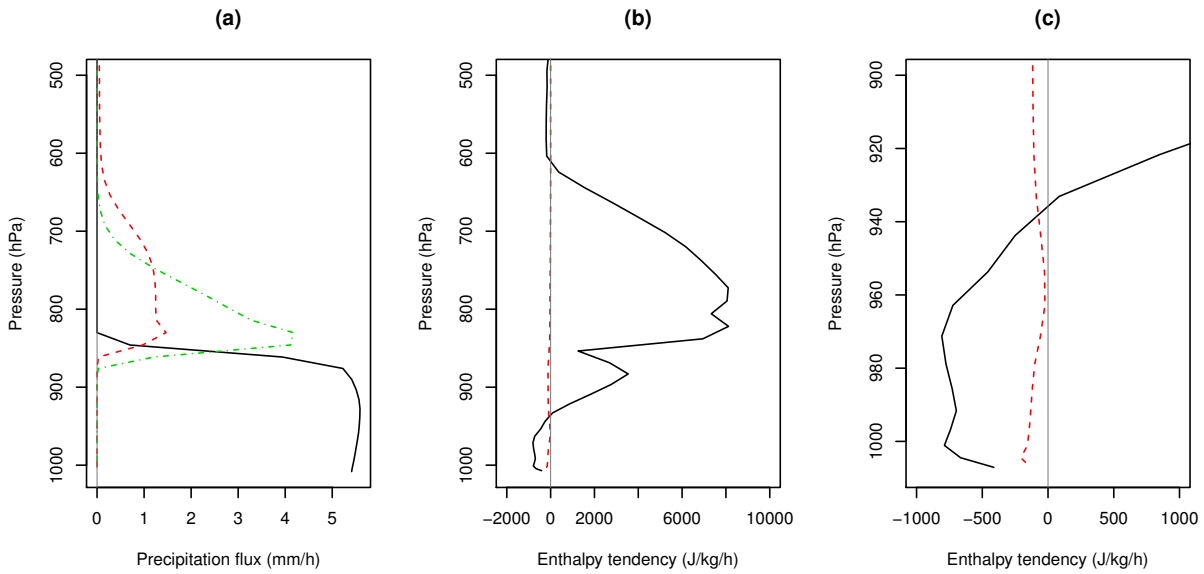

Figure 8: Vertical profiles in the point indicated in figure 7b with the flux-conservative interface. (a) precipitation fluxes: rain (solid line), snow (dashed line) and graupel (dash-dotted line); (b) cold pool-generating phenomena: latent heat effect due to phase changes (solid line) and sensible heat advection (dashed line); (c) same as (b) but focused on near-surface. All fluxes and tendencies are time-averaged between 1200 UTC and 1800UTC.

Catry, B., J.-F. Geleyn, M. Tudor, M., P. Bénard, and A. Trojáková, Flux-conservative thermodynamic equations in a mass-weighted framework, Tellus A, 59, 71-79, 2007.

Degrauwe, D., Y. Seity, F. Bouyssel, and P. Termonia, Generalization and application of the flux-conservative thermodynamic equations in the models of the ALADIN system, to be submitted to Geoscientific Model Development, 2015.

De Meutter, P., L. Gerard, G. Smet, K. Hamid, R. Hamdi, D. Degrauwe, and P. Termonia, Predicting Small-Scale, Short-Lived Downbursts: Case Study with the NWP Limited-Area ALARO Model for the Pukkelpop Thunderstorm, Monthly Weather Review, 143, 742-756, 2014.

Engerer, N. A., D. J. Stensrud, and M. C. Coniglio, Surface Characteristics of Observed Cold Pools, Monthly Weather Review, 136, 4839-4849, 2008.

Evaluation of the atmospheric instability during the warm half year of 2014 based on ALADIN forecasted thermodynamic conditions

Boryana Tsenova, Milena Koleva, Andrey Bogatchev

1 Introduction

Nowadays the study of atmospheric electricity and especially lightning is developing rapidly as technology advances. The evaluation of lightning electric and magnetic field is important as because of their fundamental importance, as well for its more precise forecast. Thunderstorms are dangerous phenomena and their accurate in terms of time and location forecast is necessary. Due to the established relations between the nature of lightning and other dangerous natural phenomena such as tornadoes, torrential rains, floods, hail storms, destructive winds and forest fires, the better understanding of lightning behaviour could improve the nowcasting of some hazards by a timely accurate numerical forecast of thunderstorm development probability. The last years an increase of the number of developed convective clouds with intensive lightning activity over Bulgaria is observed.

Since 2013, an operational scheme for predicting the lightning probability was included in the ALADIN-BG forecast post-processing (Tsenova and Bogatchev, 2012). This scheme, based on an evaluation of the atmospheric instability according to the predicted by ALADIN model meteorological fields, separates cases in four groups – very low, low, medium and high lightning probability at each point of the model grid (7x7 km) of the ALADIN-BG domain for the whole integration time (72 h) with a frequency of 3 h. It was established based on data for lightning activity for the three years 2010-2012 from the meteorological stations (taking into account the specifics of meteorological observations at main and intermediate periods imposed by WMO) in Bulgaria versus some atmospheric instability indices (as K, Cross Totals, Vertical Totals, Total Totals, SWEAT and Lifted indices) calculated based on the ALADIN forecast production. The verification of the scheme showed a relatively good skill. However, a high percent of thunderstorm cases were predicted as cases with medium lightning probability, a group including also a high percent of cases without thunderstorm formation. The aim of the present work (in the frame of the Master degree thesis of Milena Koleva) was to start an eventual improvement of the actual scheme for numerical forecast of lightning probability by a more accurate verification that considers the lightning activity based on ATDnet lightning detection network that gives a precise information for the time of lightning initiation and covers the whole region of Bulgaria. ATDnet is the most recent version of the VLF lightning location network of the Met Office, introduced in 2007 (Gaffard et al., 2008). In the present work, some of the evaluated instability indices (K, Cross Totals, Vertical Totals and Total Totals indices) were compared with data from ATDnet for the period April-September 2014. Also, as the atmospheric instability is evaluated based on the forecasted by ALADIN model meteorological fields instead of radiosounding measurements (which are performed at the territory of Bulgaria only once daily at 12 UTC and only over the region of Sofia), a comparison between measured and forecasted thermodynamical characteristics of the atmosphere over Sofia for the warm half year of 2014 was performed.

2 Data and results

Instability indices

Thunderstorm formation and further development depends on the environmental conditions. Usually different instability indices are considered as main characteristics of the environmental conditions with the aim to determine thresholds for thunderclouds formation that vary for the different parts of the earth. In the scientific community (Showalter, 1953; George, 1960; Boyden, 1963; Jefferson, 1963; Miller, 1967; Litynska et al., 1976; Peppler, 1988; Peppler and Lamb, 1989) about 13 instability indices were introduced, including only thermodynamical variables, only wind data, or combination of thermodynamical variables and wind data. In the present work the following instability indices, obtained from ALADIN-BG output are considered - K Index, Vertical Totals Index (VTOT), Cross Totals Index (CTOT) and Total-Total Index (TTOT), as Vertical Totals Index (VTOT) and Cross Totals Index (CTOT) are components of Total-Total Index (TTOT).
K Index: introduced in George (1960), it is calculated by:

$$K = (T_{850} - T_{500}) + T_{d850} - (T_{700} - T_{d700}) , \quad (1)$$

where T_{850} is the air temperature at 850 hPa, T_{d850} - dew point temperature at 850 hPa, T_{700} and T_{d700} are respectively air and dew point temperature at 700 hPa and T_{500} – air temperature at 500 hPa. The first member of (1) gives an information about the temperature gradient in the layer 850 - 500 hPa; the second member – gives an information about the humidity in the lower layers; the third member of the equation shows the moisture deficiency at 700 hPa. In dry air at 700 hPa the values of K will be lower, but the presence of moisture below 700 hPa may destabilize the air mass causing updraughts. At higher values of K strong showers may be observed. K increases with the increasing of relative humidity at 700 hPa which favours thunderstorm formation during the summer.
Cross Totals Index (CTOT), Vertical Totals (VTOT), and Total Totals (TTOT): defined by Miller (1967) and calculated by:

$$CTOT = T_{d850} — T_{500} \quad (2)$$
$$VTOT = T_{850} — T_{500}$$
$$TTOT = CTOT + VTOT$$

It is visible that CTOT depends highly from the moisture at 850 hPa, while VTOT represents the temperature gradient in the layer between 850 and 500 hPa.
The considered above instability indices are calculated based on ALADIN forecasted air and dew point temperatures at needed levels at each point of the model grid (7x7 km) of the ALADIN-BG domain for the whole integration time (72 h) with a frequency of 3 h.

Comparison between measured by radiosonde and forecasted by ALADIN thermodynamical conditions of the atmosphere over Sofia for the period April-September 2014

Because of the restrictions of the radiosonde data over the region of Bulgaria, which are obtained only once daily at 12 UTC and only over the region of Sofia, the atmospheric instability is evaluated based on the forecasted by ALADIN model meteorological fields. To assess the ability of ALADIN model to represent the actual thermodynamical atmospheric conditions, a comparison between the measured by radiosonde and forecasted thermodynamical characteristics of the atmosphere over Sofia for the warm half year of 2014 was performed. For this purpose, ALADIN data over the region of Sofia (determined as the domain of 20x20km with a center Sofia – 42,41N/23,19E) were averaged at each considered level for the comparison with the measured ones.

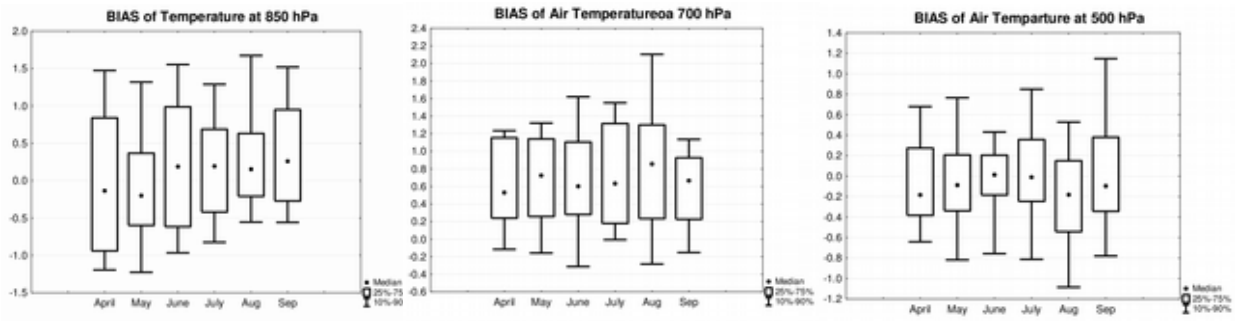

Figure 1. Bias of air temperature over Sofia for April, May, June, July, August and September 2014 at 850, 700 and 500 hPa

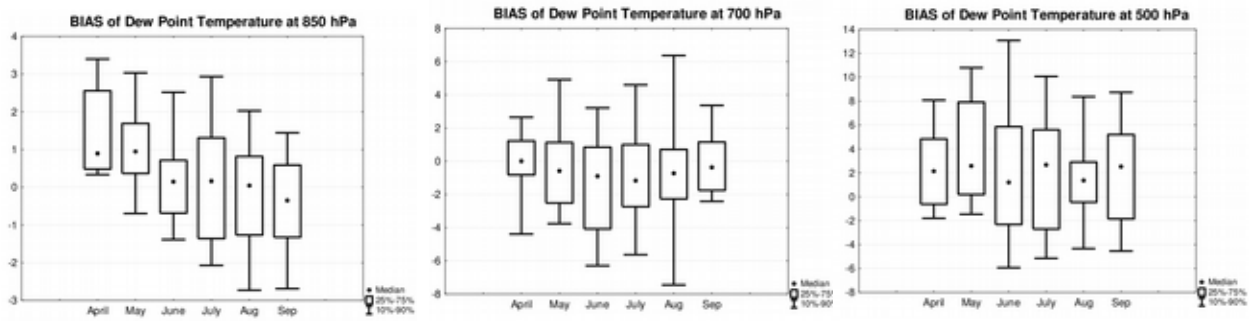

Figure 2. Bias of dew point temperature over Sofia for April, May, June, July, August and September 2014 at 850, 700 and 500 hPa

Figures 1 and 2 show box and whiskers box of respectively the bias of air and dew point temperature for the different months at the different considered levels. In Table 1 are given the correlation coefficients between the measured and the forecasted air and dew point temperature.

Table1. Correlation coefficient (R) between the sounding measured and the forecasted by ALADIN air (T) and dew point (T_d) temperatures at the levels 850, 700 and 500 hPa for the warm half year of 2014

	R_T	R_T_d	R_T_{850}	R_T_{d850}	R_T_{700}	R_T_{d700}	R_T_{500}	R_T_{d500}
April	0.99	0.97	0.98	0.87	0.98	0.72	0.98	0.85
May	0.99	0.96	0.97	0.82	0.96	0.79	0.97	0.79
June	0.99	0.96	0.96	0.79	0.95	0.81	0.98	0.70
July	0.99	0.96	0.93	0.58	0.94	0.55	0.94	0.76
August	0.99	0.97	0.96	0.67	0.92	0.84	0.96	0.90
September	0.99	0.96	0.98	0.86	0.99	0.87	0.93	0.80
All	0.99	0.96	0.98	0.89	0.98	0.80	0.99	0.8

From Figure 1 it is visible that the median of the bias of the air temperature at 850 hPa is about 0.2K – positive for April and May, and negative for the other months. The maximum value of the 90th percentile of the bias is reached in August (1,6K) while the lowest value of the 10th percentile – in May (-1,2K). The correlation coefficient (Table 1) between the forecasted and the measured temperature at 850 hPa for the whole considered period (April-May) is 0.98. It is the lowest in July (0,93) and the highest in April and September. At 700 hPa the median of the bias of the air temperature is always positive with values between 0.5K (April, with correlation coefficient of 0.98) and 0,9K (August, with correlation coefficient of 0,92). The lowest value of the 10the percentile is in June (-0,3K) and the highest value of the 90th percentile – in August (2,1K). For the whole period of consideration the correlation coefficient between the forecasted and the measured temperature at 700 hPa is 0.98. At 500 hPa the medians of the bias of the air temperature are between 0K in June

(correlation coefficient 0.98) and -0.2K in April (correlation coefficient 0.98). The lowest value of the 10th percentile is in August (-1.1K) and the highest value of the 90th percentile – in September (1.15K). The correlation coefficient between the measured and the forecasted air temperature at this level for the period April-September is 0.99. For all levels together for each month, as well for the entire period the correlation coefficients are 0.99 (2nd column in Table 1). Results the dew point temperature (3rd column in Table 1) show also a high correlation coefficient 0.96 (and 0.97 for April and August) between the determined by sounding measurements and by forecasted from ALADIN fields dew point temperature at all considered levels together. However, at the different levels the correlation is not so evident. At 850 hPa, for all months the correlation coefficient is 0.89, with lowest correlation in July (0.58) and highest in April (0.87). From Figure 2 it is visible that at this level, the median of the bias is between 1K (in May) and -0.3K (in September), with values very close to 0K for June, July and August. The highest value of the 90th percentile of the bias is in April (3.4K) and the lowest value of the 10th percentile – in August (-2.7K). The median of the bias of dew point temperature at 700 hPa is between 0K (April with correlation coefficient for the month R=0.72) and -1K (July, with R=0.55). In August (R=0.84) are the highest value of the 90th percentile of dew point temperature bias (6.5K) and the lowest value of the 10th percentile (-7.5K). At this level the correlation coefficient between the measured and the forecasted dew point temperatures for the whole period is relatively high 0.8, but in July for example it is 0.55. At 500 hPa the correlation coefficient between the measured and the forecasted dew point temperatures for the whole period is also 0.8, as at 700 hPa, with relatively higher correlations during the different months. However, at 500 hPa box and whiskers plot show highest values of the 90th percentile reaching 13K and lowest values of the 10th percentile -6k in June, where the correlation coefficient is R=0.7.

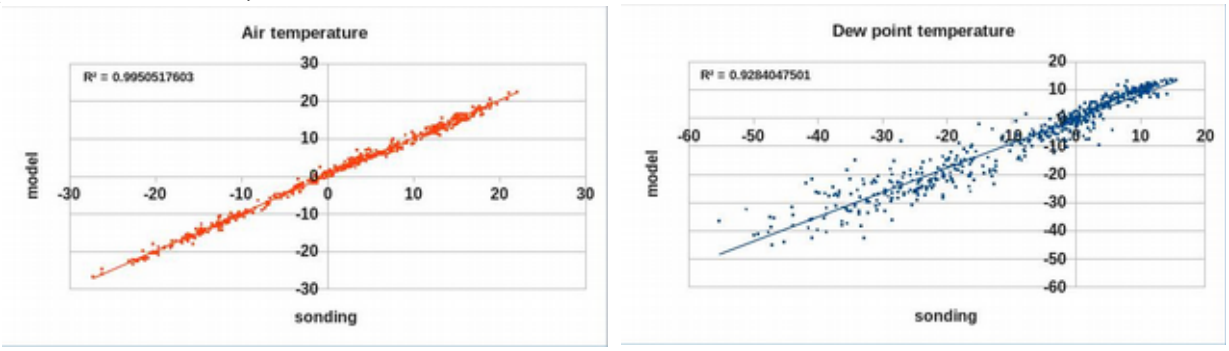

Figure 3. Scatterplots of sounding measured air and dew point temperatures at 850, 700, and 500 hPa as a function of the forecasted by ALADIN ones for the period April-September, 2014

From Figure 3 where scatterplots of measured and forecasted air and dew point temperatures are shown, we may generalize that air temperature is well forecasted, while dew point temperature seems to be overestimated, which would lead of a more humid forecasted environment in comparison to the measured one. However, it has to be stressed that accurate measurement of the relative humidity in height is one of the most difficult items in meteorology.

If we compare the instability indices evaluated in the present work obtained by sounding measurements with those obtained by the forecasted data for air and dew point temperature (Figure 4), for the case without and with lightning detected by ATDnet over the region of Sofia for the warm half part of 2014, one can see that for the K index especially, forecasted data (mod) give a better discrimination of the values of K for the cases with from those for the cases without thunderstorm. Values of K obtained from ALADIN output for the cases with detected lightning are higher (having a median of 34°C and 10the and 90th percentiles respectively 26°C and 37°C) than those obtained from sounding measurements (with a median of 36°C and 10th and 90th percentiles respectively 32°C and 41°C).

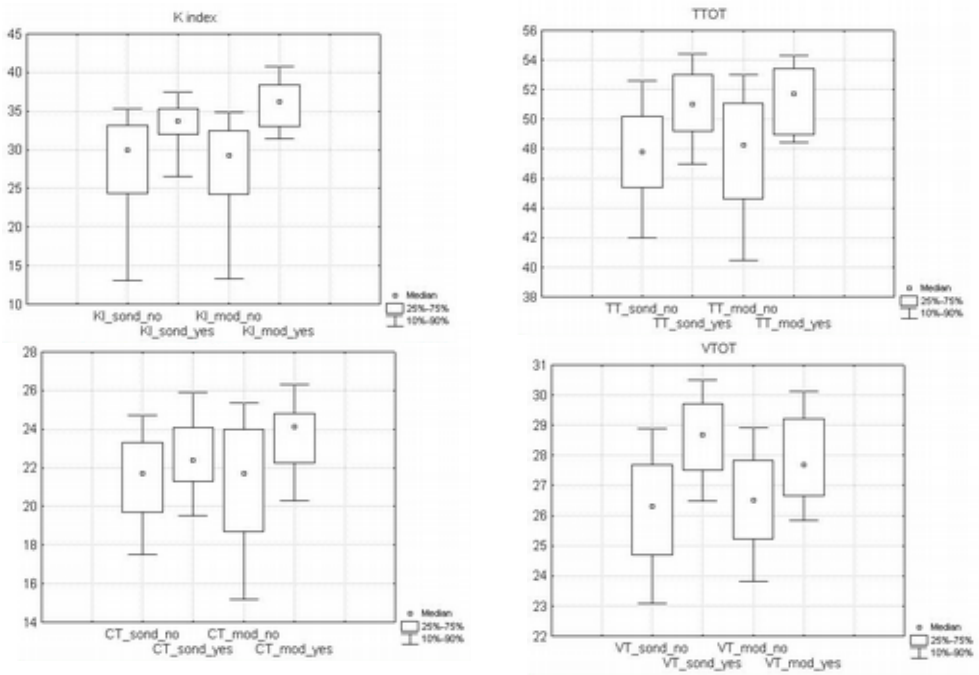

Figure 4. The instability indices obtained based on sounding measurements (sond) and on ALADIN output (mod) for the cases without (no) and with (yes) lightning activity over the region of Sofia according to ATDnet for the warm half-year of 2014.

For TTOT index, results are similar as with forecasted, as well with measured air and dew point temperatures. For the cases without any lightning detection over the considered region, values of TTOT determined based on measurements have a median of 47ºC and respectively 10th and 90th percentiles of 42ºC and 53ºC. The respective values for TTOT obtained based on ALADIN output are: median of 49ºC, 10th and 90th percentiles of 40.5ºC and 52.5ºC. For cases with detected by ATDnet lightning activity, the median of values of TTOT with measures data is 51ºC and with forecasted data – 51.5ºC. From the distributions of the values of CTOT and VTOT obtained with measured and forecasted temperatures for the cases without and with lightning it is visible that, values for VTOT (which takes into account air temperature at 850 hPa) obtained from sounding data are better discriminated than those obtained with model. It is the contrary for CTOT index (which takes into account dew point temperature at 850 hPa). This discrepancy with the results obtained for the different correlations between measured and forecasted air and dew point temperatures suggest the particularity of the different considered cases with or without detected lightning activity and their respective thermodynamic conditions, forecasted or measured.

Relationships between the forecasted instability indices and the respective data for lightning detected by ATDnet

Here will be shown some evaluations of the statistical distribution of K, CTOT, VTOT and TTOT indices for cases without and with detected by ATDnet lightning activity over 13 meteorological stations in Bulgaria given in Figure 5.

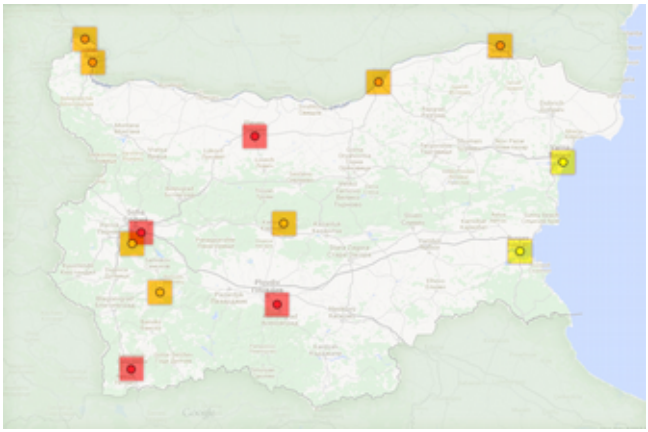

Figure 5. Location of the 13 meteorological stations considered in the present work (the squares indicate the regions of consideration for ALADIN data, as well for lightning activity data from ATDnet)

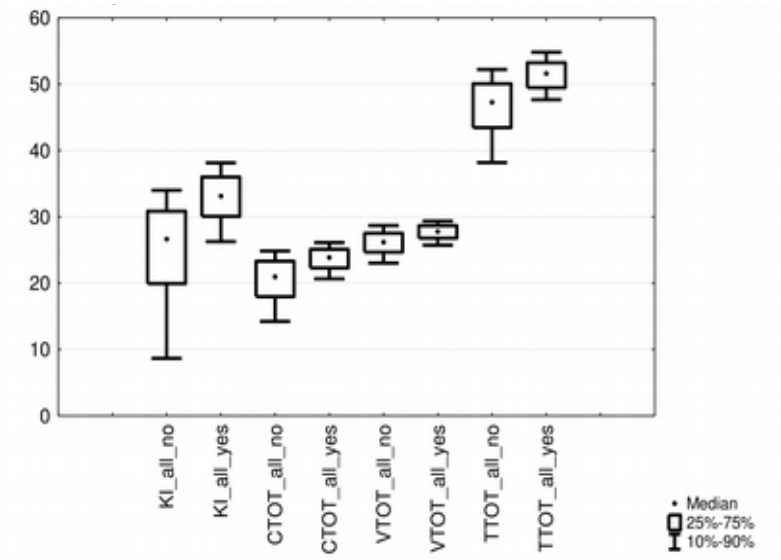

Figure 6. Box and whiskers plots of the obtained from ALADIN output instability indices for the cases without and with detected lightning activity over the regions of the considered meteorological stations for the period April-May 2014.

Figure 6 shows some parameters of the distributions of the obtained by ALADIN values of the considered here instability indices for the cases without (indicated with «no») and with (indicated with «yes») lightning activity according to ATDnet over the regions of the considered meteorological stations for the period April-September 2014. It is visible that for all considered indices there is a discrimination of their values for the cases with lightning activity from those without lightning. The f- and t-tests of the respective data samples showed that differences of the means for each considered index in the corresponding two groups (cases with and cases without lightning) are statistically significant. The median of the values of K index for the cases with lightning is 33.14, while this for cases without lightning is 26.66. However, about 50% of cases with and without lightning activity according to ATDnet have similar values of K index. Similar is the behaviour of TTOT index for cases with and without lightning (with respective medians of 51.62 and 47.29). TTOT is the sum of CTOT and VTOT, which indices values are similar for about 75% of cases with and without lightning.

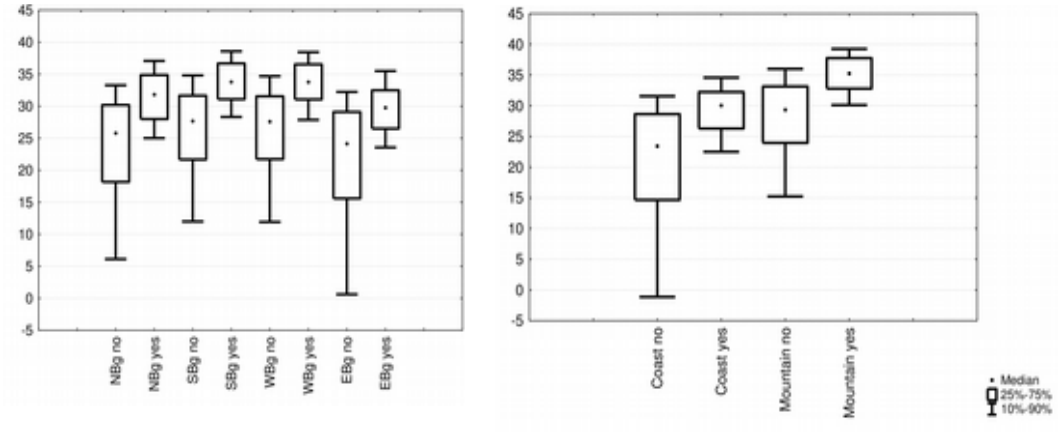

Figure 7. Box and whiskers plots of the obtained from ALADIN values of K index for the cases without and with detected lightning activity for the stations (left panel) in Northern, Southern, Western and Eastern part of Bulgaria and (right panel) in coastal and mountain regions for the period April-May 2014.

From the left panel of Figure 7 it is visible that the values of K index are slight higher in Southern part of Bulgaria in comparison with those in the Northern part. Even more pronounced is the difference in K index values over the Western part in comparison to the Eastern part of the country. Also, there is a large difference (right panel of Figure 7) between the obtained values of K over the coasts and over the mountains (where K are significantly higher). The values of the K index for cases with lightning over coasts are in the range of values of K index for cases without lightning over the mountains.

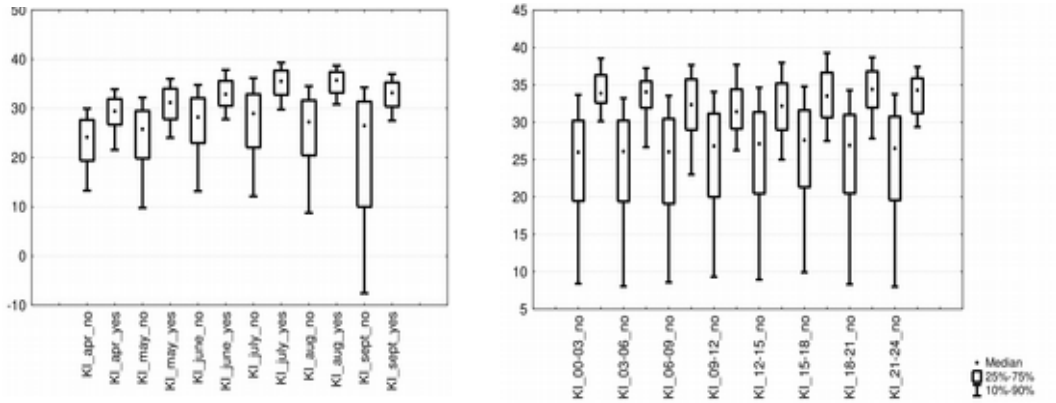

Figure 8. Monthly (left panel) and diurnal (right panel) distributions of the obtained from ALADIN values of K index for the cases without and with detected lightning activity over all considered stations the period April-May 2014.

Figure 8 shows that there is also a relatively well pronounced monthly and diurnal rate of the values of K index. The best discriminations of K values for cases with lightning from those without are in July and August (left panel). These are also the months with highest values of K index. Although, the better differentiations during nocturnal hours (right panel) is due to the significantly smaller number of cases with lightning in these hours, especially between 00 and 03 UTC, and between 03 and 06 UTC.

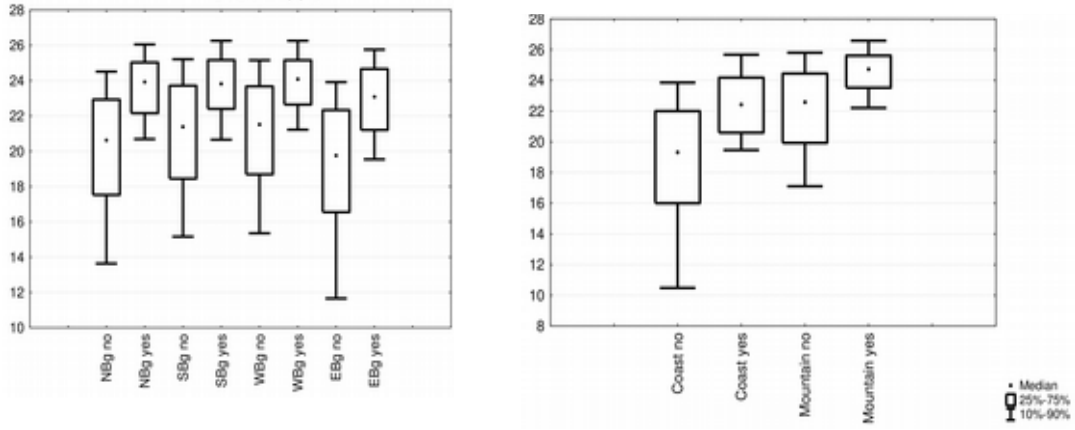

Figure 9. Box and whiskers plots of the obtained from ALADIN values of CTOT index for the cases without and with detected lightning activity for the stations (left panel) in Northern, Southern, Western and Eastern part of Bulgaria and (right panel) in coastal and mountain regions for the period April-May 2014.

Figure 9 (left panel) shows that the values of CTOT index are similar in Southern and in Northern parts of Bulgaria, but values of CTOT are lower in Eastern part in comparison to those over the Western part. Similarly to K index, there is a large difference (right panel of Figure 9) between the obtained values of CTOT over the coasts and over the mountains. The values of CTOT index for cases with lightning over coasts are in the range of values of CTOT index for cases without lightning over the mountains.

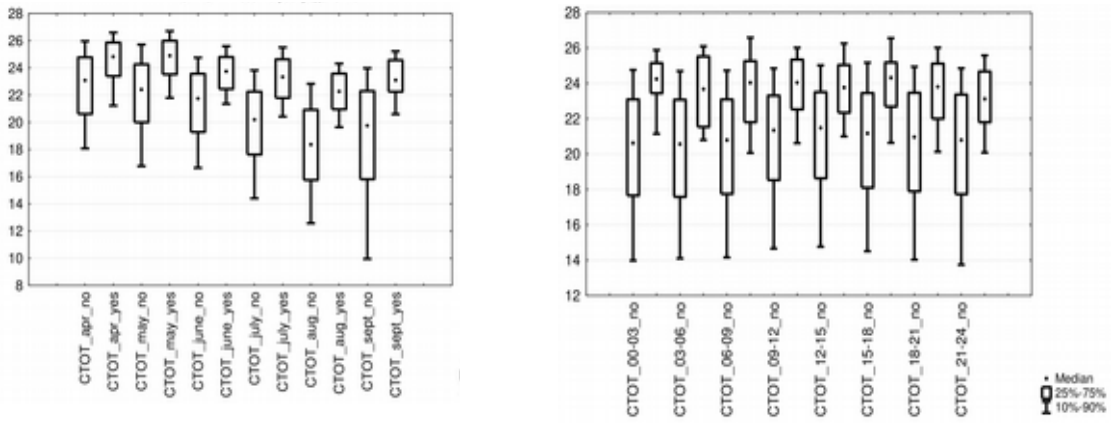

Figure 10. Monthly (left panel) and diurnal (right panel) distributions of the obtained from ALADIN values of CTOT index for the cases without and with detected lightning activity over all considered stations the period April-May 2014.

Figure 10 shows a relatively well pronounced monthly and not well pronounced diurnal rate of the values of CTOT index. The best discriminations of CTOT values for cases with lightning from those without are in August and September (left panel), while the highest values of CTOT are in April and May. Here again, the best differentiation between 00 and 03 UTC (right panel) is due to the significantly smaller number of cases with lightning in this time interval.

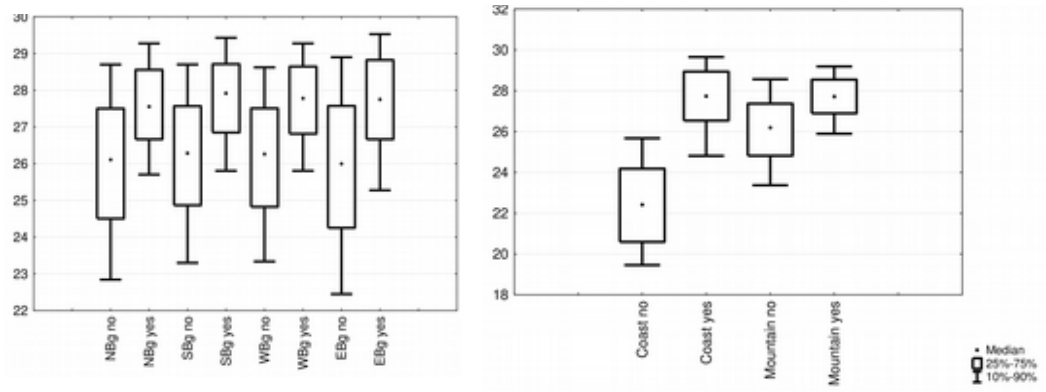

Figure 11. Box and whiskers plots of the obtained from ALADIN values of VTOT index for the cases without and with detected lightning activity for the stations (left panel) in Northern, Southern, Western and Stern part of Bulgaria and (right panel) in coastal and mountain regions for the period April-May 2014.

Figure 11 (left panel) shows that the values of VTOT index, unlike the previous considered instability induces, are similar in the different parts of Bulgaria. For the cases with lightning activity according to ATDnet the values of VTOT index are similar over coasts and over mountains. However, they are considerably different for cases without lightning activity over coastal and over mountainous regions. Additionally, based on these results, over coastal regions VTOT index seems to be a good predictor for lightning activity.

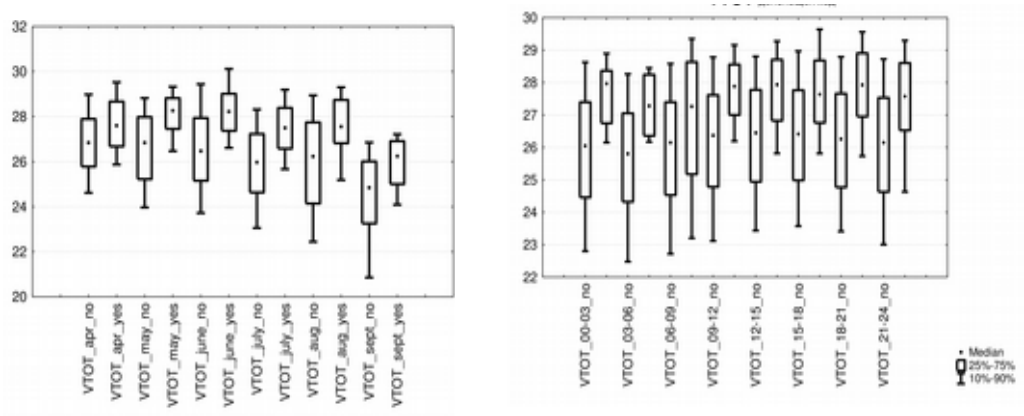

Figure 12. Monthly (left panel) and diurnal (right panel) distributions of the obtained from ALADIN values of VTOT index for the cases without and with detected lightning activity over all considered stations the period April-May 2014.

Figure 12 shows a relatively well pronounced monthly and diurnal rate of the values of VTOT index. The highest values of VTOT are in May and June (left panel).

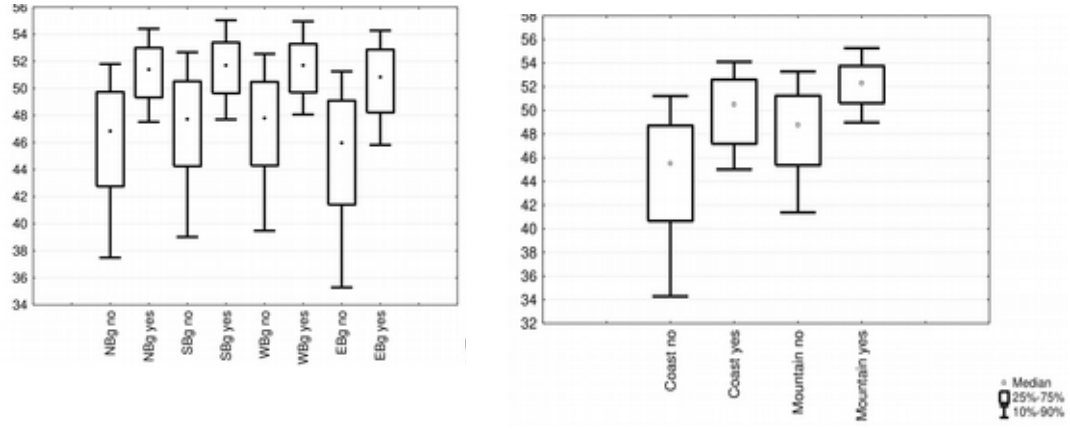

Figure 13. Box and whiskers plots of the obtained from ALADIN values of TTOT index for the cases without and with detected lightning activity for the stations (left panel) in Northern, Southern, Western and Stern part of Bulgaria and (right panel) in coastal and mountain regions for the period April-May 2014.

Figure 13 (left panel) shows that the values of TTOT index (similarly to CTOT index, see Fig. 9) are similar in Southern and in Northern parts of Bulgaria, but values of TTOT are slightly lower in Eastern part in comparison to those over the Western part. There is a slight difference (right panel of Figure 13) between the obtained values of TTOT over the coasts and over the mountains.

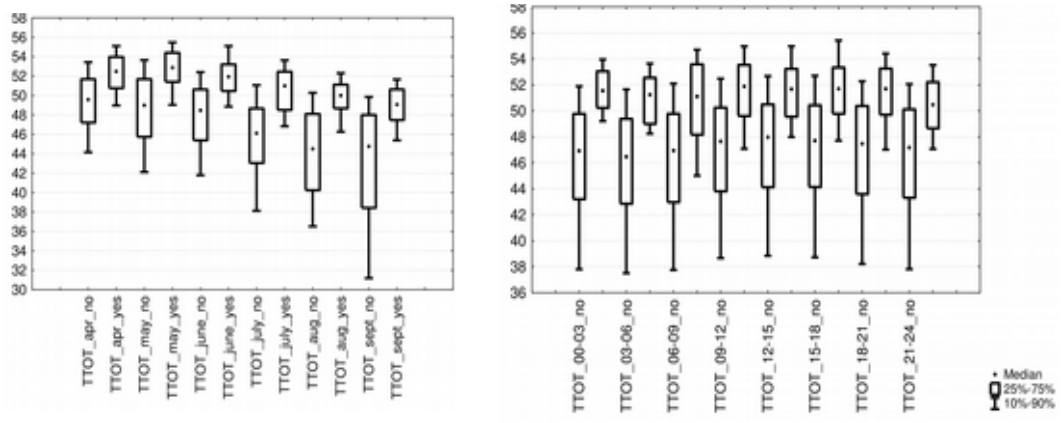

Figure 14. Monthly (left panel) and diurnal (right panel) distributions of the obtained from ALADIN values of TTOT index for the cases without and with detected lightning activity over all considered stations the period April-May 2014.

From Figure 14 the monthly and the diurnal rates of the values of TTOT index can be seen. The highest values of TTOT are in the first three months of the considered period.
From all considerations above it could be drawn that:
- all considered here instability indices obtained from ALADIN output discriminate relatively well with statistically significant differences in their means cases with from those without lightning activity according to ATDnet system;
- values of all indices vary towards the month and the region of the meteorological station;
- values of CTOT and TTOT indices are almost independent of the diurnal time interval, while VTOT and especially of K indices vary according to the time interval;
Our results showed that for 43% of cases with lightning activity the values of K index are between 30 and 35 — interval determined by George, 1960 as «scattered thunderstorms»; 33% of cases with lightning have values of K index above 35, determined as «numerous thunderstorm», and there is only

1% of cases with detected lightning and K index below 20, determined as «None probability for thunderstorm». Also, we obtained highest values of K index in August, which is similar to the results in Tsenova and Kolev, 2008 obtained for cases with observed lightning activity over Sofia based on sounding measurements for the period 1991-2000. Markova, 2013 based on data from meteorological stations in the Eastern Bulgaria for 340 cases of convective clouds (from the period between 2006-2009) and using data from GFS model obtained threshold value of K index of 29.5 for lightning initiation. For 75% of the considered here cases with lightning activity the value of K index was above 29.5. Our results for TTOT index show, that more than 70 % of cases with lightning have TTOT obtained based on ALADIN output greater than 48.5, threshold value determined from Markova, 2013 for lightning initiation.

Results show that none of the considered instability indices could used separately as a discriminator of cases with from those without lightning activity. Based on Tsenova and Bogatchev, 2012, a scheme for lightning probability evaluation is included in ALADIN-BG postprocessing in the National Institute of Meteorology and Hydrology, which is based on different combinations of threshold values of some instability indices, including among others the considered here. The obtained here results show that for a better forecast of lightning activity probability the monthly and the regional distributions of the different instability indices should be taken into consideration.

3 Conclusions

In the present work atmospheric instability indices, based on ALADIN – BG forecast are evaluated versus data for lightning activity from ATDnet system. The comparison between the measured by radiosonde and forecasted thermodynamical characteristics of the atmosphere (needed for the determination of the instability indices) over Sofia for the warm half year of 2014 showed a good performance of the model, with high correlation coefficients between the measured and the forecasted air and dew point temperatures at the main isobaric levels. Results showed that all considered here instability indices discriminate relatively well with statistically significant differences in their means cases with lightning activity from those without according to ATDnet data. Values of the considered instability indices vary with months, day time period and location. It was concluded that for a better forecast of lightning activity probability the monthly and the regional distributions of the different instability indices should be taken into consideration.

4 References

1. Boyden, C, 1963, A simple instability index for use as synoptic parameter, Meteorol. Mag., 92, 198-210

2. Gaffard, C., Nash, J., Atkinson, N., Bennett, A., Callaghan, G., Hibbett, E., Taylor, P.,Turp,M.,and Schulz, W., 2008, Observing lightning around the globe from the surface,in: the Preprints, 20th International Lightning Detection Conference, Tucson, Arizona, 21–23
George, J., 1960, Weather Forecasting for Aeronautics, Academic Press, New York

3. Jefferson, G., 1963, A further development of the stability index, Meteorol. Mag., 92, 313-316

4. Litynska Z., Parfiniewicz, J., and Pinkowski, H. 1976. The prediction of air mass thunderstorms and hails, W.M.O., No. 450, 128–130

5. Markova, B., 2013, The impact of the environmental conditions on thundercloud formation over Weastern Bulgaria, PhD thesis

6. Miller, R., 1967, Notes on analysis and severe storm forecasting procedures of the Military Weather Warning Center, Report: Technical Report 200, AWS, USAF: Scott AFB, IL

7. Peppler, 1988; A., A review of static stability indices and related thermodynamic parameters, Illinois State Water Survey Misc. Publ. 104, (Illinois State Water Survey, 2204

Griffith Drive, Champaign, IL 61820), 87 pp.
8. Peppler and Lamb, 1989, Tropospheric static stability and central North American growing season rainfall, Mon. Wea. Rev.,117, 1156–1180
9. Showalter, 1953, A stability index for thunderstorm forecasting, Bull. Amer. Meteorol. Soc., 34, 250–252
10. Tsenova, B and S. Kolev, 2008, Climatical study of the relationships between thunderstorms lightning activity and the environmental conditions over western Bulgaria, Preprints: 15th International Conference of Clouds and Precipitation, Cancun-Mexico, July 7-13
11. Tsenova, B. and A. Bogatchev, 2012, Evaluation of instability indices computed using ALADIN-BG output and their relationship with the thunderstrom activity over Bulgaria, Preprints: 15th International Conference of Clouds and Precipitation, Leipzig, Germany

Operational forecast and research in Croatia in 2015

Martina Tudor, Antonio Stanešić, Stjepan Ivatek-Šahdan, Alica Bajić, Mario Hrastinski, Tomislav Kovačić, Kristian Horvath and Iris Odak Plenković

The operational model version used is AL38T1 with ALARO0 physics for 8 and 4 km forecasts, AL29mxl for 2 km dynamical adaptation and AL36T1bf08 for 2 km NH run.. Operational forecast run for:

- 8 km resolution, 4 times per day, 3D var and surface OI, 6 h cycling, to 72 hours, coupled to IFS, 37 levels.
- 4 km resolution, 00 UTC up to 72 hours, surface OI, 6h cycling, coupled to IFS, 73 levels, to do: 3D var.
- 2 km dynamical adaptation, hourly, up to 72 hours,
- 2 km non-hydrostatic, 06 UTC up to 24 hours.

1 INTRODUCTION

1.1 Background surface fields

The “clim” files contain “climatological” background. The 12 monthly files per domain can be produced in Meteo France by running the configuration (e)923, the procedure requires the input databases. There are some features in the fields of climate files that are unrealistic and rather different from nature.

The usage of SURFEX PGD allows using new topography from the new database. Using the topography and land sea mask from the new file is invoked by setting LNORO=T in the namelist NAMCLA, and for new land sea mask (LNLSM=T). If PGD topography is imported (LIPGD=T), envelope is added to the topography.

Consequently, clim files are created as a combination from several databases. Land-sea mask and height of topography are taken from one database, but proportion of land, standard deviation of orography, roughness length and other parameters describing topography are taken from another database.

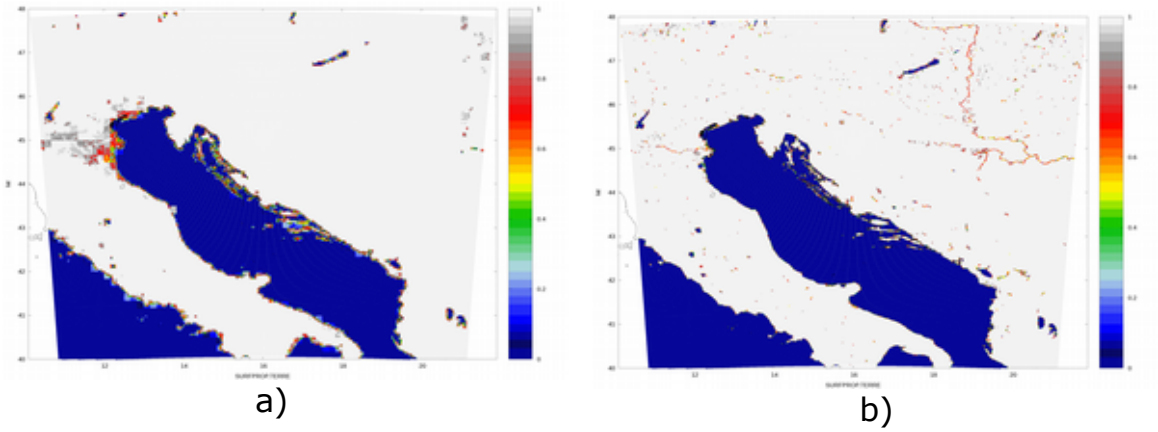

Fig. 1: Proportion of land after the Step1 (a) and computed from the SURFEX PGD file (b). These figures show data for 2 km resolution domain.

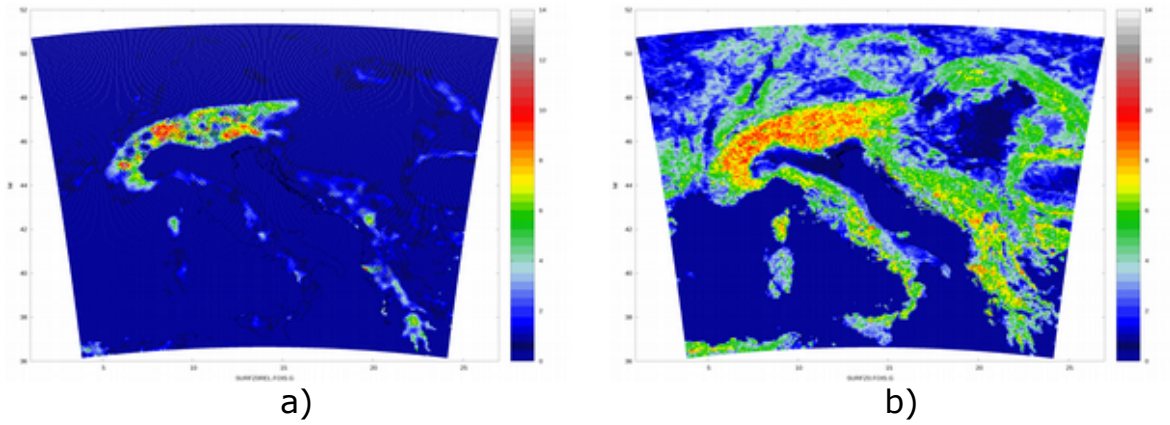

Fig. 2: Surface roughness length (a) and corrected field (b) in 8 km resolution (the values in the figures were divided by 9.81).

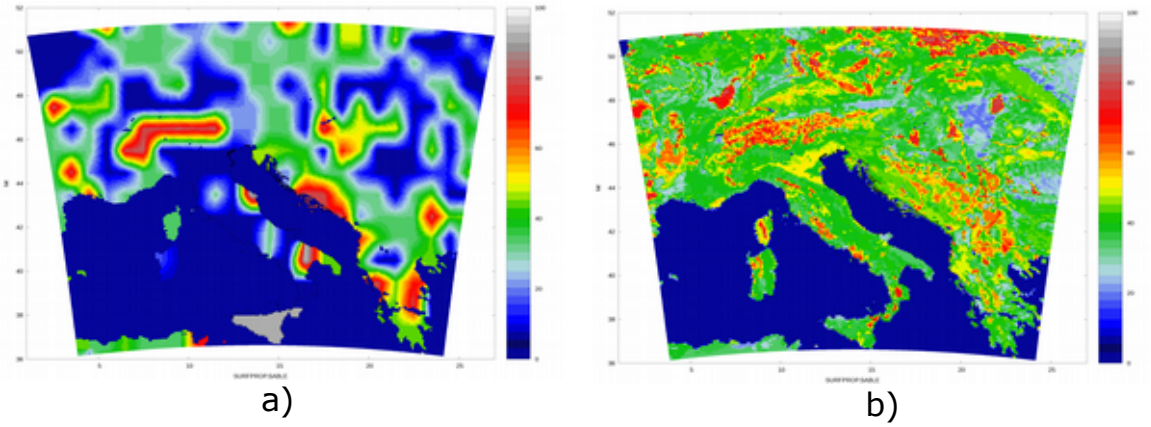

Fig. 3: Proportion of sand in the clim file (a) and after the correction using data from the SURFEX PGD file (b).

1.2 SST in the coupling files from ARPEGE and IFS

Sea surface temperature (SST) influences the model forecast of land/sea breeze and the intensity of precipitation downstream. SST is taken from initial file and remains constant during the model forecast, currently there is no local assimilation of SST.

There are two sets of SST fields provided in the coupling files, from operational forecasts of IFS and ARPEGE.

Here we compare the SST from the coupling files with the values measured on stations. Several of these unnatural features in SST have been fixed. However, there are still large discrepancies in measured and model SST in certain regions, especially in autumn and winter along western Adriatic coastline.

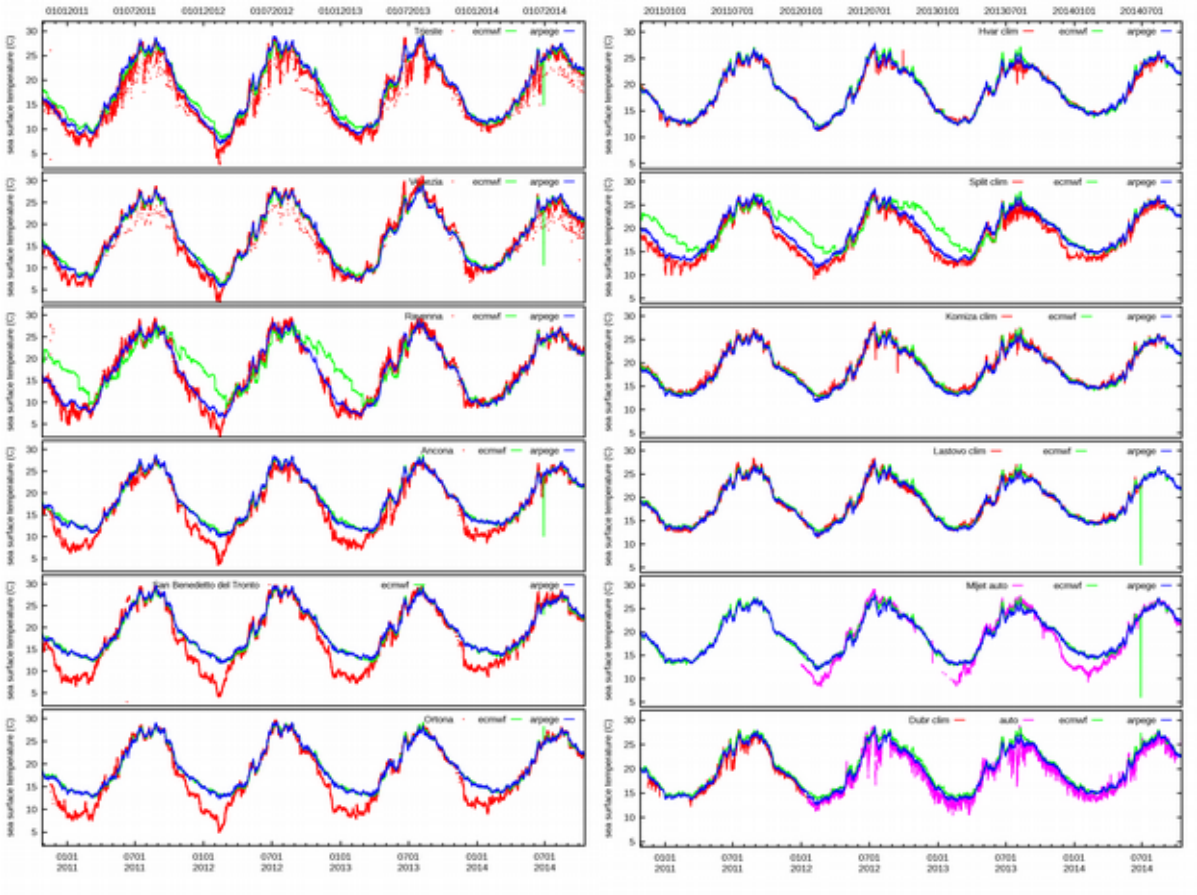

Fig. 4: SST measured on stations (red), and from the nearest sea point in ARPEGE (blue) and ECMWF (green) coupling files for stations in Italy (left) and Croatia (right) on Adriatic Sea for the period from 27th October 2010 to 16th October 2014.

2 Case with severe torrential rain and flash floods

In the middle of May 2014, severe torrential rain over mountains and the valley in the South-eastern Europe triggered flash floods, landslides and record levels of rivers (Bosnia and Herzegovina, Serbia and Croatia). The prognostic convection scheme yields less precipitation than the diagnostic one in 8 km but more in 2km resolution.

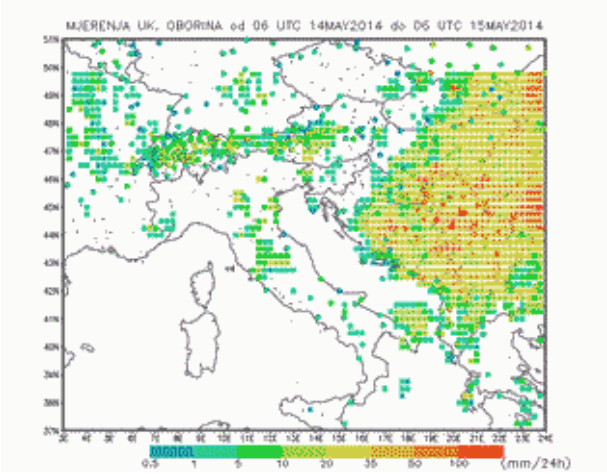

Fig. 5: Measured accumulated 24 hourly precipitation from TRMM estimates using satellite data 3B42RT (squares, no data north of 50N), and rain gauges (circles).

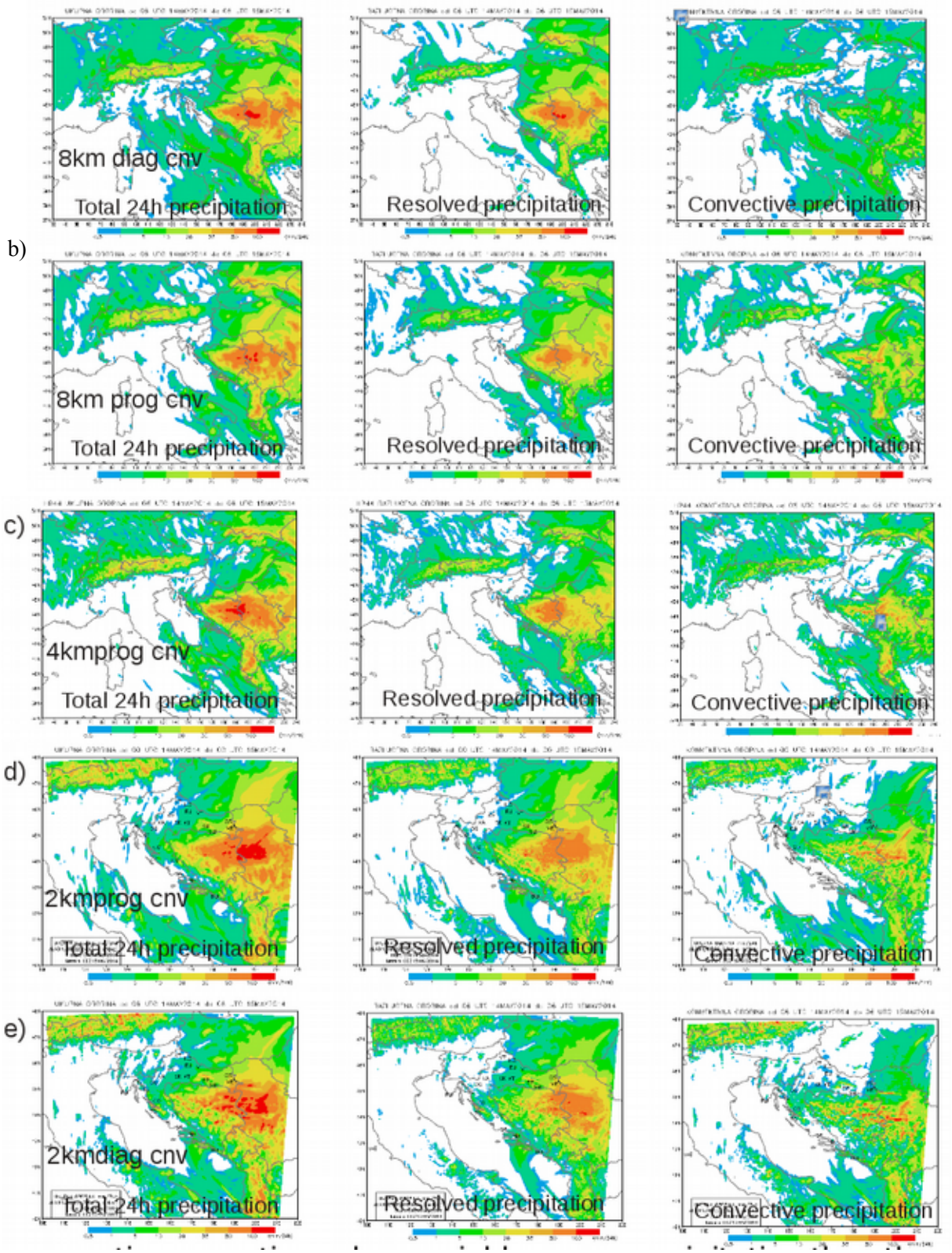

Fig. 6: Forecast using diagnostic (a) and prognostic convection in 8 km (b), 4km (c) and diagnostic (d) and prognostic convection in 2km (e) resolution of the accumulated 24 hourly precipitation (total in the left column, resolved in the middle column and convective in the right column) for the case with severe flash floods in Bosnia and Herzegovina, Serbia and Croatia, that occurred on 15th May 2015.

The absence of convective precipitation (and clouds) from the model forecast is often interpreted as the absence of convection. This issue gets worse with increasing of the resolution. Parametrization of deep convection computes precipitation that is added to the resolved precipitation and plotted on a map as total precipitation and later validated against (in situ) measurements. But, it should be taken as subgrid variability in precipitation added to the resolved precipitation.

Fig. 7: Usual interpretation of convective (unresolved) precipitation (left) and two alternatives (centre and right) depending on the convective mesh fraction.

3 ALADIN and IFS as background for NWC SAF

Numerical model information is mandatory for moisture and orographic corrections. Convective rainfall rate (CRR) product computed from MSG SEVIRI satellite data underestimates intensive precipitation and overestimates frequency of events with weak rain (compared to in situ measurements). When ALADIN is used as background, values are closer to the real ones than product that uses ECMWF fields as background.

a) b)

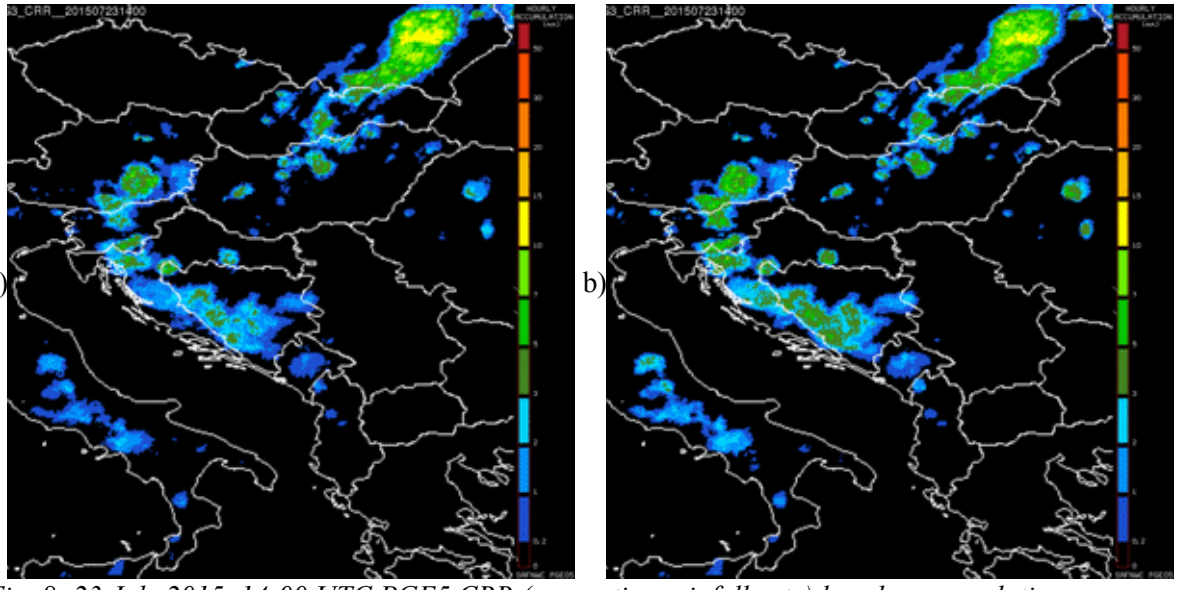

Fig. 8: 23 July 2015, 14:00 UTC PGE5 CRR (convective rainfall rate) hourly accumulation using IFS (a) and ALADIN/HR (b) fields as background.

http://www.nwcsaf.org/HTMLContributions/SUM/SAF-NWC-CDOP2-INM-SCI-ATBD-05_v4.0.pdf.

4 When is 2 km NH forecast better?

Severe bura events in Makarska can be missed by dynamical adaptation but correctly predicted by non-hydrostatic forecast using the full physics package.

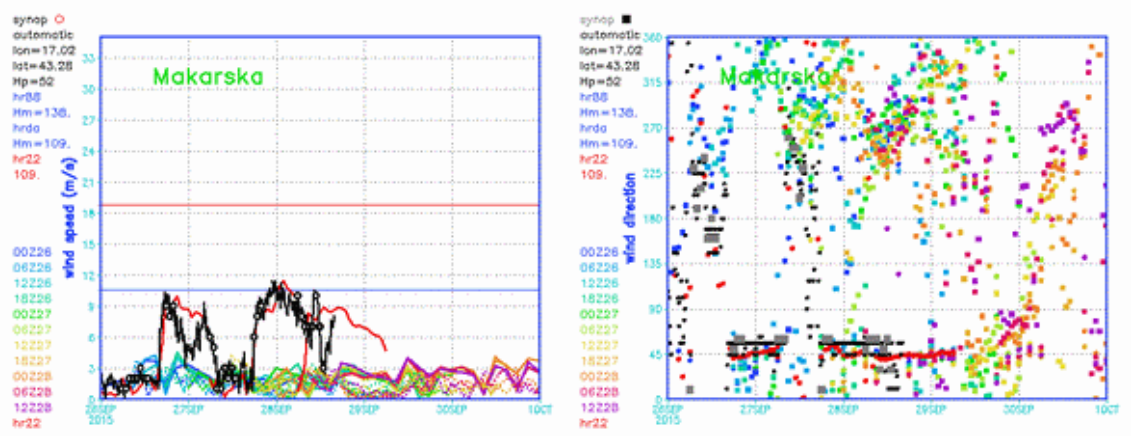

Fig. 9: Measurements (black) 8 km forecasts (full lines) 2 km DADA (dashed) and 2 km NH (red).

ALARO-1 and BLENDVAR Data Assimilation

Radmila Brožková, on behalf of the CHMI NWP Department

1 Introduction

In 2015 there were two major changes in the operational configuration of the ALADIN model in CHMI. By the end of January a new model physics version has been introduced in the operations, denoted as ALARO-1 version A. The second substantial improvement of the operational system has taken place in August - the introduction of an original data assimilation algorithm called BLENDVAR for preparing forecast initial conditions.

2 ALARO-1 version A

Turbulence scheme TOUCANS

New parameterization scheme of turbulence called TOUCANS (Third Order moments Unified Condensation and N-dependent Solver) follows recent evolutions in the theory of turbulence. Stability functions, valid for all ranges of Richardson numbers without a need to deploy a critical value, make the backbone of the scheme. Novelties are the use of prognostic turbulent kinetic energy together with prognostic moist total turbulent energy, parameterization of third order moments and turbulent diffusion of cloud water. Improved description of boundary layer processes is for example demonstrated by better scores of screen level temperature shown on Fig. 1, where both bias and root mean square errors are statistically significantly reduced. Boundary layer cloudiness forecast get also improved, as shown on Fig. 2.

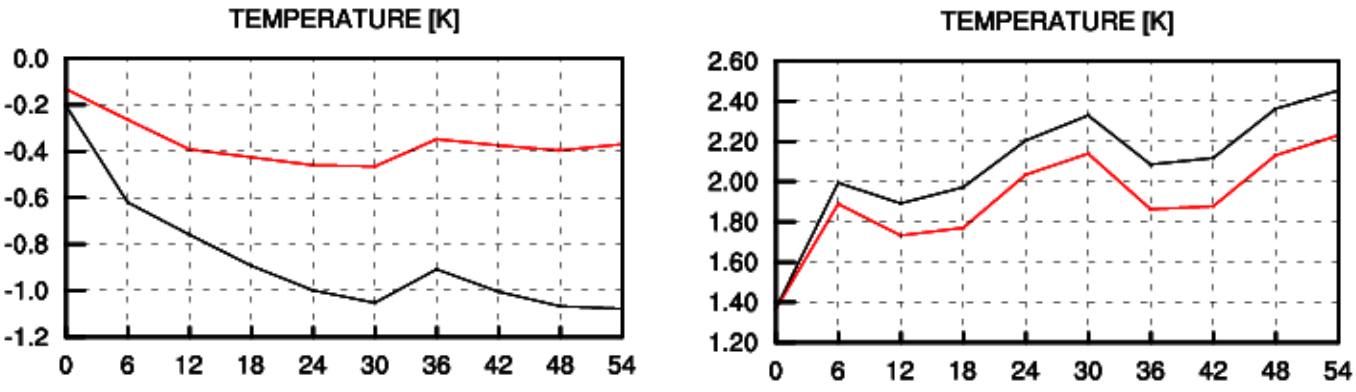

Figure 1: Bias (left panel) and root mean square error (right panel) of the 2m temperature forecast by the previous version of the ALADIN model (black line) and by the new version (red line). Forecast length in hours is plotted on the horizontal axis. The verification period runs from 3.1.2015 to 23.1.2015 for the area of Central Europe.

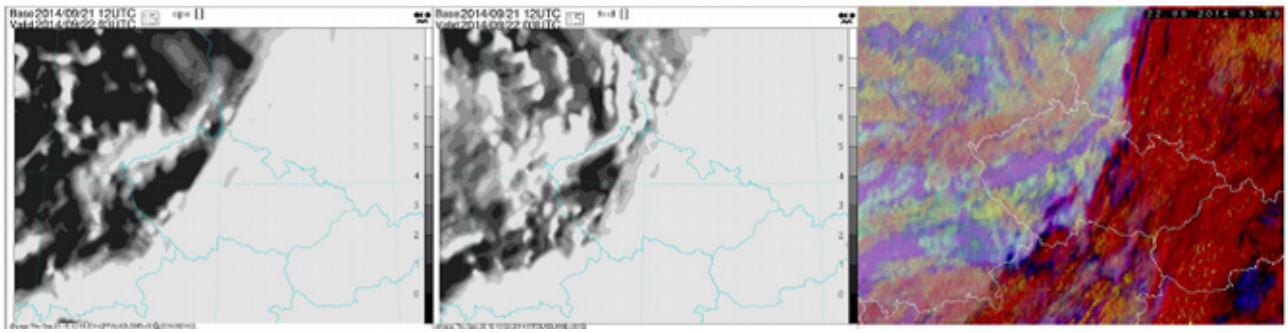

Figure 2: Cloud scene behind the severe cold front. Total cloudiness forecast by the reference model version (left) and by the ALARO-1 model version (right). Right: verifying satellite picture, where thick clouds are red, medium and low clouds are ochre, lowest clouds are green and terrain is rose . Forecast base is 21 September 2014 at 12h UTC, validation time is 22 September 2014 at 03h UTC.

Radiation scheme ACRANEB 2

The parameterization of radiative transfer underwent an important change as well. The scheme is a broadband one with one thermal and one solar spectral interval. This choice allows a relatively cheap computation of the radiation and cloudiness interaction at every time-step of the model, which is an important property when going to higher resolutions. Gaseous radiative transfer functions were substantially reviewed, including an original solution for the absorption saturation problem. Recent reference data were used to fit the coefficients of the cloud optical properties. The cost effectiveness of the scheme is greatly improved by introducing the intermittent computations, where radiative transfer terms evolving in order of hours are not computed at every model time-step in contrast to the above mentioned interaction with cloudiness. Verification of the solar radiation flux is shown on Fig. 3 at the Kuchařovice station for the case of 20. 3. 2015, where the scheme accounted for the solar eclipse. In addition to the introduction of these two completely new schemes, microphysics of clouds and precipitation has also been updated. Rain drop distribution is improved especially for small sizes of drops. There is a higher number of small raindrops which by consequence evaporate more easily; thus the problem of forecasting excessive drizzle is reduced. The parameterization of vertical overlaps for clouds and falling precipitation is also improved moving the model cloud scene closer to reality compared to the assumption of the maximum overlap for adjacent levels.

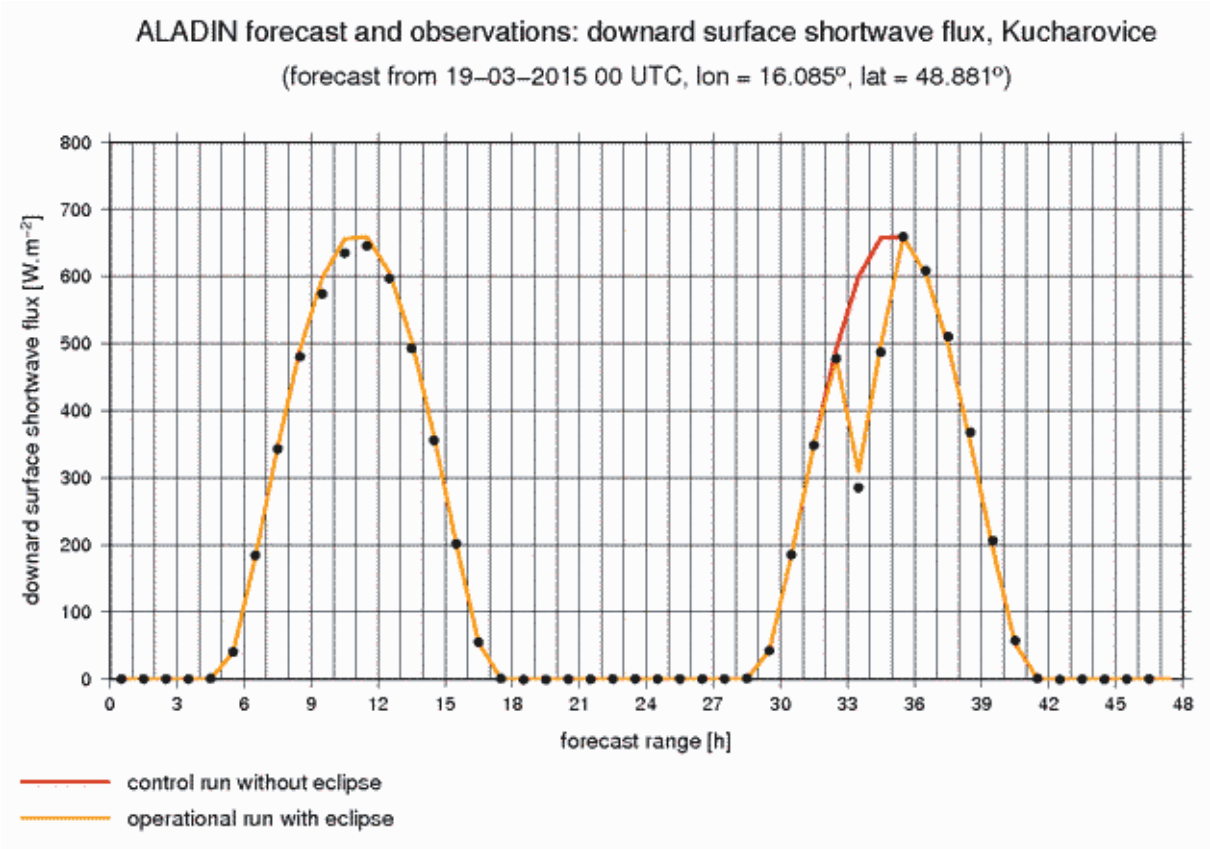

Figure 3: Comparison of the solar flux forecast by the model ALADIN with the observations at the Kuchařovice station, the forecast base is on 19. 3. 2015 at 0h UTC, capturing the case of the solar eclipse on 20. 3. 2015

3 BLENDVAR

The algorithm exploits the method to combine large scale analysis of the global model with fine scales of the ALADIN model first guess, known as the Digital Filter Blending, completed by a 3DVAR analysis at high resolution. The assimilation cycle build on BLENDVAR has been tuned using the diagnostics of first guess and analysis departures from observations. At high resolution the system assimilates, observations from surface stations, radio-sounding stations, satellite wind observations, MSG SEVIRI observations and aircraft AMDAR observations. Beside the improvement of the objective forecast scores thanks to a better quality of the initial conditions, the new scheme has also been tested for the June 2013 flood case. It showed improved precipitation forecast regarding both the amounts and spatial location, as demonstrated by the Fraction Skill Score on Fig. 4 and cumulated precipitation (Fig. 5) .

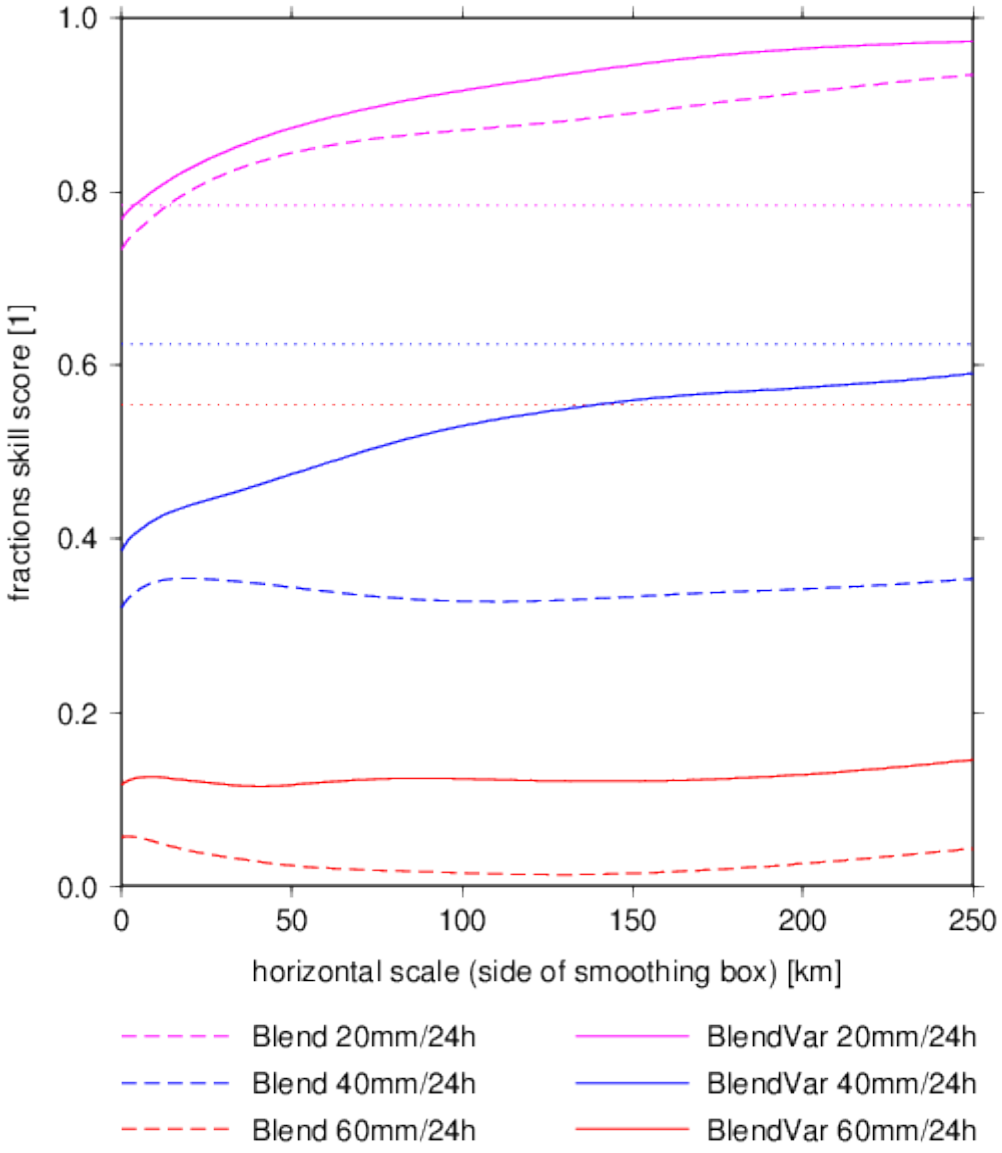

Figure 4: Fraction skill score of precipitation amounts for the 20, 40 and 60 mm/24 hours thresholds of the ALADIN model forecast from 06:00 UTC 1 June 2013. FSSuniform is denoted by horizontal dotted lines with colour corresponding to the thresholds. Reference is denoted by Blend.

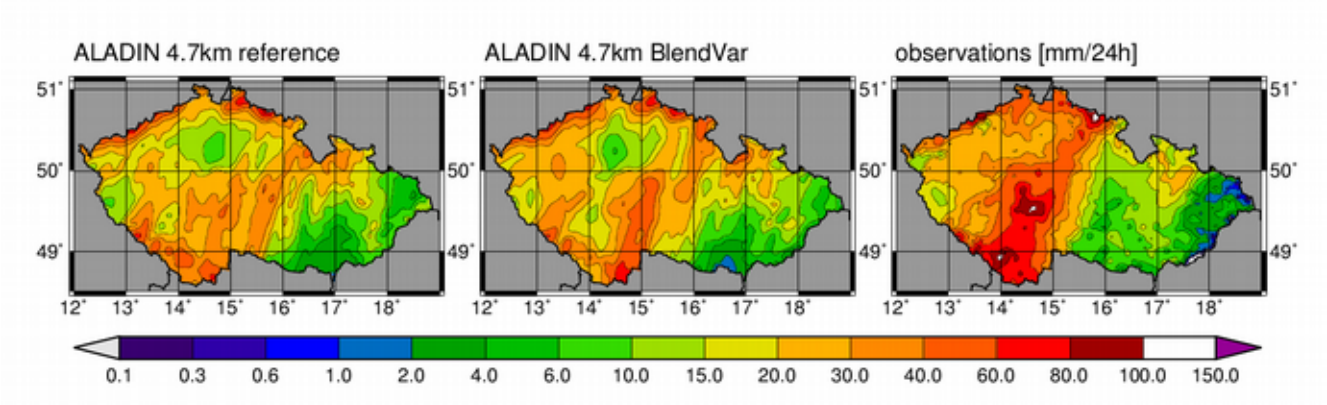

Figure 5: 24-hour precipitation amount predicted by the ALADIN model and a verifying observation. Reference setup is denoted in the left column and BLENDVAR configuration is in the middle.

4 Outlook

The two above mentioned enhancements of the operational system are investments on which ensuing developments are going to capitalize. To mention some of them, there are a new shallow convection scheme, unification of cloudiness, prognostic mixing length in preparation on the side of turbulence, while in data assimilation the effort is concentrated now on the assimilation of MODE-S aircraft data (both EHS and MRAR types).

Radar assimilation at higher density in the operational AROME model at 1.3 km horizontal resolution

Eric WATTRELOT

1 Introduction

This paper presents results from radar data assimilation experiments which have been purposed to increase the density of the assimilated radar observations in the AROME assimilation system (nonhydrostatic limited-area model Application of Research to Operations at Mesoscale).
Radial velocities from the Doppler radars of the "Application Radar la Météorologie InfraSynoptique" (ARAMIS) French radar network have directly been assimilated in the 3D-Var AROME system since 2009 (Montmerle and Faccani, 2009). Reflectivity data have been introduced in the assimilation system in 2010, but their assimilation is done in two steps: first, a vertical inversion of the reflectivity profiles to retrieve relative humidity pseudo-observations and in a second time the introduction of these retrieved columns of humidity in the 3D-Var algorithm. The methodology needs a detailed observation operator to convert the model control variables and other prognostic fields as those related to precipitating hydrometeors into a model equivalent radar measurement of reflectivity at observation location. This two-step methodology and in particular the 1D Bayesian inversion avoids the difficulties to treat nonlinear moist processes involved in the definition of the observation operator, and the retrievals then assimilated in the 3D-Var allow to benefit from the multivariate analysis scheme (Wattrelot et al., 2014).
The AROME assimilation system has been recently updated (on the 13th April 2015): it currently mainly consists in a 1-hour assimilation cycle instead of 3-hour before, and an increase both horizontal resolution (from 2.5 to 1.3 km) and vertical resolution (from 60 levels to 90 levels with a large increase in the boundary layer). The higher resolution of this new AROME configuration should allow to assimilate radar data at higher density, in particular because the part of the observation error due to the representativeness errors should decrease.
Results are shown from preliminary experiments in the AROME with a 2.5 km mesh (Section 2). Section 3 provides a detailed description of the high-resolution model (Section 3.1) and results of experiments with a 3-hour assimilation cycle (Section 3.2) and a 1-hour cycle, with the help of a posteriori diagnostics (Section 3.3). An illustration on a case study of the positive impact of the latest configuration with high-density of radar data is shown in Section 4. Finally, results are summarized and discussed in Section 5.

2 Preliminary experiments in the AROME at 2.5 km horizontal resolution

Using the operational 3-hour cycle assimilation AROME system with 2.5 km horizontal resolution, different experiments have been performed. In this operational AROME model, radar data are thinned every 15 km because observation-error correlations are not accounted for in the 3D-Var assimilation). Before testing a higher density radar assimilation in the higher resolution of the model, the behaviour of the assessment of a higher density radar assimilation is evaluated at 2.5 km of model resolution.
Previous tests to increase the radar density (up to 15 km of horizontal thinning) had been carried out with one of the first operational version of AROME system which were operationally running in 2009 (used with a 2.5-km mesh covering a France domain vertically divided in 41 layers from 17 m above the ground up to 1hPa and coupled to the ALADIN model). These experiments led to a clear degradation of forecasts scores (Wattrelot et al. 2014). New experiments using different thinning are performed and evaluated in the operational AROME system running in 2011, with a larger computational domain, a direct coupling with the global model ARPEGE with a 10 km resolution over western Europe, background error covariances deduced from an ensemble data-assimilation technique

(Brousseau et al. 2011), an increased number of vertical levels to 60, and radiances from the Infrared Atmospheric Sounding Interferometer (IASI) at 80-km thinning etc. :

1. thinning of radar reflectivities and radial winds at 15 km as in the operational e-suite of AROME (OPER_AROME25)
2. thinning of radar data at 8 km (RAD8_AROME25)
3. thinning of radar data at 4 km and at 30 km (not shown)

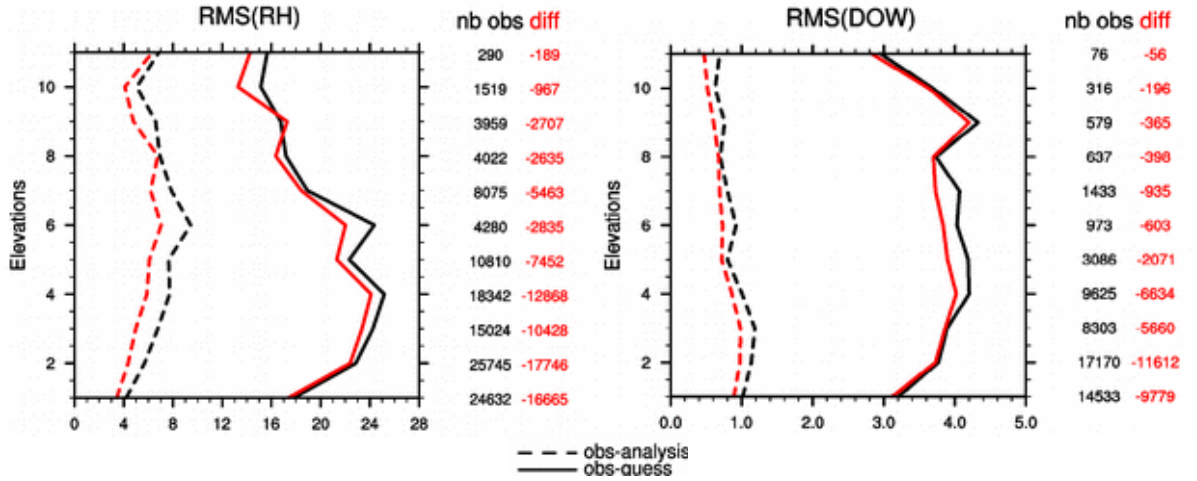

Figure 1: Root-Mean-Square of observation minus guess (full line) and of observation minus analysis (dashed line) for relative humidity (left) in % (X-axis) and radial wind (right) in m/s (X-axis), for each elevation (Y-axis). Results are shown for experiments with 3-hour cycled assimilation between 25 October 2011 and 31 October 2011: the red line is for the reference OPER_AROME25 and black line is for the experiment RAD8_AROME25 .

The experiment RAD8_AROME25 shows a systematic growing of the fit of both the analysis and the guess to the radar observations of relative humidity retrievals and radial winds by comparison at the OPER_AROME25 reference. It is illustrated here once the first days of the experiment (Figure 1). It seems to be a degradation of the assimilation system, even it is always difficult to compare analyses and model forecasts against different sampling of assimilated observations. The same behaviour is observed (Figure 2) against conventional observations (as radiosounding data) or Aircraft observations (Airep). After three weeks of runs, the classic scores and in particular precipitating scores have shown a clear degradation of the assimilation system (not shown).

3 Higher density radar assimilation in AROME at 1.3 km horizontal resolution

3.1 Experimental set-up

In order to prepare the first version of the higher resolution AROME-France assimilation system, a lot of tests have been performed. The first set of experiments run on summer 2013. The used version of AROME model consists of a larger AROME domain (38°-53°N, 8°W – 12°E, Figure 3) and model forecasts at a higher resolution with a 1.3 km mesh instead of 2.5 km before. This configuration has more vertical levels (90 against 60 before) which allow to increase the vertical resolution in particular in the boundary layer as shown in Figure 3. This first stable version exists through both the work of Yann Seity (which has made choices on the vertical discretisation and on different options on Physics and dynamics to allow a reasonable cost on the new parallel supercomputer BULL), and the work of Pierre Brousseau which has done a new B-matrix of background-error covariances (built with an ensemble of AROME forecasts from the ARPEGE forecasts ensemble AEARP) adapted at the new 1.3 km horizontal resolution.

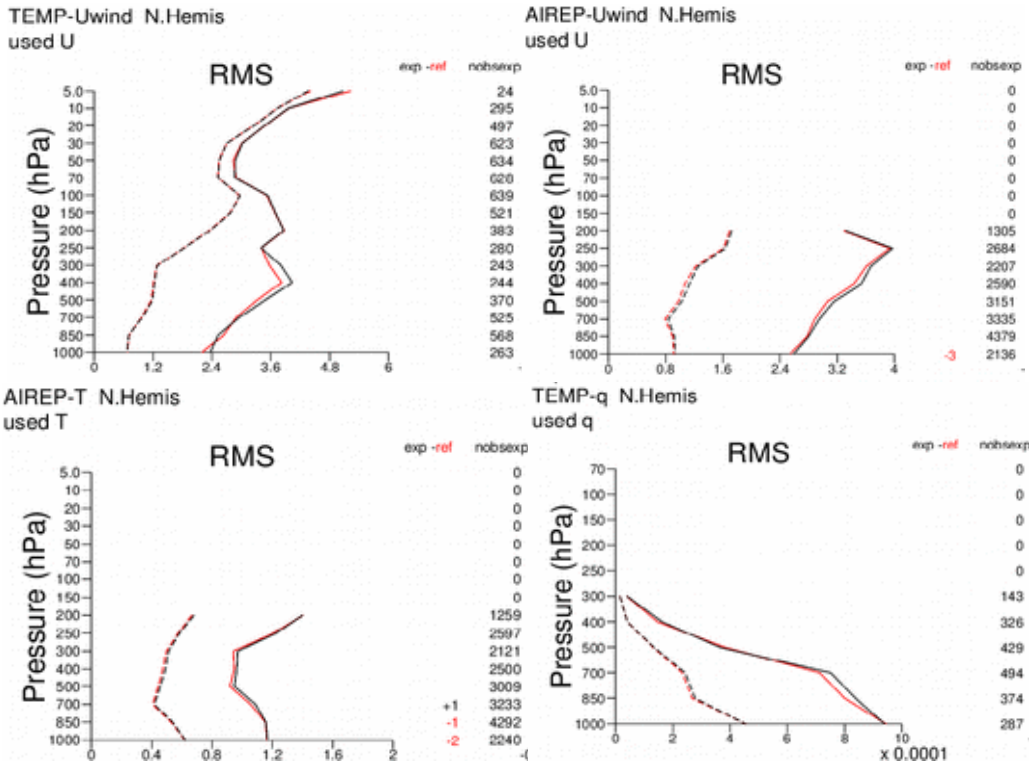

Figure 2: Root-Mean-Square of observation minus guess (full line) and of observation minus analysis (dashed line) for relative humidity (left) in % (X-axis) and radial wind (right) in m/s (X-axis), for each elevation (Y-axis). Results are shown for experiments with 3-hour cycled assimilation between 25 October 2011 and 31 October 2011: the red line is for OPER_AROME25 and black line is for RAD8_AROME25.

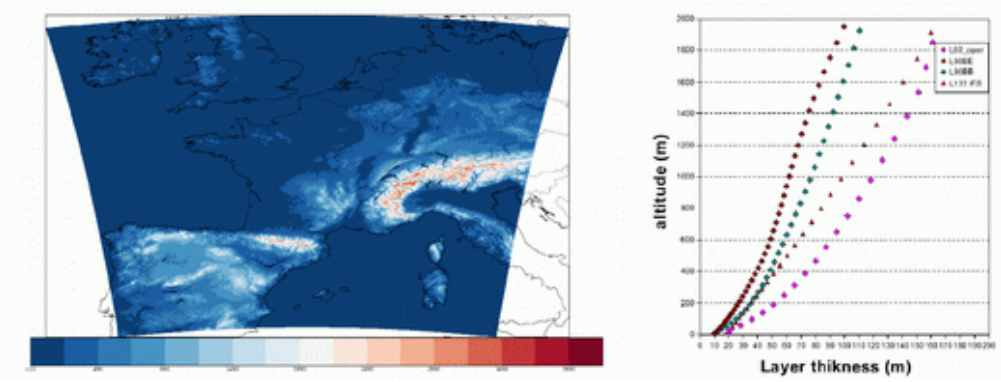

Figure 3: New AROME domain (left) for the higher resolution model (1.3 km) and the increase of the vertical resolution with 33 levels in the boundary layer below 2000 m altitude of height instead of 21 and the lowest level at 5 m instead 10 m (right, in blue diamond-shaped) .

Two kinds of experiments for reference have been used to test the higher radar density:

- the first set of experiments in test over Summer 2013 time run with a 3-hour assimilation cycle (Section 3.2).
- a second set of experiments refers to the hourly-assimilation system in preparation to the version of AROME which became operational at Météo-France on the 13th April 2015 (Brousseau et al. 2016). This set of experiments has been running for Summer time and Autumn time in 2014 (Section 3.3).

Table 1: Definition of the experiments

Experiments	AROME 1,3 km horizontal resolution						
	3 hour assimilation cycle				1 hour assimilation cycle		
	Thinning of 15 km for radar data	Thinning of 8 km for radar data	No cycled (guess from CY3H_REF)	No cycled (guess from HDRAD_CY3H)	Thinning of 15 km for radar data	Thinning of 8 km for radar data	Tuning (observation error, revision of the main parameters of the 1D Bayesian inversion)
CY3H_REF	X						
HDRAD_CY3H		X					
HDRAD_CY3H_NOC		X	X				
LDRAD_CY3H_NOC	X			X			
CY1H_REF					X		
HDRAD_CY1H						X	
LDRAD_CY1H_TUN					X		X
HDRAD_CYC1H_TUN						X	X

3.2 Experiments in the 3 hour assimilation cycle

Results from these experiments at 1.3 km horizontal resolution which have been run under a 3-hour assimilation cycle are shown between 15 and 30 July 2013. Over this time period, the higher radar density allows to improve precipitating forecast events between 12 and 24 hour forecast range (Figure 4). Subjective evaluation have shown a slight improvement on convective situations over this time period. Over this time period, an improvement of the fit of both the AROME analysis and guess to the radar observations for the HDRAD_CY3H experiment (by comparison at CY3H_REF experiment) is shown in Figure 5a for the pseudo-observations of relative humidity retrieved from radar reflectivity. In particular, the better fit of the guess to the radar pseudo-observations (not still assimilated in the 3D-Var AROME) indicates a good capability of the AROME system to well use the high density of radar reflectivity observations. It is much less clear for radial winds. The degraded fit of the analysis to the radar wind observations (Figure 5b) could indicate the need for decreasing the standard deviation of observation error (it will be confirmed by a posteriori diagnostics of observation error, i.e. section 3.3.2).

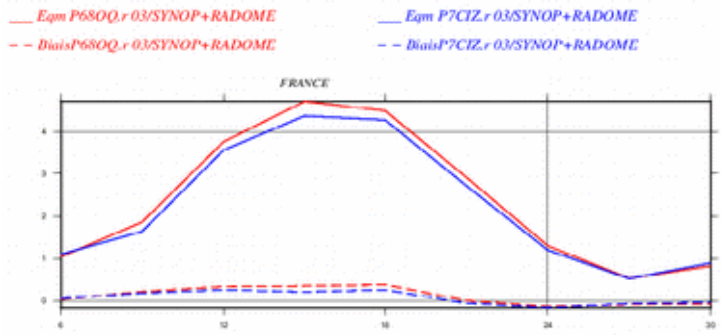

Figure 4: Root-Mean-Square (full line) and Bias of the 6-hour precipitating accumulation (RR6) model forecasts against the ground observations from 00h and 30h forecast range (X-axis). The red line is for reference experiment (referred as CY3H_REF in Table 1) and the blue line for the experiment (referred as HDRAD_CY3H in Table 1).

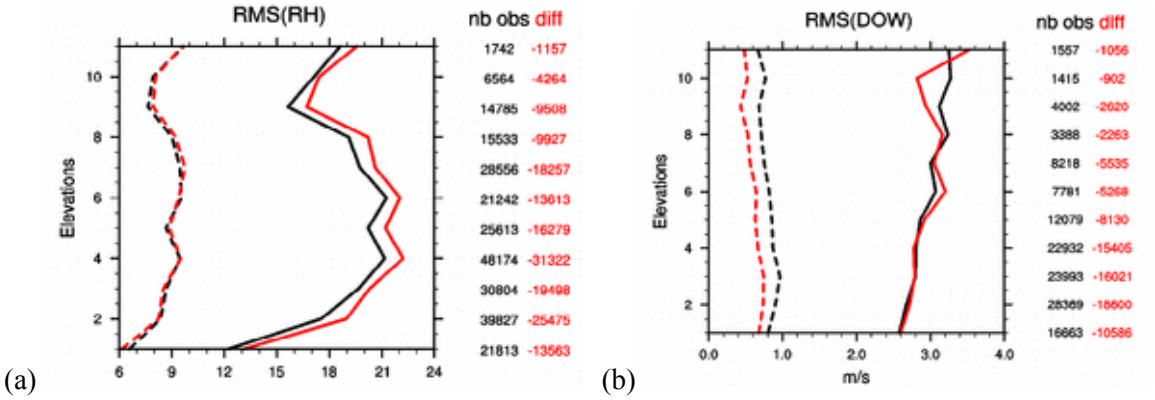

Figure 5: Root-Mean-Square of observation minus guess (full line) and of observation minus analysis (dashed line) for relative humidity (left) in % (X-axis) and radial wind (right) in m/s (X-axis), for each elevation (Y-axis). Results are shown for experiments with 3-hour cycled assimilation between 15 July 2013 and 28 July 2013: the red line is for reference experiment CY3H_REF and black line is for the experiment HDRAD_CY3H .

However, the fit of the guess to the radial winds shows ambivalent results: if an improvement is observed for the middle elevations, a slight degradation is shown for the highest elevations. But it is always a difficulty to conclude with such comparison because the sampling of radar data is not the same in both experiments. Unlike the comparison between CY3H_REF and the experiment LDRAD_CY3H_NOC, which assimilates the same sampling of radar data at 15 km of horizontal density but with a first-guess from HDRAD_CY3H (forecast from a high density analysis): the fit of the cycled "high density" guess to the radar observations is slightly improved for both reflectivity and radial wind observations (Figure 6). Moreover, the comparison between the experiments HDRAD_CY3H and HDRAD_CY3H_NOC shows that the first-guess from the cycled experiment HDRAD_CY3H is better than the one from the non-cycled experiment and the analysis shows the same difficulties to fit the radial wind observations (Figure 7). As a conclusion, the cycled assimilation of radar data at 8 km of resolution doesn't induce any evident degradation of the system and the reduction of standard deviation of radial wind observations can be tested.

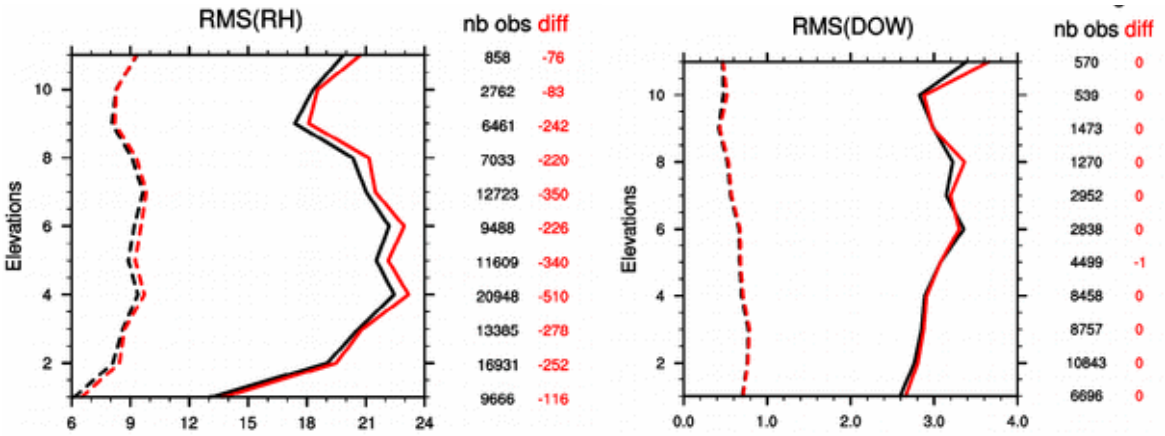

Figure 6: Same as Figure 5 but results are shown for experiments with 3-hour cycled assimilation between 15 July 2013 and 30 July 2013: the red line is for the reference CY3H_REF and black line is for the experiment LDRAD_CY3H_NOC.

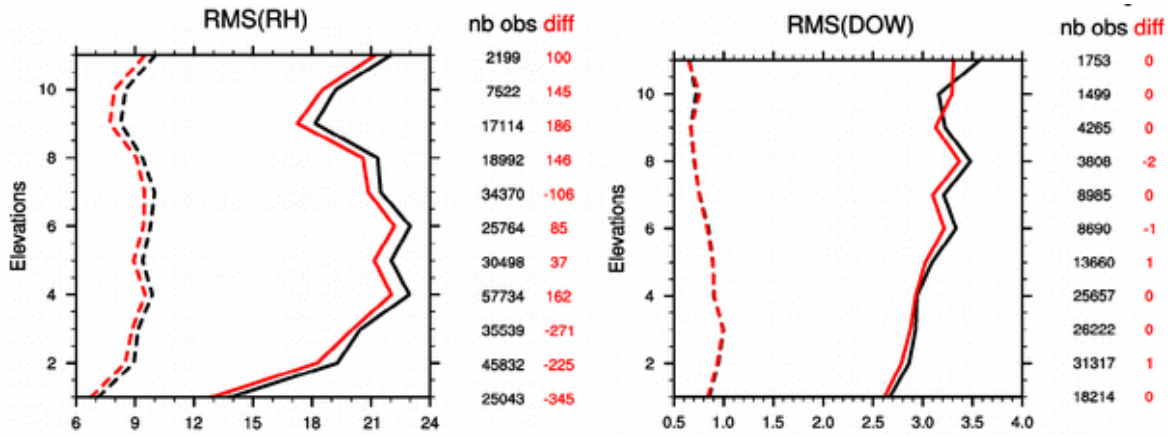

Figure 7: Same as Figure 5 but the red line is for the experiment HDRAD_CY3H and black line is for the experiment HDRAD_CY3H_NOC.

3.3 Experiments in the 1 hour assimilation cycle

3.3.1 General results from first experiments

The experiments CY1H_REF and HDRAD_CY1H with a hourly cycle assimilation have run for the long time period of three months between the 7th July and 29th September 2014. Although subjective evaluation shows some improvement of forecasted precipitating patterns of specific convective events during this time period, in particular at short-time (not shown), long term scores are rather neutral as the averaged regional BSS_NO shown in Figure 8. In a first approach, it can be surprising because an improvement is systematically observed for short term forecasts up to 12h forecast range for all threshold of rain rates. But, the averaged regional BSS_NO is an averaging over 4 forecast ranges between 6h and 24h and a slight degradation can be observed for the longer forecast ranges 18h and 24h (Figure 9). Further studies are needed to implement and evaluate the radar assimilation at higher density.

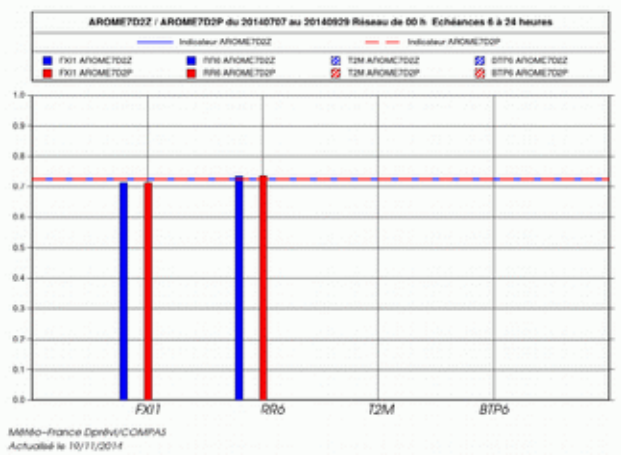

Figure 8: Averaged Regional Brier-Skill Scores for wind gusts (FX1) and 6-hour precipitating accumulation (RR6) for CY1H_REF (red) and HDRAD_CY1H (blue) experiments. The score is averaged over 4 forecast ranges (6 h to 24 h) and over three thresholds (0.5, 2 and 5 mm) for rain rates and maximum wind gusts over 1 hour exceeding 40 km.h^{-1}. The combined synthetic index (dashed line) is used to monitor the quality of the High Resolution operational model AROME. Higher scores reflect improved forecast skill. The BSS shown here takes into account a 52 km neighbourhood (Amodei et al. 2015).

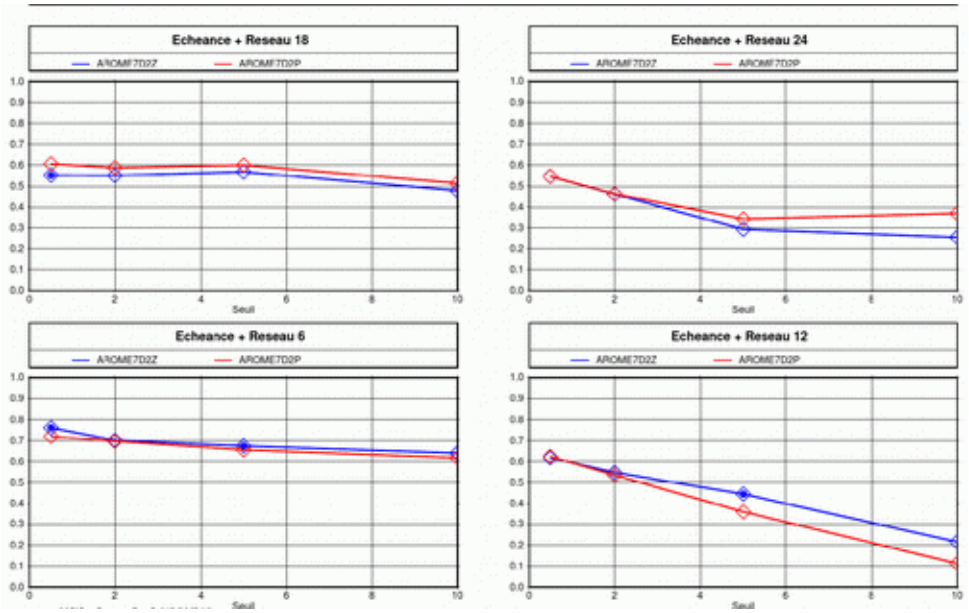

Figure 9: Regional Brier-Skill Scores for 6-hour precipitating accumulation (RR6) for CY1H_REF (red) and HDRAD_CY1H (blue) experiments for 4 forecast ranges (6 h to 24 h) and over different thresholds (0.5, 2, 5 mm and 10 mm) for rain rates.

3.3.2 Estimates of observation error correlations : a posteriori diagnosis.

In order to better specify the observation errors of radar data in the assimilation AROME system, and also to much better understand the behaviour of the system when the density of assimilated observations is increased, some a posteriori diagnostics of the assimilation system have been done. Different methods have been applied, unfortunately all of them with drawbacks and hypotheses which may be not verified. The “Höllingsworth-Lönnberg” and “Desroziers” methods have shown that the observation error standard deviation for Doppler radial winds was overestimated through a ratio of 2/3 of the specified value, in the AROME at 1.3 km of resolution (not shown). However, there may be a risk to decrease too much the observation error standard deviation: it can lead to a degradation of the first-guess provided by a wrong analysis, in particular in the case of observation error spatial correlations. But, some diagnostics of spatial correlations have also been computed through the Background-error method (method which uses the estimate of background-error from an assimilation ensemble). Two AROME ensemble assimilation systems (for 2.5 km and 1.3 km) with 90 members have been used. These diagnostics have shown a large decrease of observation error spatial correlations between the AROME at 2.5 km and 1.3 km of horizontal resolution (from 40 km to 25 km for the lengthscale of observation error correlations). It confirms that the observation error correlations (thanks to less representativeness error) decrease in the AROME 1.3 km horizontal resolution.

3.3.3 Revised set-up of radar assimilation

The long term evaluation of the first tests with a 8 km horizontal thinning has demonstrated rather neutral results (over summer and autumn time in 2014). Moreover, some specific events were even more poorly forecasted with this AROME configuration using radars at higher density (as for the “case study” considered hereafter on the 19th September 2014). An important tuning of various parameters of the radar assimilation has been done. First, according diagnostics, the observation error standard deviation for radial winds has been decreased up to 2/3 of the initial value. Afterwards, an change of various parameters of the radar reflectivity assimilation has been done, thanks to the new parallel computing capabilities. This configuration has been needed, to give more weight to radar observations and to allow some triggering of the convection in the model simulations when the model was very far from the observed convection. Results of this new configuration are evaluated in particular over the chosen two weeks described hereafter.

Table 2: New parameters of the 1D Bayesian inversion of reflectivity

	Radius of the neighborhood	Profiles	Sigma_o for the 1D inversion	Quality Check || Zana – Zobs||
AROME OPER	100 km	81	0.2	~ 7 dbZ
New configuration	200 km	225	5	~ 20 dbZ

Choice of the meteorological time period

In autumn 2014, a lot of convective weather period have been observed. During the time period between the 16th and 30th September, many thunderstorms developed over the South of France. Figure 10 shows that on the 16th September the weather situation is already controlled by an altitude minimum, centered over the Iberian Peninsula, which leads a cyclonic southern flow and generates some wet and hot air at low levels. Associated at this barometric situation strong thunderstorms developed and some convective clouds moved from Spain or Mediterranean to cover the South of France. This weather situation remained over Western Europe during several days (Figure 10).

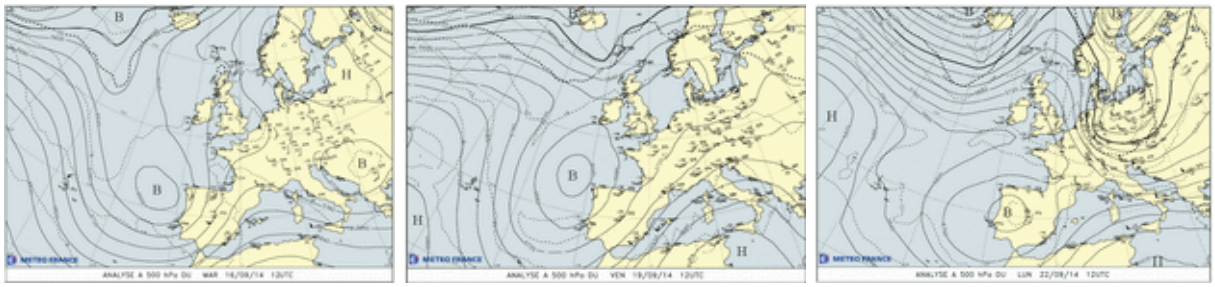

Figure: 10: Geopotential at 500 hPa for the 16th September 2014 12h TU (left), the 19th September 2014 12h UTC (middle) and the 22th September 2014 12h UTC (right).

This time period has also been chosen because some convective events of this specific period have been badly forecasted by the operational AROME model, and the potential of improvement could be tested. The positive impact of this revised set-up on the "higher-density radar" configuration is displayed (between HDRAD_CYC1H_TUN and LDRAD_CY1H_TUN) in Figure 11 through the averaged Brier-Skill Score and the combined synthetic index over the most convective week of the time period. It shows the better impact of the radar assimilation at higher density with the new tuning.

The improvement of the precipitating forecast scores between HDRAD_CY1D_TUN and CY1H_REF is also shown up to 18 and 24 hours (unlike for HDRAD_CY1H against CY1H_REF) in Figure 12 for the same time period.

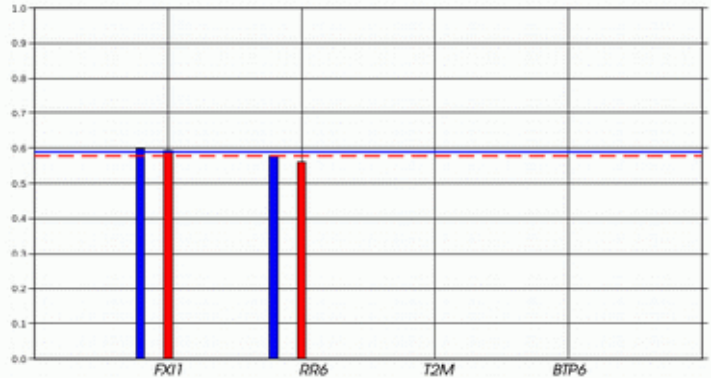

Figure 11: Same legend as figure 8 but for HDRAD_CY1H_TUN (blue) and LDRAD_CY1H_TUN (red)

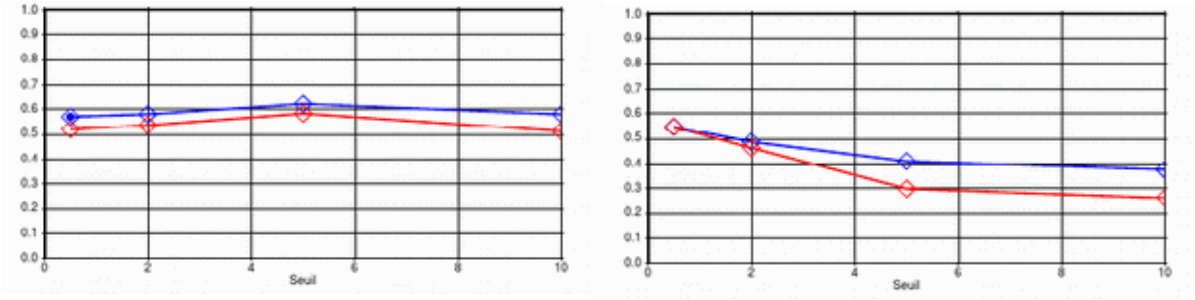

Figure 12: Same legend as figure 9 but for the forecast range 18h (left) and 24h (right) for HDRAD_CY1H_TUN (blue) and CY1H_REF (red)

An AROME version (included the assimilation of the radar at higher density and the revised set-up) in preparation in July 2015 run for one month (between 5 July and 6 August 2015) and the much better capability of the AROME system to simulate intense convective events is displayed in Figure 13, through significant BSS for the high threshold 10 mm in 6 hours, computed against the quantitative precipitation estimation ANTILOPE[1].

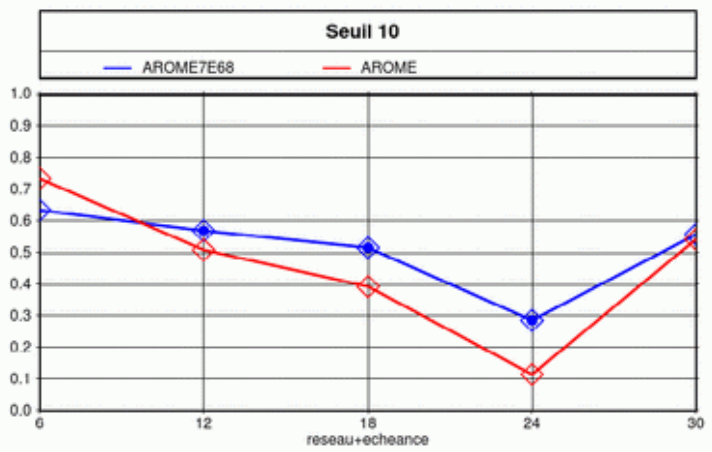

Figure 13: Same legend as Figure 9 but for the time period between the 5th July and 6th August 2015 between HDRAD_CY1H_TUN (blue line) and CY1H_REF (red line) for the threshold 10 mm, against the quantitative precipitation estimation ANTILOPE.Significant statistics are displayed by full diamond.

4 Illustration on a case study: focus on the 19th September 2014

4.1 Meteorological situation

As introduced in the previous section, on the 19th September 2014, an high level trough centered over the near Iberian Peninsula controls the weather over the Southern France and generates the development of strong thunderstorms over the Mediterranean which reached in particular South-Eastern France on the 19th September.

We focus on the strong convection on the South-East of France on the morning of 19th September 2014. This specific date has been chose because of the strong sensitivity of the AROME experiments to allow the triggering of the convection.

[1] The quantitative precipitation estimation ANTILOPE (ANalayse par spaTIaLisation hOraire des PrEcipitations) is an objective analysis computed by a blending radar and rain-gauges data.

4.2 Analyses increments

The comparison between the experiment LDRAD_CY1H_TUN and HDRAD_CY1H_TUN allows to identify the impact of the only higher density radar assimilation with the revised set-up. The convection on the "Bouches du Rhône" French department is absolutely not forecasted either at 06h, 07h, 08h, or 09h UTC in LDRAD_CY1H_TUN unlike the experiment HDRAD_CY1H_TUN (not shown, but see Figure 15 for the radar composite images). Figure 14 shows the analyses differences between at 07h UTC where the importance of the relative humidity field in the triggering and in the development of convection is highlighted. Indeed, this latest fields has to be compared to the radar composite at 07h UTC (Figure 15) and to the fact that the experiment LDRAD_CY1H_TUN doesn't simulate the expected convection.

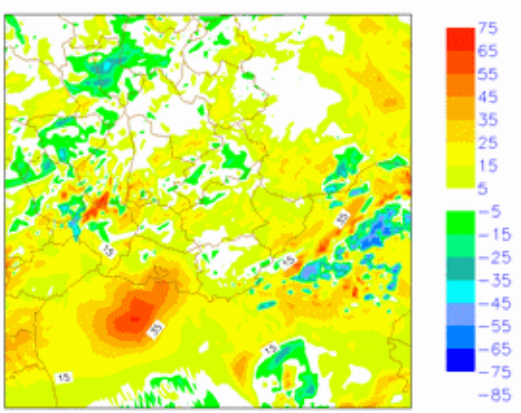

Figure 14: Analyses differences of relative humidity (left) at 600 hPa altitude between HDRAD_CYC1H_TUN and LDRAD_CY1H_TUN on 19 September 2014 – 07h UTC.

4.3 Illustration on radar reflectivity forecasts

Although the experiment HDRAD_CY1H improves the cumulative precipitating scores (against the AROME operational system CY1H_REF, not shown) the displacement of convection over the Mediterranean at 06h to cover the extreme South-East part of France at 07h, 08h and 09h TU is much better forecasted in the HDRAD_CY1H_TUN experiment (Figure 15): in the experiment CY1H_REF, the convection on the "Bouches du Rhône" French department is absolutely not forecasted either at 6h, 7h, 8h, or 09h UTC unlike the experiment HDRAD_CY1H_TUN. With the high-density radar data, the convection is triggered at the correct location (and is kept after every 1-hour analysis), even if the model fails to reproduce both the observed extent and intensity. It confirms the positive effect of the combined changes on the onset of heavy convection in cases where the model first guess and the radar data have large discrepancies.

5 Conclusion

Through the resolution increase of the AROME model, additional smaller scale meteorological features can be simulated, and also progressively analyzed. The updated version of the AROME model with a 1.3 km horizontal resolution allows to consider the assimilation of radar data at higher density. However, the assimilation of radar observations in the AROME model at 2.5 km resolution showed that their horizontal density can not be less than 15 km, in order to avoid observation error correlations induced by the differences between the scales of real precipitating features and the resolved model scales. Indeed, some experiments in the AROME at 2.5 km horizontal resolution have shown a degradation of the behaviour of the assimilation.

In agreement with a number of diagnostics of the assimilation system, it became possible to consider a radar density at 8 km after retuning some parameters from the reflectivity inversion and also revisiting the observation error standard deviation for radial Doppler winds. Indeed, although the only higher density of radar assimilation provides an improvement of short-term precipitating forecast scores, rather both neutral scores over long time period and a slight degradation at longer forecast ranges have

been observed. As a conclusion, with the combined changes, a clear positive impact of the radar high-density has been shown, in particular by an improvement of the precipitating forecast scores up to 18 hours. Such positive impact on precipitating scores has been observed for an AROME experiment in preparation of the e-suite AROME became operational on the 8th December 2015. Moreover, on a specific convective case, the triggering of some convective cells, hardly simulated with the AROME system at 2.5 km resolution (and 15 km of radar density), have been described with this new configuration.

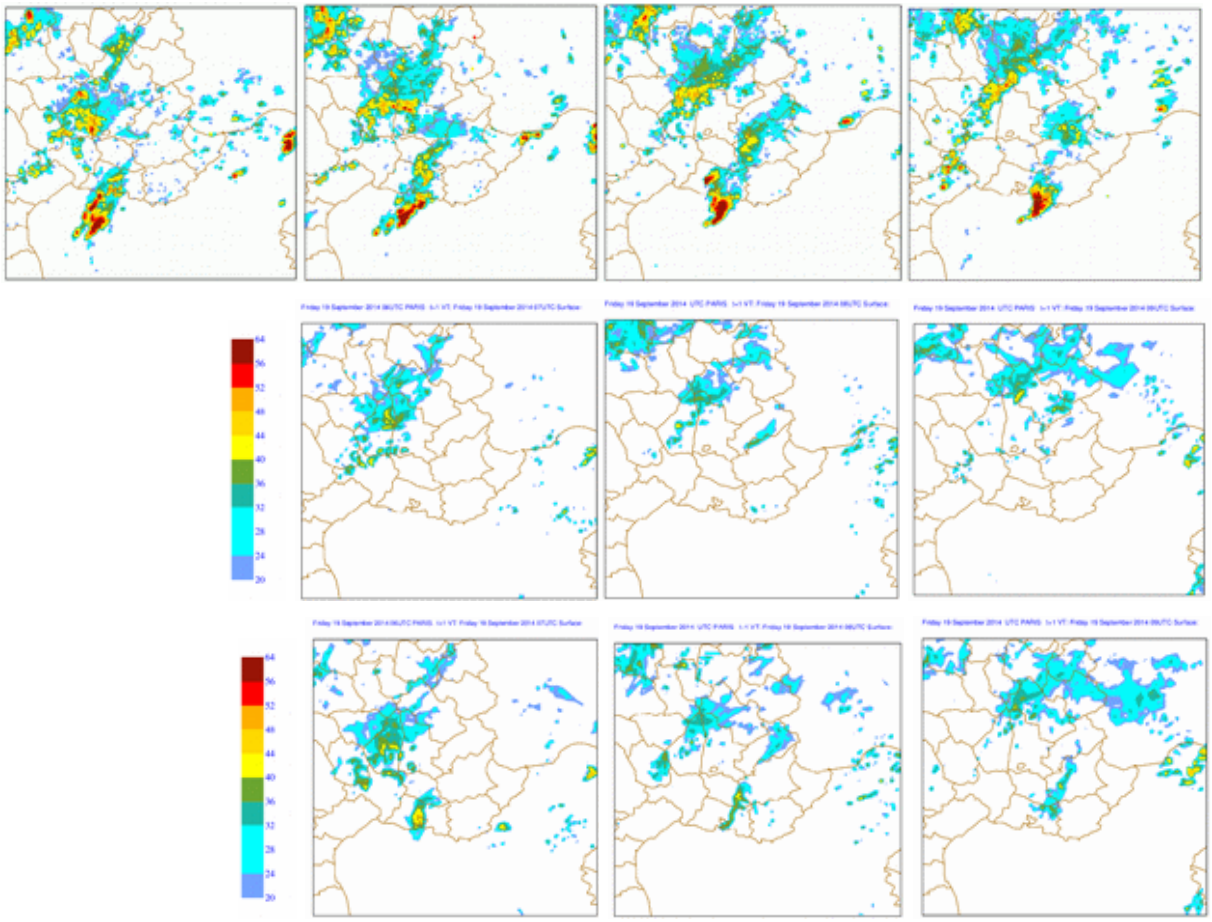

Figure 15: Over the South-East of France and on the 19th September 2014: Radar composites (top) from left to right at 06h UTC, 07h UTC, 08h UTC and 09h UTC. Simulated reflectivities at 700 hPa of the 1-hour AROME forecasts at the valid time 07 UTC, 08 UTC and 09 UTC for CY1H_REF (middle) and HDRAD_CY1H_TUN (bottom) experiments.

6 References

Amodei, M., I. Sanchez and J. Stein, 2015 : Verification of the French operational high-resolution model AROME wit the regional Brier probability score, *Meteorological Applications, Royal Meteorological Society,* **22**, 731-745**.**

Brousseau P., Y. Seity, D. Ricard and J. Leger, 2016: Improvement of the convective activity forecast with the AROME-France system. *QJRMS, submitted.*

Brousseau, P.L. Berre, F. Bouttier, and G. Desroziers, 2011 : Background-error covariances for a convective-scale data assimilation system: Arome-france 3D-Var. *Quaterly Journal of the Royal Meteorological Societ,* **137 (655),** 409-422.

Montmerle, T., & Faccani, C. (2009). Mesoscale assimilation of radial velocities from Doppler radars in a preoperational framework. *Monthly Weather Review*, 137(6), 1939-1953.

Wattrelot, E., Caumont, O., & Mahfouf, J. F. (2014). Operational implementation of the 1D+ 3D-Var assimilation method of radar reflectivity data in the AROME model. *Monthly Weather Review*, 142(5), 1852-1873.

Modelling activities at the Hungarian Meteorological Service

Viktória Homonnai, Máté Mile, Dávid Lancz, Balázs Szintai, Mihály Szűcs, Helga Tóth
Hungarian Meteorological Service

1 Introduction

This short paper describes the current research and development activities at the Hungarian Meteorological Service (OMSZ) related to the ALADIN/AROME modelling system. At the end of 2015, three limited are systems from the ALADIN/AROME model family are run operationally at OMSZ, which are described in Table 1.

Table 1: Operational model configurations at OMSZ.

	AROME	**ALADIN**	**ALADIN-EPS** (11 members)
Resolution	2.5 km	8 km	8km
Levels	60	49	49
Number of points	500x320	360x320	360x320
Boundaries	ECMWF deterministic (1h coupling)	ECMWF deterministic (3h coupling)	PEARP (6h coupling)
Runs per day	00 (+48h), 06 (+39h), 12 (+48h), 18 (+39h)	00 (+54h), 06 (+48h), 12 (+48h), 18 (+36h)	18 (+60h)
Data Assimilation	3 hourly (SYNOP, TEMP, AMDAR)	6 hourly (SYNOP, TEMP, AMDAR, SEVIRI, AMV, ATOVS)	-

This paper describes the developments related to these operational systems as well as research work on the next generation of numerical weather prediction models.

2 Research and development activities

Experimental AROME Data Assimilation with non-conventional observations

During the last year, AROME DA system was further tested with Meteosat (MSG) SEVIRI radiances and High Resolution Winds (HRW) AMV products in Hungary. Experiments with both types of observations have already been done in ALARO DA system, even SEVIRI radiances became operational.

The so called HRW is one of the NWCSAF products which provides Atmospheric Motion Vectors (AMV) and is calculated from the measurements of MSG SEVIRI channels. Our motivation was to test HRW in mesoscale AROME model through its operational DA system. The HRW with a previous configuration of NWCSAF package (v2011) was already tested in ALARO DA system. Beside HRW AMV the standard AMV from MSG (so called Geowind or MPEF) available through Eumetcast

broadcasting service was also included in the AROME experiments. The impact was investigated on a summer period including different weather situations (both convective and synoptically stable conditions). Overall HRW has neutral impact regarding objective verification scores, however in particular case studies positive impact for precipitation forecast was observed. In an example (see figure 1.), 3 hours accumulated precipitation forecasts started from 00UTC on 6th of August were studied with respect to AROME operational configuration, AROME oper with MPEF (Geowind) AMV and AROME oper plus HRW AMV. The frontal precipitation band was mainly captured by all model configurations, but the distribution of accumulated rain was the closest to the RADAR when HRW AMV was assimilated.

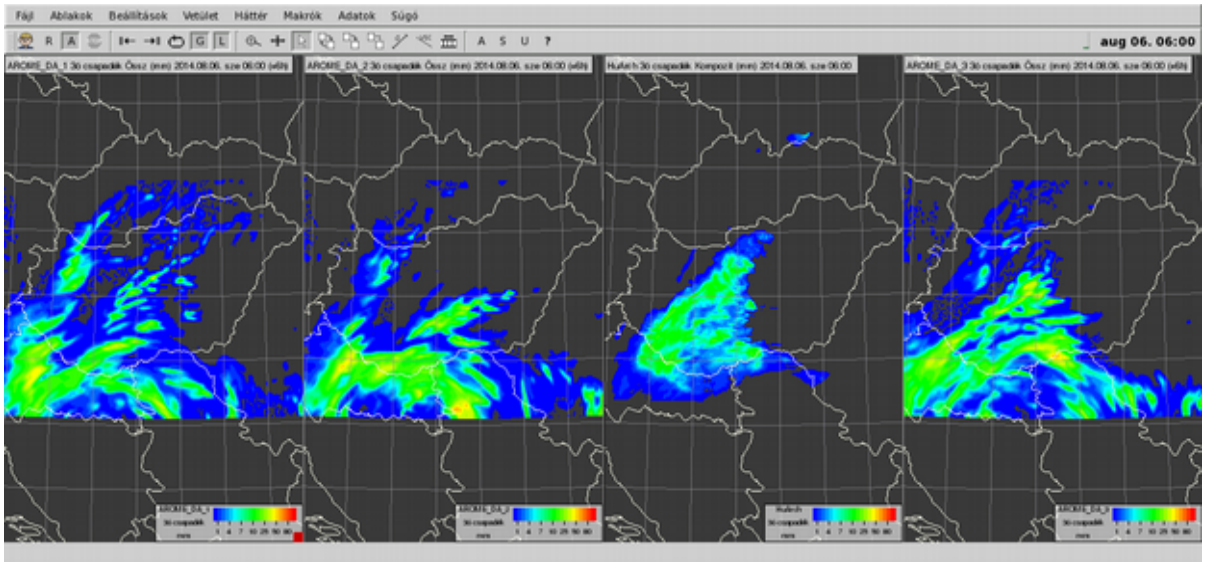

Figure 1. 3h AROME/Hungary precipitation forecasts for 6th of August, 2014. 1.panel: Without AMV, 2.: with MPEF AMV, 3.: RADAR observation, 4.: with HRW AMV

Concerning radiances of MSG SEVIRI sensor another study has been made with AROME-Hungary. For variational bias correction, a passive assimilation experiment was carried out with coldstart initialization of all SEVIRI channels except 1, 5 and 8. Predictor number 3 (surface temperature) and smaller adaptivity parameter were selected to increase correction during the examined period. SEVIRI window channels and surface characteristics (surface emissivity and surface temperature) have been used with the default settings which should be further tuned. Preliminary results showed neutral to positive impact on AROME analyses and forecasts.

ImagineS project

In the framework of the ImagineS project a Land Data Assimilation System (LDAS) is applied at the Hungarian Meteorological Service (HMS - OMSZ) to monitor the above ground biomass, surface fluxes (carbon and water) and the associated root-zone soil moisture at the regional scale (spatial resolution of 8 km x 8 km) in quasi real time. In this system the SURFEX (SURFace EXternalisée) 7.3 model is used, which applies the ISBA-A-gs photosynthesis scheme to describe the evolution of vegetation. SURFEX is forced using the outputs of the ALADIN numerical weather prediction model run operationally at HMS. First, SURFEX was run in open-loop (i.e. no assimilation) mode. Secondly the Extend Kalman Filter (EKF) method was used to assimilate LAI Spot/Vegetation and SWI ASCAT/Metop satellite measurements. The EKF run was compared to the open-loop simulation and to observations (LAI and Soil Moisture satellite measurements) over the whole country and also to in-situ measurements of a selected site in West-Hungary (Hegyhátsál). The ability of the modeling system to simulate inter-annual variability has also been validated in 2D over Hungary. Six years (2008-2013) have been simulated using SPOT/VGT GEOV1 LAI assimilation and open-loop runs.

These six years were used as a baseline to calculate monthly anomalies for the 2012. Negative anomaly is appearing in the soil moisture measurements of Hegyhatsal in 2012 (Fig. 2).

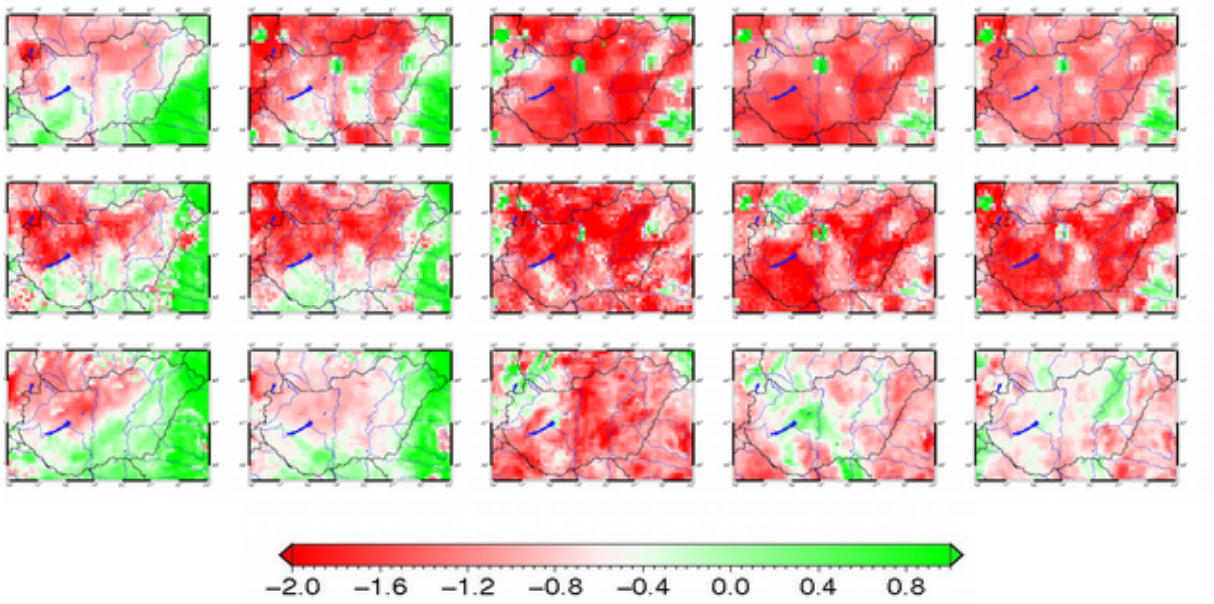

Figure 2: Monthly anomalies for the year 2012 from May to October: ASCAT/SWI-10 product (first row) assimilated WG2 (second row) and open-loop WG2 (third row)

It has been shown that the above-ground biomass simulated by ISBA-A-gs over wheat relates very well to agricultural yields if the assimilation of both satellite observations (LAI and SWI) is performed (Fig. 3).

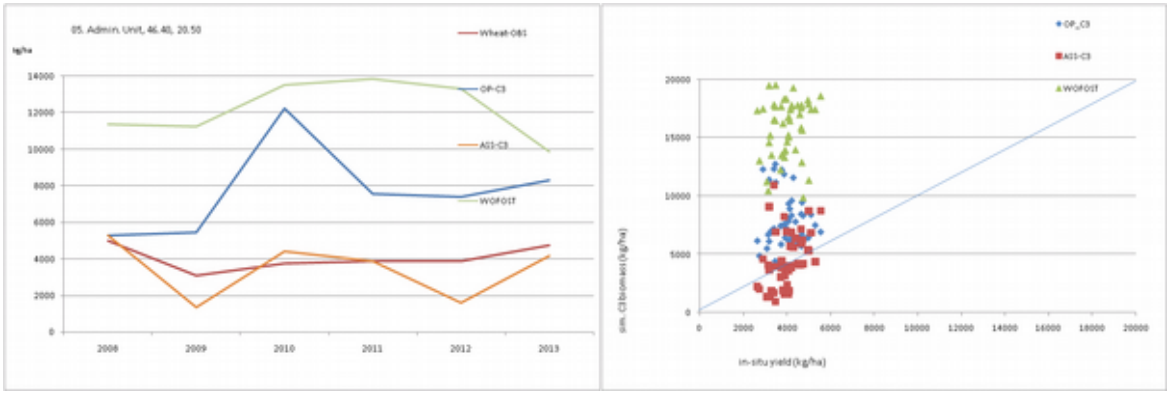

Figure 3: left: Wheat type biomass production vs. observed yield vs. WOFOST estimate for a selected administrative units, right: Scatter plot: Simulated above-ground biomass of straw cereals (open-loop, assimilation and WOFOST estimation) vs. observed yield, over 8 administrative units in Hungary for period of 2008-2013

Microphysics tuning in AROME related for wintertime low cloud events

Wintertime thermal inversion with fog and stratus cloud is a common phenomenon over the Carpatian Basin. The most NWP models usually predict well the nighttime fog but they tend to dissolve the stratus layer in daytime. Former sensitivity experiments indicated that the reason of the underestimation of low cloud cover can be searched in the microphysics parameterization. It was suggested to tune the autoconversion function and by now this modification has become operational. It was experienced that increase of the critical value of the autoconversion is not able to solve the problem in all of the cases, so developments continued with implementation of the OCND2 modifications into the ICE3 microphysics scheme. This modification pack consist of a more rigorous

separation of the liquid water and ice phases in the calculation of the mixed phase clouds. The OCND2 option was tested on longer time periods (winter and summer). Results show better cloud cover forecasts but the bias of 2m-Temperature continues to deteriorate in summer so further studies are needed.

Research of shallow convection parameterization in the grey zone in AROME

The current shallow convection parameterization in AROME is based on the Mass-Flux scheme, which supposes that a thermal, with far smaller horizontal size than the mesh-size of the simulation, is responsible for the non-local vertical turbulent transport in the planetary boundary layer. At low horizontal resolutions (dx > ~ 1 km) these thermals are entirely parametrized but at higher resolutions, the dynamics starts to partly simulate them. For these resolutions (called grey zone), where the shallow convection is partly treated by the dynamics and it is still needed to partly be parametrized, the parametrization has to be modified, so that it becomes scale-adaptive.
In our research we propose and test a modified version of the Mass-Flux, where the surface initialization of the thermals is dependent on the horizontal resolution (Fig. 4). This modfication is base on MesoNH large eddy simulations (LES). The first real case tests and validations were already made but the tuning is not done yet (Fig. 5).

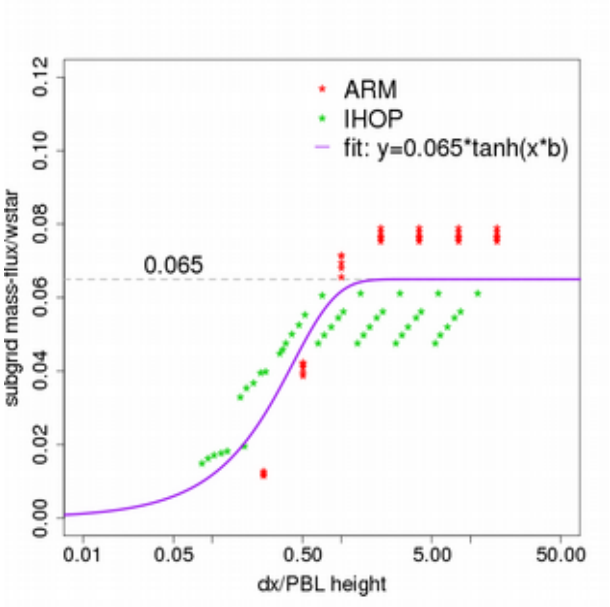

Figure 4. The normalized subgrid mass-flux values at the surface from the IHOP and ARM cases at various resolutions. The fitted curve was used as the new coefficient in the EDKF.

Data source: Rachel Honnert, CNRM, Toulouse

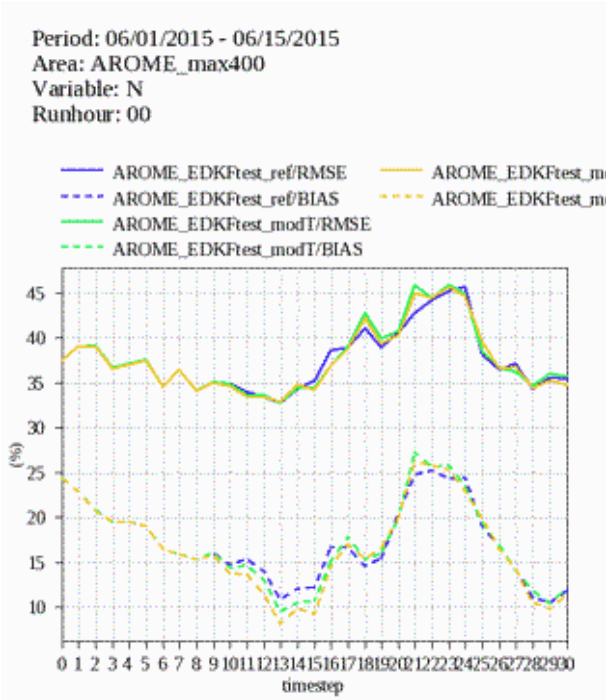

Figure 5. Verification of the cloudiness - RMSE and BIAS, blue: reference 1km test-AROME, green: modified AROME LUPBLH=T, orange: modified AROME LUPBLH=F (LUPBLH is a possible switch in the modification)

Limited area ensemble activity

Hungarian Meteorological Service is running its operational limited area ensemble system. It uses ALARO-0 baseline physics package and runs on 8km resolution. This system is the simple downscaling of French PEARP (ARPEGE EPS) and runs daily once at 18UTC for 60 hours. As convection-permitting ensemble systems are getting more focus in Europe, OMSZ has also started its test with AROME-EPS on 2.5km resolution.

After the extension of ECMWF's optional BC project OMSZ has started to test coupling to the ENS in the high-atmosphere but keeping the downscaled ARPEGE fields on the surface. First results show that the new coupling strategy can lead to a system with smaller error but less spread which underlines the importance of the local perturbations. An additional advantage of ENS usage is that it can ensure fresh LBCs four time per day which can make a positive impact on coupled data assimilation cycles.

We have been focusing mainly on two methods to generate local perturbations, both in ALARO-EPS and in AROME-EPS. Ensemble data assimilation (EDA) system was tested to get more precise initial condition fields and to estimate its uncertainty better. Results were quite promising especially in AROME-EPS where near-surface verification showed a clear improvement if EDA was implemented. Furter tests are needed to find the settings which can work optimally with the possible new coupling strategy.

Stochastically Perturbed Parameterized Tendencies (SPPT) is a method what we tried to use to give a representation of the model uncertainty. Tests are still in their early stage, and it looks quite challanging to find a version of the scheme which can effectively increase the spread of the system without causing unexpected errors.

Highlights of NWP activities at FMI in 2015

Carl Fortelius, Karoliina Hämäläinen, Markku Kangas, Ekaterina Kurzeneva, Laura Rontu, Niko Sokka

1 Operational activity

FMI operates two suites of deterministic short-range forecasts on the domains shown in Fig. 1. The Scandinavian domain is covered by AROME/HARMONIE on a grid spacing 2.5 km horizontally, while the larger domain is covered by the HIRLAM reference runs (RCR), having a grid spacing of about 7.5 km. Both of the suites use hourly lateral boundary data from the ECMWF BC programme.

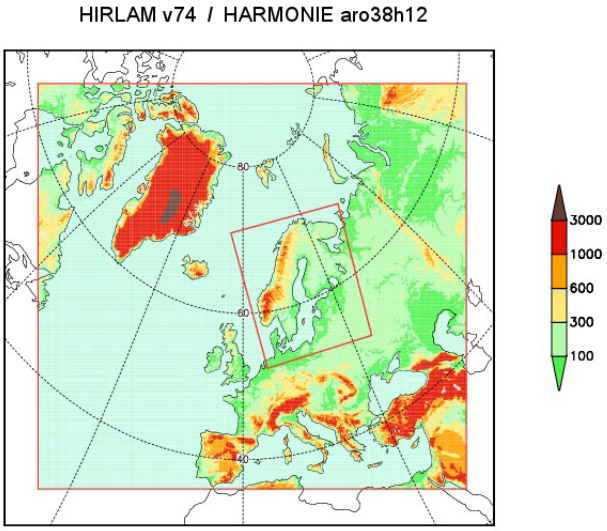

Figure 1: The domains of FMI's two operational suites

The operational HARMONIE system was upgraded to cy38h1.2 early in 2015. Changes to the micro physics introduced in cy38h1.2 have yielded a significant improvement of the winter time temperature forecasts by removing a cold bias. However, there is now more over-prediction of low level clouds and fog over land-areas.

2015 has seen a continued development of the on-line monitoring facility on http://fminwp.fmi.fi/mastverifnew/. As a part of our effort to cater for utilisation of renewable energy sources, the short wave direct normal irradiance was added to the suite of observations at Sodankylä. Forecasts of FMI duty forecasters were also added at Finnish stations. A report on the Sodankylä facility was prepared (Kangas et al. 2015).

2 Research and development

Radiation parameterization Several minor improvements to the default IFS radiation scheme were suggested and tested in HARMONIE cycles 38h1 and 40h1 (Gleeson et al., 2015a). 3D and 1D (MUSC) experiments were run to compare the results of IFS, HLRADIA and ACRANEB2 radiation schemes in the framework of AROME physics. The importance a correct definition of aerosol optical properties for solar radiation was demonstrated (Gleeson et al., 2015b and Toll et al., 2016). Long-wave radiation fluxes by three radiation schemes were tested against Sodankylä observations and shown to agree generally well with each other and with the observations. In case of optically thick clouds, the HLRADIA scheme seemed to overestimate the down welling radiation (Kangas et al., 2015). Orographic radiation parametrizations were suggested and shown to influence significantly the local radiation fluxes over slopes and mountains but have a minor impact on screen-level temperatures (Wastl et al., 2015a, 2015b, Rontu et al., 2015, 2016). A discussion paper by Räisänen et al., 2015 reports new parametrizations for the optical properties of blowing snow. The approach may open perspectives for a proper parametrization of radiative effects of precipitating snow and graupel, which are presently (option OCND2 since harmonie-38h1) handled in an ad-hoc way by treating them as a part of cloud ice crystals.

Surface modelling FMI scientists continue research and developments to represent lakes in NWP and climate models. A study was initiated to build the new structure functions of the lake water surface temperature basing on in-situ and satellite observations. Monitoring and development of the global lake database continue: the bathymetry for 1400 Finnish lakes was included into the database, a technical problem with rivers was fixed. FMI researchers actively participated in the 4th workshop "Parameterization of lakes in NWP and climate modelling", presenting studies of the lake EKF behavior, modelling of Arctic lakes and the lake database developments. Technical testing of the lake model FLake in SURFEX/ ECOCLIMAPII and in HARMONIE is in progress. A gap in SURFEX PGD interpolation/aggregation methods with grids of different resolution was recognized; developments to improve this are planned.

FMI NWP actively participates in COST Action ES1404 HarmoSnow. The main purpose of the Action is harmonization of snow observations, with the perspective to advance snow data assimilation in European NWP and hydrological models and show its benefit for relevant applications.

A study comparing three urban land surface models (CLM, SUEWS and SURFEX) at two sites in Helsinki was completed in 2015 (Karsisto et al., 2015). The modeled net all-wave radiation, turbulent fluxes of sensible and latent heat and snow depth were compared against observations, focusing on seasonality, snow cover, and near-surface stability. No model was found to outperform the others, but rather the performances were dependent on season, site and the flux in question. All models simulated the net all-wave radiation well and the largest uncertainties were related to the snow- melting period in spring. The largest uncertainties in the sensible heat flux seemed to relate to the modeling of the anthropogenic and storage heat fluxes particularly at the more densely built Hotel Torni site. The latent heat flux was underestimated by all the models at both sites during the growing season. Wintertime stability, determined by the Obukhov-length, was better simulated at the suburban site than downtown, where SUEWS and SURFEX showed more stable and neutral cases than the observations indicate, while CLM did not show stable cases at all.

Icing of structures FMI NWP has implemented an ice accretion model for wind turbines, post processing AROME output into the icing rate and related production loss. The system has already been used to compile an icing-atlas for Finland (Hämäläinen and Niemelä, 2016, http://tuuliatlas.fmi.fi/en/), and is currently providing trial-forecasts for the icing season of 2015/16 in a collaboration with the energy company Puhuri.

Cloud computing Within the Glenna Nordic Cloud project (https://wiki.neic.no/wiki/Glenna), FMI NWP participated in preparing a use case implementing the HARMONIE MUSC single column model as a cloud application. This allows MUSC users to focus immediately on research questions rather than on installing and configuring the system, and eliminates platform-induced differences between experiments. The cloud application is thus ideally suited for use in education and training.

New projects FMI NWP is involved in the new research project BC-DC (Academy of Finland, 2015-2020) aiming to produce research-based models for the development of variable distributed production of energy. FMI will work on aspects of short-range local weather forecasting relevant for energy production, including assimilation of radar radial wind data and Metop AMV data, modelling of ice accretion on wind turbines, and post processing of radiation and wind forecasts into energy production.

3 References

Gleeson, E., K. P. Nielsen, V. Toll, L. Rontu, E. Whelan (2015a): Shortwave Radiation Experiments in HARMONIE: Tests of the cloud inhomogeneity factor and a new cloud liquid optical property scheme compared to observations. http://www.cnrm.meteo.fr/aladin/IMG/pdf/nl5.pdf (p. 92)

Gleeson, E., V. Toll, K. P. Nielsen, L. Rontu, and J. Mašek (2015b): Effects of aerosols on solar radiation in the ALADIN-HIRLAM NWP system. http://www.atmos-chem-phys-discuss.net/15/32519/2015/acpd-15-32519-2015.html

Hämäläinen, K. , and S.Niemelä (2016): Production and verification of Finnish Icing Atlas, Wind Energy (under review)

Kangas, M., L. Rontu, C. Fortelius, M. Aurela and A. Poikonen (2015): Weather model verification using Sodankylä mast measurements. Geosci. Instrum. Method. Data Syst. Discuss., 4, 1-22, 2015 www.geosci-instrum-method-data-syst-discuss.net/4/1/2015/ doi:10.5194/gid-4-1-2015.

Karsisto, P., Fortelius, C., Demuzere, M., Grimmond, C. S. B., Oleson, K. W., Kouznetsov, R., Masson, V. and Järvi, L. (2015): Seasonal surface urban energy balance and wintertime stability simulated using three land-surface models in the high-latitude city Helsinki. Q.J.R. Meteorol.Soc.
doi:10.1002/qj.2659 http://onlinelibrary.wiley.com/doi/10.1002/qj.2659/abstract

Rontu, L., S. Niemela, C. Wastl, A. Mary and Y. Seity (2015): OLYMPIC HARMONIE 2014 - Influence of the details of topography in a NWP model :
http://streaming.uibk.ac.at/medien/c707/c707101/icam2015/poster/P2.44.pdf

Rontu, L., C. Wastl, and S. Niemela (2016): Influence of the details of topography on weather forecast - evaluation of HARMONIE experiments in the Sochi Olympics domain over the Caucasian mountains. Under review for Frontiers study topic
http://journal.frontiersin.org/researchtopic/3327/the-atmosphere-over-mountainous-regions

Räisänen, P., A. Kokhanovsky, G. Guyot, O. Jourdan, and T. Nousiainen (2015): Parameterization of single-scattering properties of snow. http://www.the-cryosphere.net/9/1277/2015/tc-9-1277-2015.html

Toll, V., E. Gleeson, K.P. Nielsen, A. Männik, J. Mašek, L. Rontu, P. Post (2016): Impacts of the direct radiative effect of aerosols in numerical weather prediction over Europe using the ALADIN-HIRLAM NWP system. Under review for Atmospheric Research.

C. Wastl, C., A. Mary, Y. Seity, L. Rontu, C. Wittmann (2015a): Parameterization of orographic effects on surface radiation in AROME-SURFEX. http://www.cnrm.meteo.fr/aladin/IMG/pdf/nl5.pdf (p. 81)

C. Wastl, C. Wittmann, A. Mary, Y. Seity, L. Rontu, M. Dian, 2015b. Parameterization of orographic effects on surface radiation in AROME. http://streaming.uibk.ac.at/medien/c707/c707101/icam2015/poster/P2.43.pdf

HARMONIE activities at IMO in 2015

Bolli Palmason, Sigurdur Thorsteinsson, Nikolai Nawri, Guðrún Nína Petersen, Halldór Björnsson

1 Introduction

HARMONIE has been run operationally at the Icelandic Meteorological Office (IMO) since autumn 2011, establishing a growing reputation within the institute. In winter 2013, it became the main short-range forecast model used by IMO's forecasters. Another milestone was reached in summer 2014 when the model became the basis for the short-range weather forecasts on IMO's public website (www.vedur.is).

In the year 2015 our main activities were:

- To improve the physiography databases (PGD) used in HARMONIE for Iceland. A major upgrade of the IMO HARMONIE system using the new PGD was made in the autumn.
- Start a reanalysis project, ICRA-2015, running HARMONIE with ERA-Interim on the boundary covering the years 1980 to 2015.

2 The model setup

The IMO HARMONIE was updated to the current model set up on 23 September 2015. A short summary of changes can be found in Table 1. Among the changes was an increase in the horizontal domain of the operational HARMONIE model in order to diminish the known problem of too weak triggering of shallow convection over sea, see Figure 1. The figure shows results of two simulations differing only in domain size. For the smaller domain the convective precipitation is not visible until over land (left panel) while in the larger domain (right panel) the convection produces precipitation earlier, over ocean to the west of the country.

Figure 2 shows better the extent of the new HARMONIE domain.

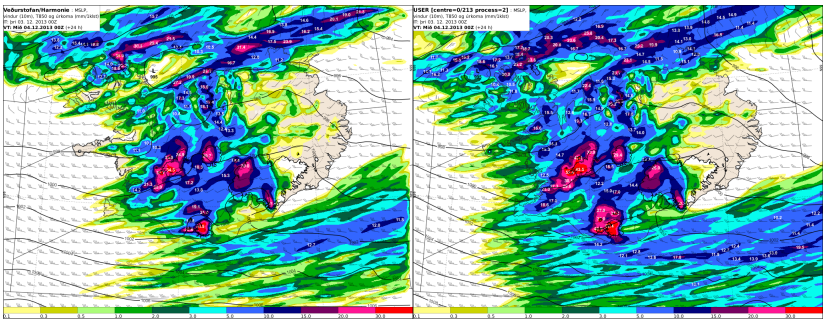

Figure 1: Simulated accumulated 24 hour precipitation (mm) on 23 December 3 2013 due to shallow convection associated with westerly flow. Smaller domain (left) and larger domain (right).

Table 1: Comparison of operational HARMONIE at IMO before and after 23 September 2015 as well as the ICRA-2015 reanalysis.

Model version	HARMONIE op.2014-2015	HARMONIE op. 2015-2016	ICRA-2015 reanalysis
Cycle	cy38h1.1	cy38h1.2	cy38h1.2
Domain size	300x280 grid points	500x480 grid points	300x280 grid points
Resolution	2.5 km	2.5 km	2.5 km
No. of levels	65	65	65
Forecast model	Non-hydrostatic, Arome physics	Nonhydrostatic, Arome physics	Non-hydrostatic, Arome physics
Initial conditions	CANARY+OI_Main, 230 SYNOP obs.	CANARY+OI_Main, 230 SYNOP obs.	CANARY+OI_Main, available SYNOP obs.
Orography	GTOPO30	Improved GTOPO30	Improved GTOPO30
Physiographic data	ECOCLIMAP-I/FAO	ECOCLIMAP-II/HWSD	ECOCLIMAP-II/HWSD
Coupling with	IFS/1 hourly	IFS/1 hourly	ERA-Interim/6 hourly
Starting times	00/06/12/18 UTC	00/06/12/18 UTC	00/06/12/18 UTC
fc length/outputs	+48 hours/every 1 hour	+66 hours/every 1 hour.	+12 hours, 6-12 hours/every 1 hour

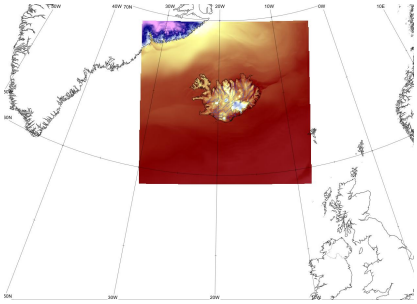

Figure 2: Example of a 2 m temperature forecast showing the size of the current Icelandic domain.

3 Upgraded physiography

The main development work at IMO during the last one and half year has been to upgrade the physiography databases for Iceland. The land-cover databases ECOCLIMAP-I/II were identical for Iceland and contained errors, e.g. in glacier extent, vegetation fraction, leaf area indices (LAI), and soil depths.

The method we used to build the new classification map ECOCLIMAP-II was to combine the existing databases available such as Corine (CLC2006) [1], soil map from the Agricultural University of Iceland (AUI) [2] and the AUI Farmland database [3]. These two databases are the best classification of bare and vegetated land in Iceland. Hence, ECOCLIMAP-II/Iceland takes advantage of the improvements provided by these three databases as they are based on supervised classification from satellite images, calibration monitoring, atmospheric correction, and normalization of surface directional effects compared to the NOAA/AVHRR datasets (acquired between April 1992 and March 1993) that were used to produce ECOCLIMAP-I. The Corine data base is the basis, with AUI Farmland database applied for vegetation and AUI soil map where vegetation is missing. Furthermore, we use MODIS LAI and albedo products to improve each land-cover type definition in the ECOCLIMAP-II/Iceland database.

The two other databases used to describe the PGD, e.g., the FAO/HWSD sand/clay database and the GTOPO30

topography database were also upgraded with the best available local data. The HWSD was improved with the help of AUI specialists to better describe the soil compositions. Figure 3 shows the new ECOCLIMAP-II/Iceland land-cover database with the 29 land-cover types used for Iceland at the 100 m working resolution.

The updates of PGD are used in the current HARMONIE system through locally modified copies of each database. The plan is to deliver the modifications to Meteo France to be included in the official ECOCLIMAP-II database and a detailed report is being written. Both will be delivered early in 2016.

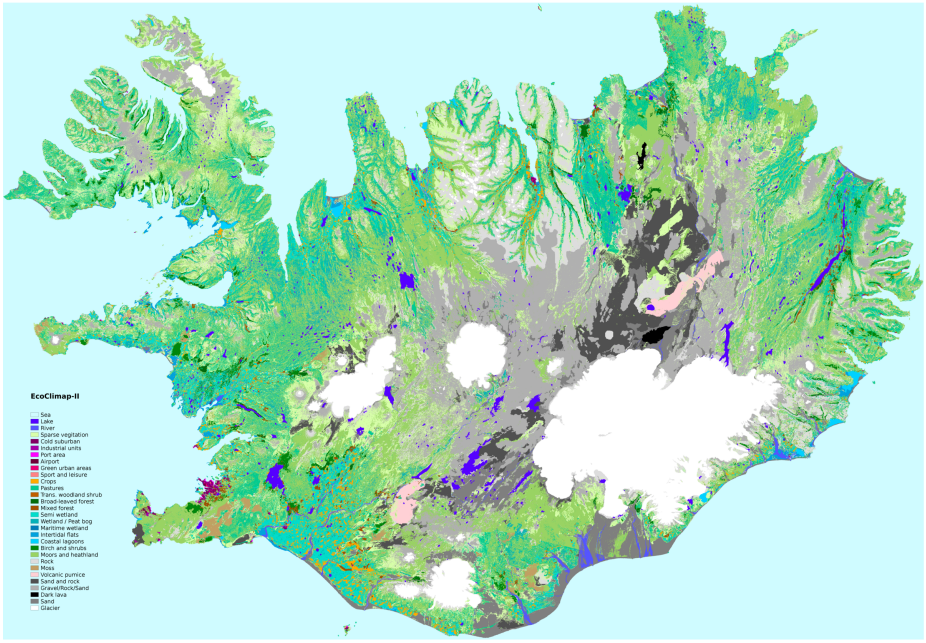

Figure 3: The new ECOCLIMAP-II/Iceland map with the 29 land-cover types used for Iceland.

4 Regional reanalysis project

After an extensive test period, a reanalysis project (ICRA-2015) was launched in spring 2015. ICRA-2015 uses a similar HARMONIE 38h1.2 setup as for the 2014 - 2015 operational run, but using ERA-Interim at the boundaries. The updates of the PGD databases are used in the reanalysis. ICRA-2015 does not use climate mode, but instead runs in forecast mode with 6 h analysis cycles and 12 h forecast lengths and the reanalysis data is comprised of key parameters for the 6-12 h forecasts with outputs at 1 hour interval. The ICRA-2015 reanalysis run is scheduled to be finished early 2016.

The goals of the reanalysis project are:

- HARMONIE model climate, to be able to produce long-term statistics, trends, and anomaly maps.
- To deliver products to hydrological applications: accumulation and melt of seasonal snow on ground (daily operational forecasts and reanalysis climate) delivered to the national power company for monitoring of hydroelectric dams.
- To deliver evaporation data to the Statistical Office of Iceland and European Commission.

Furthermore, there are interests in the project for application to road services, communities (e.g., avalanche protection), insurance companies and glaciologists.

Figure 4 gives an example of result from this work.

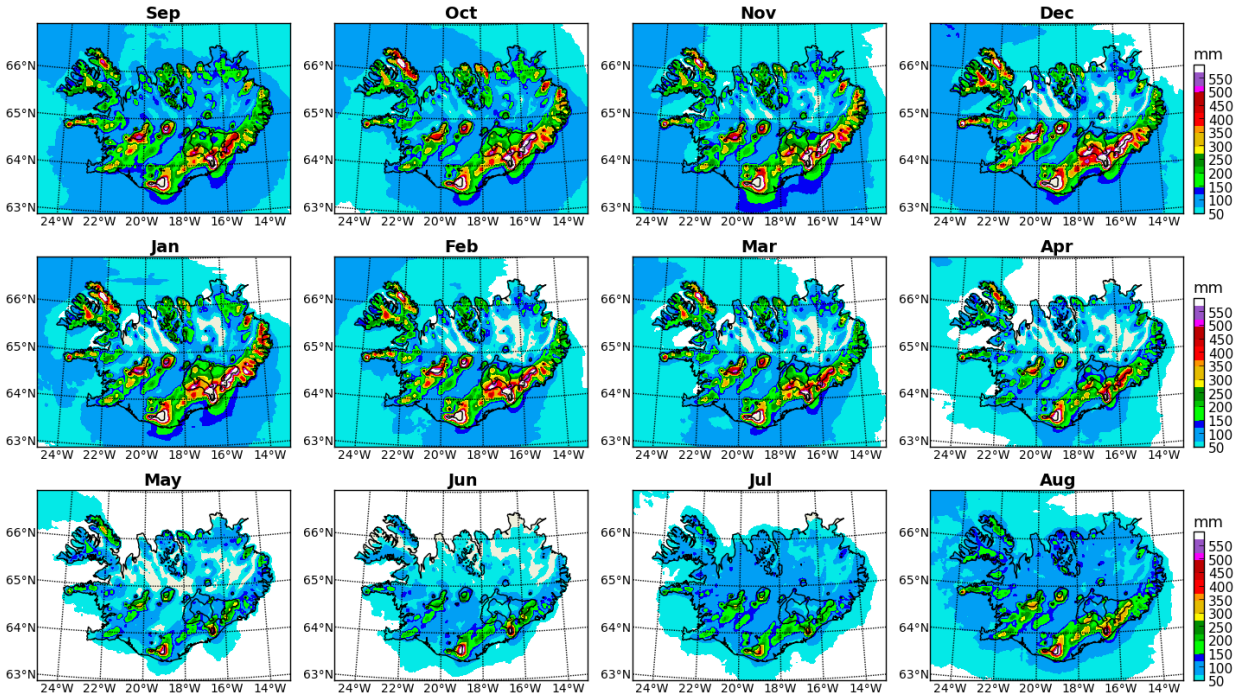

Figure 4: HARMONIE reanalysis multi-year (13 years) monthly mean maps of accumulated total precipitation (mm).

5 Acknowledgement

The IMO Harmonie team would like to thank Ólafur Arnalds and Sigmundur Helgi Brink, AUI, for all their assistance in improving the PGD. They provided us with state of the art data bases, good guidance and last but not least showed great enthusiasm for the project.

6 References

Árnason, K., Matthíasson, I.: CORINE Land Cover 2006 of Iceland. Grant agreement 3601/B2007.EEA53004. Final report. October 2009. National Land Survey of Iceland.

Arnalds O, Óskarsson H. 2009. Íslenskt jarðvegskort (Soil map of Iceland). Náttúrufræðingurinn 78:107-121. English summary.

Fanney Ó. Gísladóttir, Sigmundur Helgi Brink og Ólafur Arnalds. 2014. Nytjaland. Fjölrit LbhÍ nr. 54. URL: http://www.lbhi.is/sites/default/files/gogn/vidhengi/rit_lbhi_nr_54.pdf

Met Éireann NWP Highlights 2015

Eoin Whelan, Emily Gleeson, Sarah Gallagher, Ray McGrath

1 Introduction

HARMONIE is used operationally by Met Éireann as its short-range forecast model as well as a research tool by Met Éireann scientists. HARMONIE 36h1.4 was made operational by Met Éireann in July 2011 with cycle 37h1.1 being introduced in January 2013. This article provides a summary of the current operational HARMONIE configuration as well as summaries of some of the NWP research carried out at Met Éireann during 2015.

2 Operational NWP

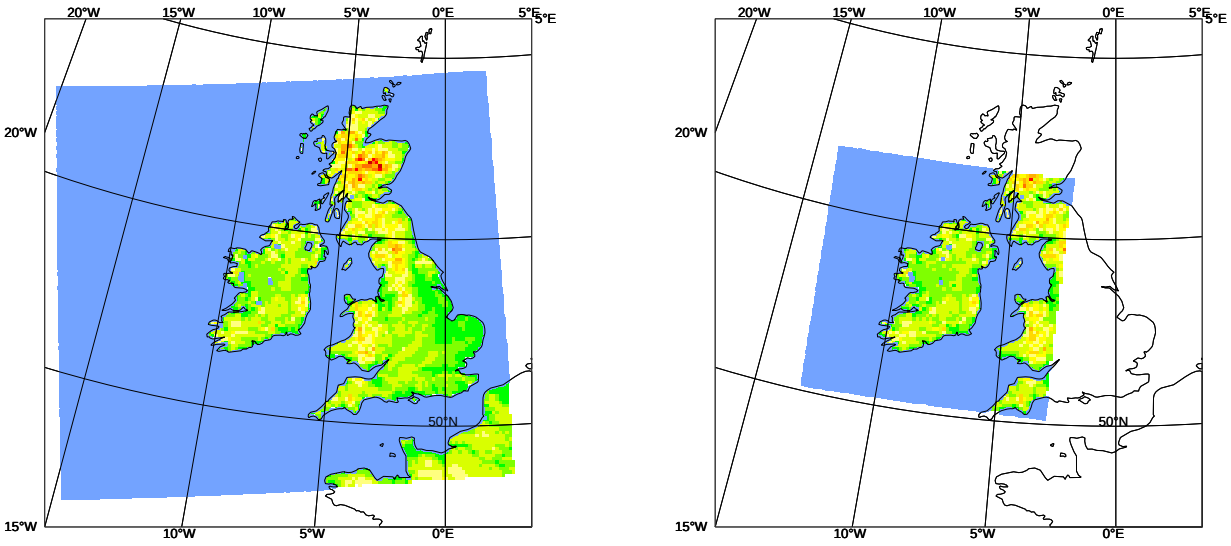

(a) Met Éireann operational HARMONIE domain

(b) Renewable energy project HARMONIE domain

Figure 1: Met Éireann HARMONIE domains

Met Éireann runs a single operational HARMONIE configuration on a domain covering Ireland, the United Kingdom and part of Northwest France. 54 hour forecasts are produced four times each day using cycle 37h1.1 on a 2.5km horizontal grid with 65 levels in the vertical and a model top at 10hPa (the operational domain is shown in figure 1(a)). No upper air analysis is carried out and optimum interpolation is used for the surface analysis. The observation cut-off is set at 45 minutes; this is enough time to collect and process the surface observations used by the surface analysis.

HARMONIE 38h1.2 is currently[1] being evaluated. The proposed operational configuration will use the same domain but 3DVAR upper air analysis using conventional observations will be enabled. The forecast cycle frequency will also be doubled so that forecasts will run eight times per day.

3 Renewable Energy

Met Éireann staff and researchers at University College Dublin (UCD) started a project at the end of 2014 which used the HARMONIE model and the WAVEWATCH III wave model (NOAA/NCEP [2016]) to produce a high resolution wind and wave atlas for Ireland based on the years 2000 to 2013 inclusive. During 2015 results from the simulations were analysed; further details are available in Gallagher et al. [2016].

Met Éireann ran HARMONIE cycle 37h1.2 on a small domain covering Ireland and its coastal waters (see figure 1(b)) for the 14 years to produce 10m winds that were used to drive the WAVEWATCH model for the period. The HARMONIE configuration for this project used ERA-Interim data (79km grid-spacing) for its boundary conditions without any intermediate model following the approach taken by Burgers et al. [2013]. This represents a downscaling ratio of approximately 32:1 which is significantly larger than the accepted maximum ratio of 5-10:1. An "intermediate" model using a grid-spacing of about 10km could have been used. However, the results presented by Burgers et al. [2013] and early tests in preparation for this project did not suggest any significant problems with this approach. HARMONIE 10m winds were found to be generally superior to ERA-Interim in predicting both wind speed and direction when compared with land observations and marine observations close to the coastline. Figure 2 shows an example of the output from the project, the winter average wind power at 90m for the south-west coast of Ireland.

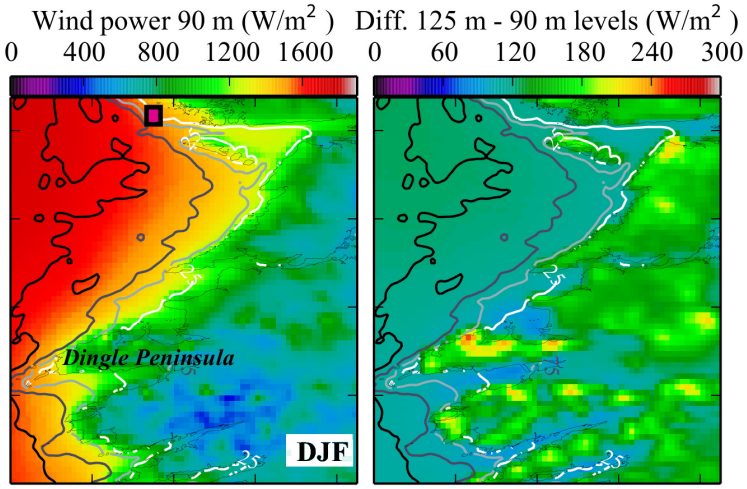

Figure 2: Winter average of the wind power at 90 m (left panel) and the difference between the 125 m and 90 m levels (right panel) for the southwest coast of Ireland. The square marker shows the proposed position of a wind energy project.

By considering the wind and wave conditions jointly, the research was able to build a unified description of the wave and wind nearshore energy potential of Ireland. This made it possible to select regions that have both a high energy density and are reasonably accessible for marine operations and maintenance. The study provides detailed information on wind and waves that reflects the current climate, an important consideration in view of climate change over past decades. This information also makes it possible to inform commercial interests

[1] January 2016

involved in marine operations in general, and in exploiting ocean renewable energy.

4 Regional re-analysis

In 2015 Met Éireann staff commenced a 35-year regional re-analysis of the Irish climate using the HARMONIE model, Met Éireann Re-Analysis (MÉRA). HARMONIE 38h1.2 was set up on the current operational domain, see figure 1(a), with 3DVAR upper air analysis of conventional observations enabled. Observations prepared from Met Éireann's climate database were used to supplement conventional observations used by ERA-Interim. The 35-year simulation period was split in to seven streams each consisting of a 1 year "spin-up" followed by 5 "production" years. Production started in February 2015 and the streams are now at the half way mark.

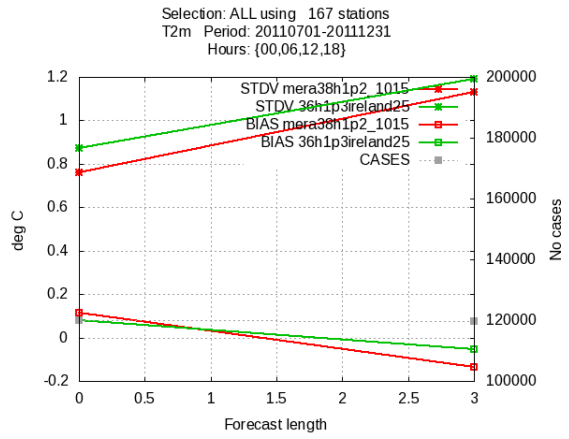

(a) Verification of 2m temperature (0-hour and 3-hour) forecasts comparing Met Éireann operational HARMONIE forecasts (36h1p3ireland25, green) and MÉRA forecasts (mera38h1p2_1015, red)

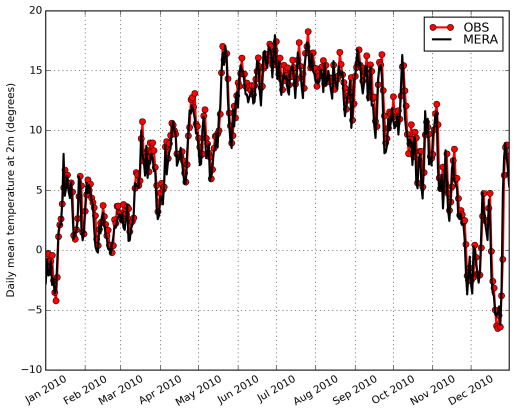

(b) A comparison between gridded observed daily mean 2m temperatures and output from the MÉRA simulations

Figure 3: MÉRA results

Initial analysis of MÉRA output suggests that the simulations are performing well. Point verification of the output has shown that MÉRA (38h1.2) performs better than the original (Met Éireann) operational configuration (36h1.3 with no upper air analysis), see figure 3(a). MÉRA output also compares well with Irish gridded observations, see figure 3(b).

References

G. Burgers, P. Baas, and H. van den Brink. Towards an extreme wind climatology for The Netherlands based on downscaling ERA-Interim with the HARMONIE-AROME high-resolution model. *Poster presented at EGU 2013, Vienna*, 2013.

S. Gallagher, R. Tiron, E. Whelan, E. Gleeson, F. Dias, and R. McGrath. The nearshore wind and wave energy potential of Ireland: a high resolution assessment of availability and accessibility. *Renewable Energy*, 88: 494–516, 2016. doi: 10.1016/j.renene.2015.11.010.

NOAA/NCEP. WAVEWATCH III® model. http://polar.ncep.noaa.gov/waves/wavewatch, January 2016.

ALADIN related activities in Morocco

Hassan Haddouch, Siham Sbii, Karam Essaouini

1 Introduction

This short article gives an overview of the most important achievements within the NWP group of the Moroccan Meteorological Service (DMN) during 2015.
AROME 2.5km forecast system was set up at Morocco weather service in addition to the operational ALBACHIR 10km model and NORAF. It is now reaching an operational status.
In addition, the high resolution e-suite for ALADIN-MAROC was installed with resolution of 7.5km in horizontal and 70 levels in vertical. It is based on CY40ope2 version.

2 GPS data assimilation In ALADIN-MAROC

10 ground-based GPS stations are installed in different Moroccan synoptic stations (Figure 1). Data from this network is collected in real time and stored in a local server. GPS data from IGS website is also downloaded, especially from stations inside and around ALADIN-MAROC domain. A suite for high quality coordinate calculation based on BERNESE software has been implemented and validated. BERNESE software provides also ZTD (zenith total delay) data (Figure 2).

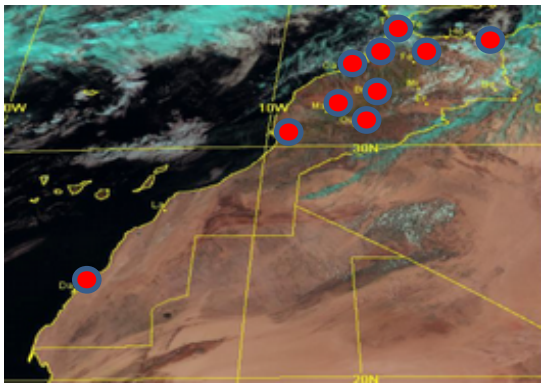

Figure 1: Network of Moroccan GPS stations

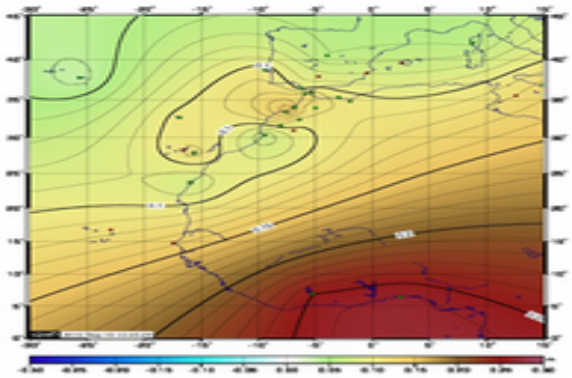

Figure 2 : ZTD anomaly map locally produced by BERNESE

The assimilation of ZTD data in ALADIN-Morocco model starts by performing monitoring of locally produced ZTD data.
First, the assimilation of only ZTD produced from Moroccan network and IGS data generates humidity increments from surface to above 500hPa. Figure 3 shows humidity increment at 850 hPa and 700hPa. The relative humidity increment reaches 18% in the north of Morocco, well covered by GPS data as shown in Figure 3. The increment in the south of Morocco corresponds to data from DAKHLA GPS station.

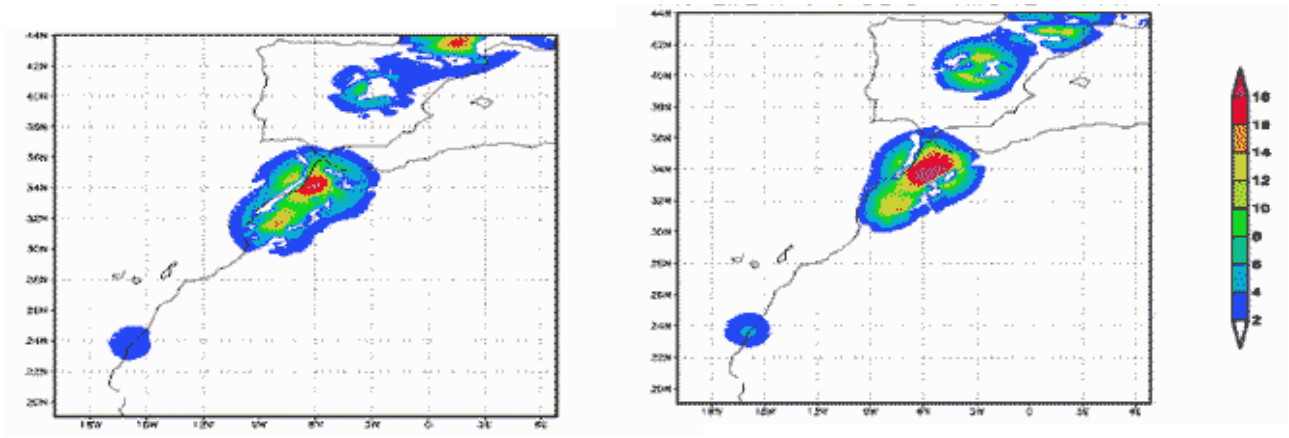

Figure 3: Relative humidity increments at 850 hPa (left) and 700 hPa (right)

An impact study was performed over 2 months from 02/09/2014 to 31/10/2014. The scores versus conventional observations were calculated by the MET software. The results shows a slightly positive impact specially for humidity at low levels (Figure 4).

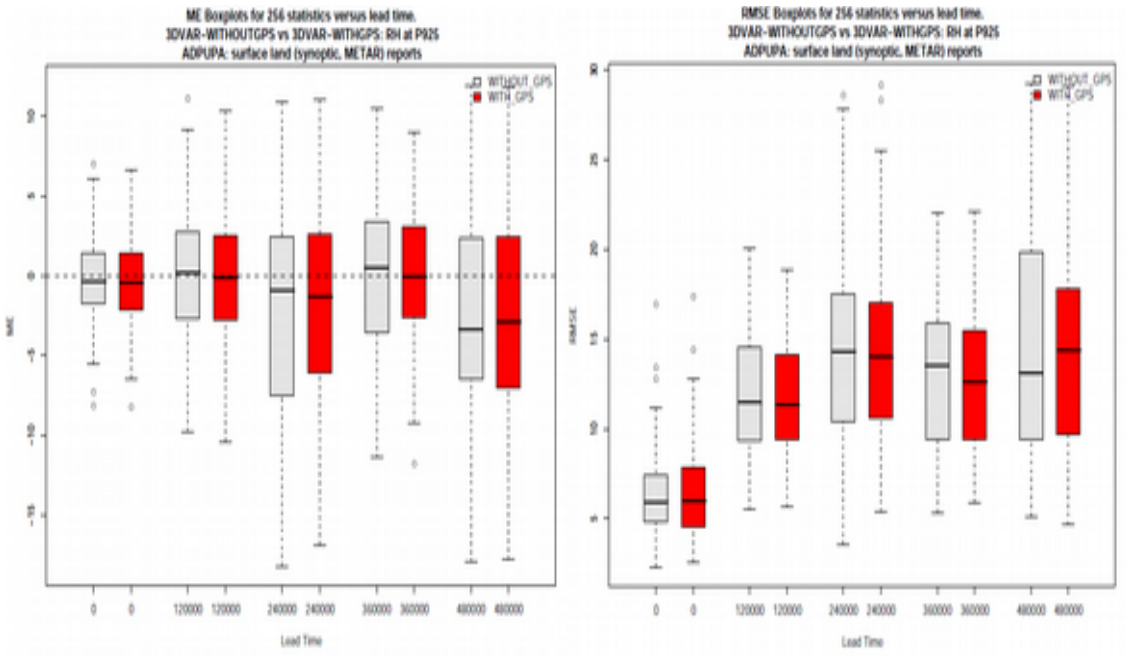

Figure 4: Bias (left) and RMSE (right) of humidity forecast errors at 925hPa

3 Installation of cy40ope2 in ALADIN-MAROC 7.5 Km, 70 l in Morocco

The cycle CY40ope2 has been compiled and implemented in the double suite for ALADIN-MAROC. Before its implementation in operation, scores and comparison to cy36t1 are ongoing for both ALADIN-MAROC and AROME MAROC.

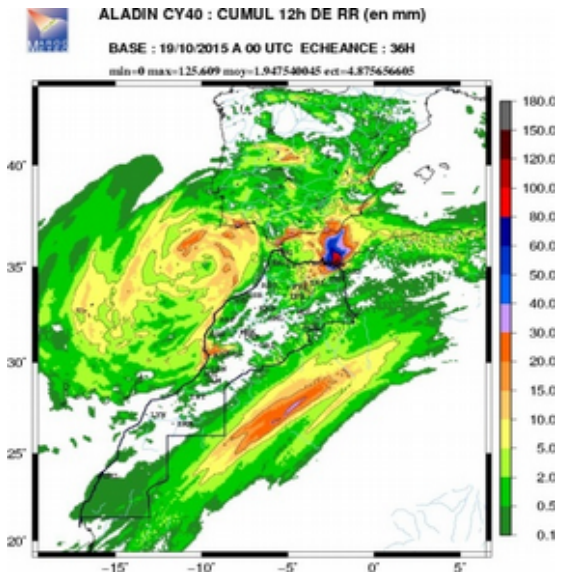

ALBACHIR cy40ope2, 7.5Km, 70 l

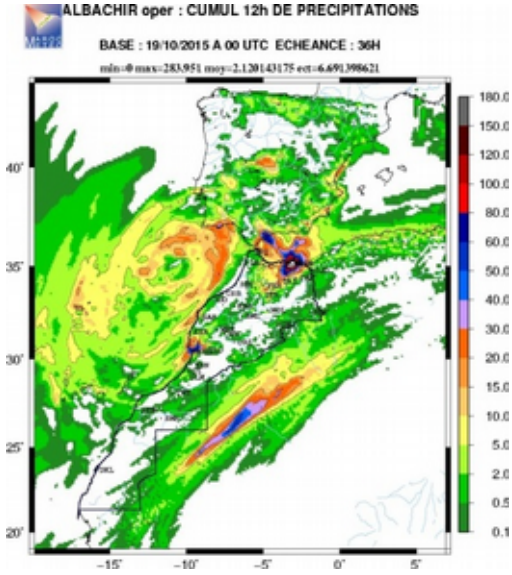

ALBACHIR cy36t1, 10 Km, 60 l

4 References

Fatima Zahra Hdidou, Zahra Sahlaoui : GPS Project documents
Siham SBII : activity report
Essaouini Karam: Activity report

Meteorological Co-operation on Operational NWP

MetCoOp-group (contact Ulf Andrae, SMHI)

1 AROME-MetCoOp

In March 2014 the meteorological cooperation (MetCoOp) between SMHI and MET-Norway, became operational. The most important feature of this cooperation is that the forecasts from daily AROME-MetCoOp runs on the Norwegian HPC (Vilje) are distributed both to SMHI and MET-Norway. Similar back-up runs are performed at the Swedish HPC (Frost). The integration domain is shown in Figure 1.

Since 8 December 2014 AROME-MetCoOp has used Harmonie Cy38h1.2 (2,5km horizontal resolution and 65 vertical levels). At that time the model used 3D-VAR data assimilation (conventional observations, AMSU-A and AMSU-B/MHS) and surface assimilation with 3-hourly cycling. The lateral boundaries were taken from ECMWF (every hour) and the forecast length was +66hr (only 00, 06, 12 and 18 UTC). During 2015 several aspects of the model system have been improved. A limited set of GNSS data (March), radar reflectivity (June) and IASI-data (November) have been included in the 3D-VAR assimilation scheme. In general, these changes result in a neutral or slightly positive impact on forecast skill. In addition, from November SICE (Simplified Sea Ice Scheme) is included, and SST for the Baltic Sea is taken from the Hiromb ocean model operated by SMHI. These latter changes give a significant local improvement of verification scores at the Swedish coast during periods with rapid changes in SST (Figure 2).

To improve the near surface temperature,effort has been spent on surface processes and on optimizing the size of the analysis increment in the surface analysis. With the reference code we see that the surface increments to the soil temperature (TG1 and TG2) don't have any impact on the forecast of near surface temperature beyond a very few hours. The surface layer has very little heat capacity and the resulting increments to the deep soil are too small. At the moment we therefore have increased the analysis increment according to Lindskog et al. (2012), even if we know that this change in combination with model snow melt feedback can give undesired effects (e.g. unrealistic very hot soil temperatures) and we have to monitor the model performance closely. A better long term solution that we are aiming for is to apply an Extended Kalman Filter for the surface data assimilation. We are currently investigating methods to improve the modelling of surface temperatures in areas of snow.

Alongside the operational forecasts, a pre-operational suit is also running on a daily basis, which is setup identical to the operational forecast, but contains additional model components that are expected to enter the operational suit after technical and scientific validation. In the present pre-operational suite, the critical condensation threshold in the Sundquist parameterization for precipitation generation was modified to be described as a function of temperature at the lifting condensation level. For lower temperatures the threshold is lower as it was reasoned that precipitation production is likely to be favored by active ice-phase processes, so that when cloud-base temperature is close to 0°C, precipitation is possible with relatively shallow convective clouds (Kain and Fritsch, 2004). This type of phenomena is particularly evident in predictions of "lake-effect snow" (e.g., Niziol et al. 1995) We believe that this change will improve a substantial model deficiency experienced during the last few years. Under conditions with an onshore wind component combined with very shallow convection in northern Norway it is often observed (heavy) precipitation, which is not captured by the model. In addition to this change, we have recently started to assimilate scatterometerdata in the pre-operational suite.

Another important milestone from 2015 is that MetCoOp has taken the new Swedish HPC (Frost) in use for operations. With the increase in computer capacity the first MetCoOp EPS (MEPS) experiments have also been conducted and we plan for daily test runs from early 2016. The first

version of MEPS will include 10 members (3 to +66hr, 7 to +36hr) 4 times a day, with the same domain and resolution as the current deterministic AROME-MetCoOp. Initial and lateral boundary perturbations will be calculated with the Scaled Lagged Average Forecasting (SLAF) method. However, the perturbation method will be under considerations and compared to methods based on ECMWF ENS output. Effort has also been put into monitoring of the observation usage, and this has shown to be very useful at several occasions (detection of missing important observations or usage of observations in an incorrect way).

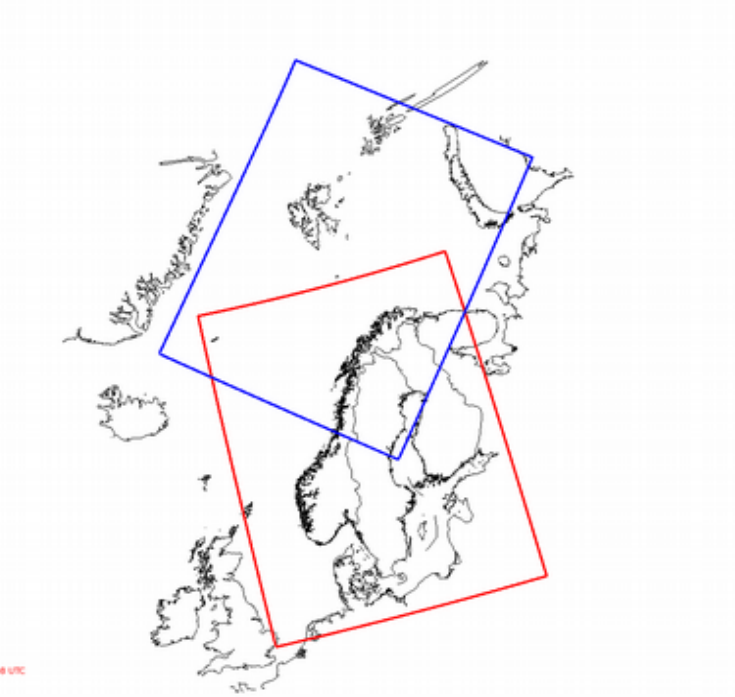

Compared to other models (i.e. ECMWF, HIRLAM) used operationally at SMHI and MET-Norway AROME-MetCoOp verifies very well. However, some deficiencies in the model performance are still noticeable. The most pronounced deficiency in 2015 might be the very long spin up of humidity, and thereby precipitation and (low) clouds (Figure 4 illustrate a particular problematic case). A part, but not all, of the spin-up problem was due to an artificial drying introduced by the assimilation of radar reflectivity. The reason for this was the handling of the lower detection limits of the radar observations. This is now solved by making the assimilation independent of the lower limits of individual radars. However, the investigation of the problem continues and we see spin-up differences in regions, seasons and for different weather types. Days with reduced forecast skill are also associated with fog and cloud cover in general and issues related to the near surface temperature and precipitation.

Figure 1. In red the AROME-MetCoOp domain operated by SMHI and MET-Norway, in blue the AROME-Arctic domain operated by MET-Norway.

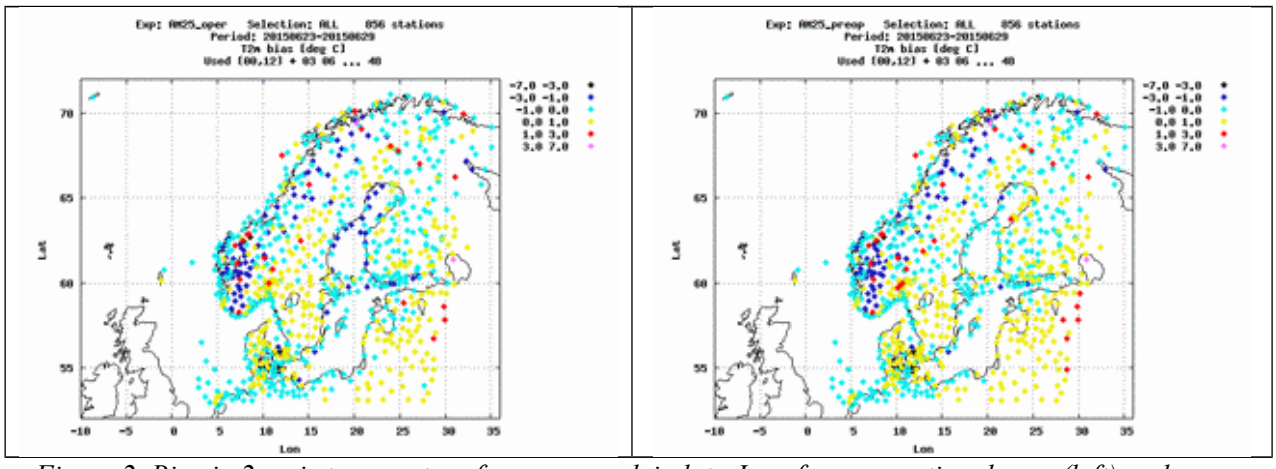

Figure 2. Bias in 2m air temperature from one week in late June from operational runs (left) and pre-operational runs (right). The difference between the two versions is that SST for the Baltic Sea is from ECMWF in the operational runs while from the Hiromb ocean model in the pre-operational runs which is reflected in the difference in bias of the Swedish coast stations.

2 The use of AROME-MetCoOp at MET-Norway

At MET-Norway AROME-MetCoOp is the main weather forecasting model. The model is used to force several downstream applications (i.e. turbulence forecasts at airports, air quality forecasts and ocean forecasts). AROME-MetCoOp is also the main model for the duty forecasters and the basis for the official weather forecasts on Yr.no (api.met.no). For the latter application the model output is post-processed for several parameters (temperature, wind, wind gust, precipitation, cloud cover, lightning).

For several severe weather events (precipitation and wind) during the last year AROME-MetCoOp has offered very good forecast guidance. In Figure 3, scatter plots of 24hr accumulated precipitation for all Norwegian observation sites are compared to AROME-MetCoOp (red) and ECMWF HIRES (blue) for the 6 wettest periods autumn 2015. However, the spin up problem, and especially in the summer, has also been the origin of frustration among users, forecasters and researchers. A summer case is illustrated in Figure 4. For the short forecasts the heavy showers seen from radar reflectivity lacks in the south east of the domain, while for the longer forecasts the location is wrong due to lack of local predictability of the system.

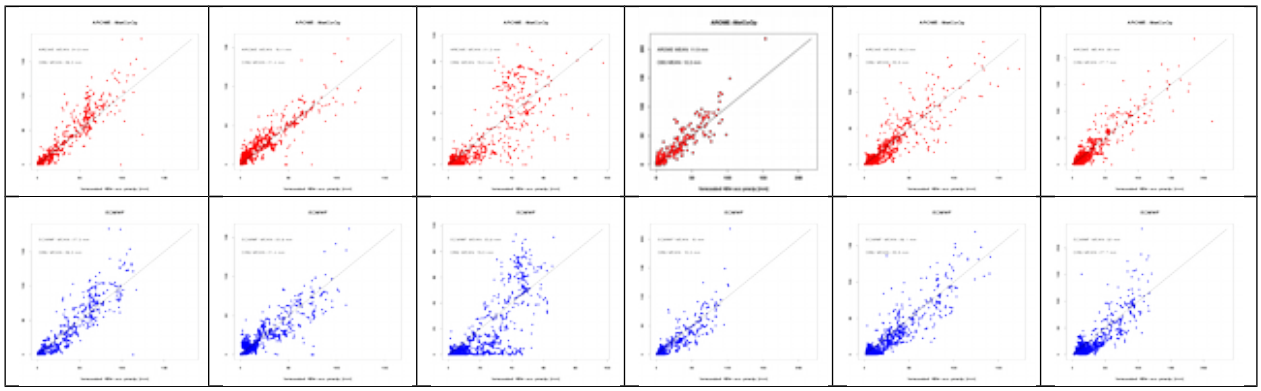

Figure 3. Examples of observations (y-axis) and forecasts (x-axis, AROME-MetCoOp in red and ECMWF in blue) of 48hr accumulated precipitation under the 6 wettest periods autumn 2015 in Norway.

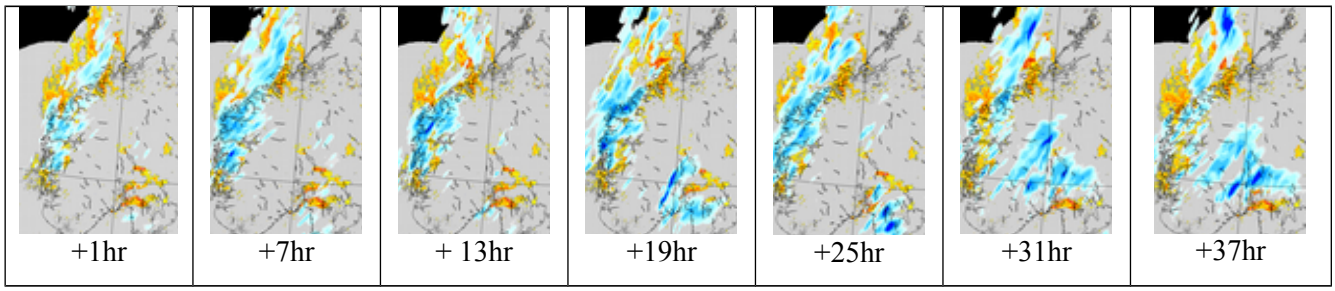

Figure 4. An example of the spin-up effect. 1hr precipitation forecast from AROME-MetCoOp and radar reflectivity. All pictures valid for 7.August 07UTC, but with forecasts for 7 different lead times.

From October 2015 MET-Norway has in addition been running daily runs with AROME-Arctic. The same domain size and model version as AROME-MetCoOp, but with somewhat different observational usage has been implemented for an Arctic domain (see Figure 1).

3 The use of AROME-MetCoOp at SMHI

At SMHI, AROME-MetCoOp is one of the models that can be chosen as input to the operational weather forecast data-base in addition to the ECMWF model, and two different set-ups of the HIRLAM modeling system, running on 11km and 5.5km grid respectively. The data-base, running at 2.75km, with rotated lat-lon grid has a great number of users, both in the commercial and public sector, as well as the internal production at SMHI. The data base contains both the standard meteorological parameters as direct model output, as well as a large variety of postprocessed variables. Methods have been introduced for e.g. cloudiness and precipitation to handle the detailed structures and their uncertainty. As an example, precipitation is given by a maximum, minimum, mean and median within a neighbourhood of 20 km.
In general the model performs well in regards to wind, wind-gusts, temperature and precipitation. The main problem in the present version is an over-prediction of low level clouds, affecting parameters important for aviation such as visibility. However, during an unusually dry period in October, 2015, forecasters reported a systematic under-prediction of low level clouds. All models available for the forecasters at SMHI captured the clouds except for AROME-MetCoOp, Figure 5 and 6. It was found that the under-prediction of low level clouds was related both to the initial amount of moisture, and to the representation of shallow convective clouds. The forecast was improved by introducing corrections to the assimilation of radar reflectivities, as well as implementing the shallow convection formulation used in the pre-operational suit mentioned above. In figure 6, middle and right, we see the combined impact of these two changes on low level cloud cover.

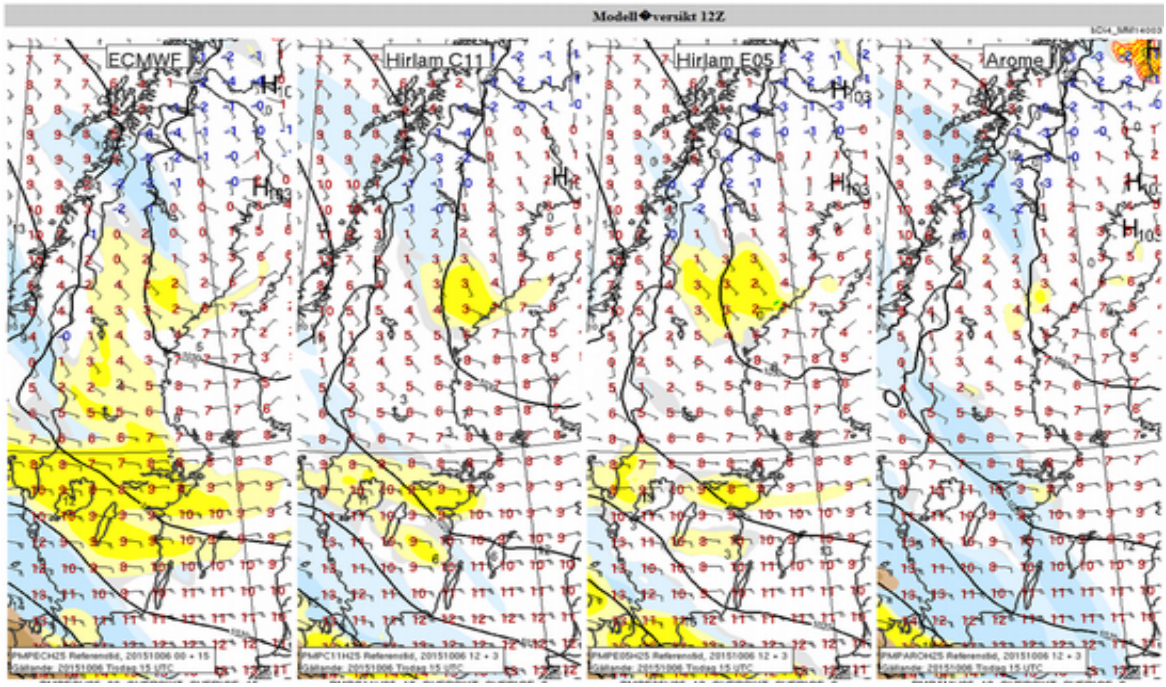

Figure 5. Forecast for 2015-10-06 15UTC from (left to right) ECMWF, HIRLAM 11km, HIRLAM 5.5km and AROME.The yellow areas indicate low level clouds .

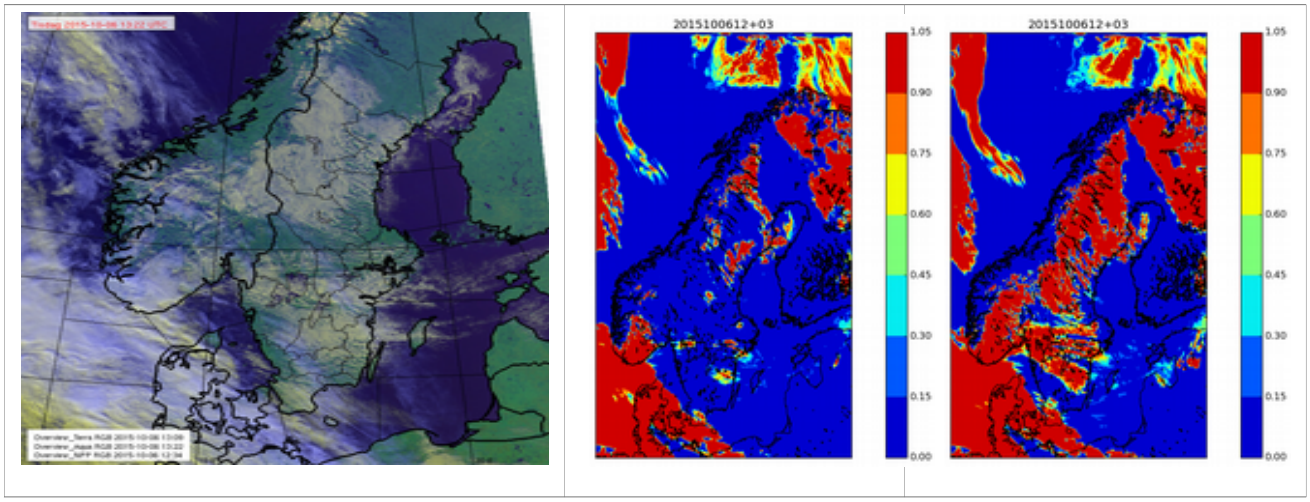

Figure 6. Left: Polar view of cloud cover from visible channels for 2015-10-06 13UTC. Middle: Operational AROME-MetCoOp low level cloud cover for 2015-10-06 15UTC. Right: Low level cloud from the updated model (see text) for the same occasion.

References

Lindskog et al, 2012: http://www.cnrm.meteo.fr/aladin/IMG/pdf/smhi_surface_asm_2012.pdf

Kain, John S. "The Kain-Fritsch convective parameterization: an update." *Journal of Applied Meteorology* 43, no. 1 (2004): 170-181.

Niziol, Thomas A., Warren R. Snyder, and Jeff S. Waldstreicher. "Winter weather forecasting throughout the eastern United States. Part IV: Lake effect snow." *Weather and Forecasting* 10, no. 1 (1995): 61-77.

ALADIN in Poland - 2015

Marek Jerczynski, Bogdan Bochenek, Marcin Kolonko, Malgorzata Szczech-Gajewska, Jadwiga Woyciechowska

1 Introduction

Various efforts were carried out at IMGW in 2015. Among them: switch to CY40T1 version of ALADIN system and exchange ALARO-0 with ALARO-1, putting into operational service new sub-regional suite also installation, testing and using of CROCUS snowpack for hydrological purposes and application of new NWP products in frame of ISOK project.

2 Operational activities

During 2015 two NWP suites were operationally exploited at IMGW. First, sub-regional one based on ALARO-1 model was put into service in this year autumn. Its domain covers almost all territory of Europe (see Figure 1) with 4.0 km resolution. Second, high resolution suite which domain covers Central Europe has 2.5 km grid-size and is based on AROME. Both suites use CY41T1 code version of ALADIN system. Table 1 summarizes main features of the suites, and figures Figure 2 and Figure 3 present examples of forecast maps for E040 domain.

Table 1: Current operational configurations

Suite	Sub-regional	HiRes
Domain	E040	P025
Model	CY40T1 / ALARO-1	CY40T1 / AROME
Resolution	4.0 km	2.5 km
Area	3156 km x 3156 km	1600 km x 1600 km
Grid	800 x 800	648 x 648
Levels	60	60
Coupling zone	16	8
Runs	4 / day	4 / day
Starting times	00, 06, 12, 18 UTC	00, 06, 12, 18 UTC
Forecast range	66h, 66h, 66h, 60h	30h
Coupling model	ARPEGE	ALARO - E040
Coupling frequency	3h	1h

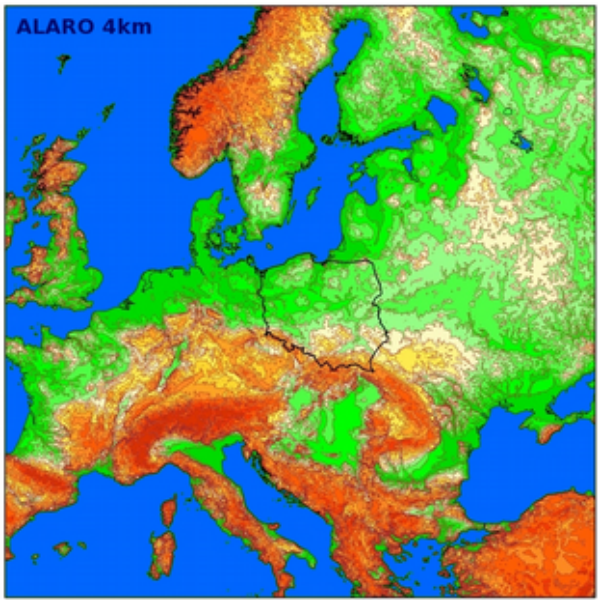

Figure 1: Domain E040

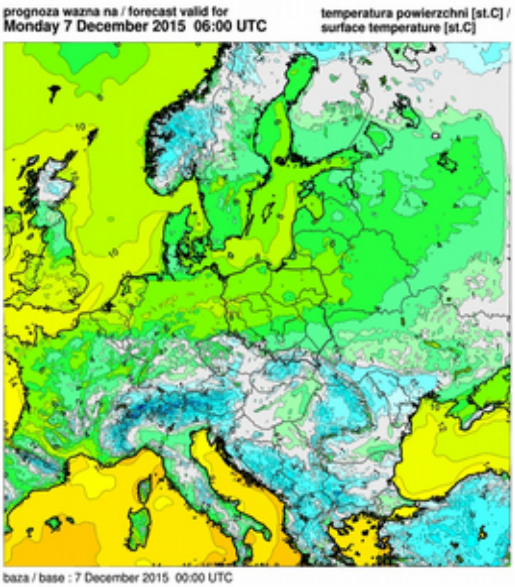

Figure 2: Forecast map for new domain – surface temperature

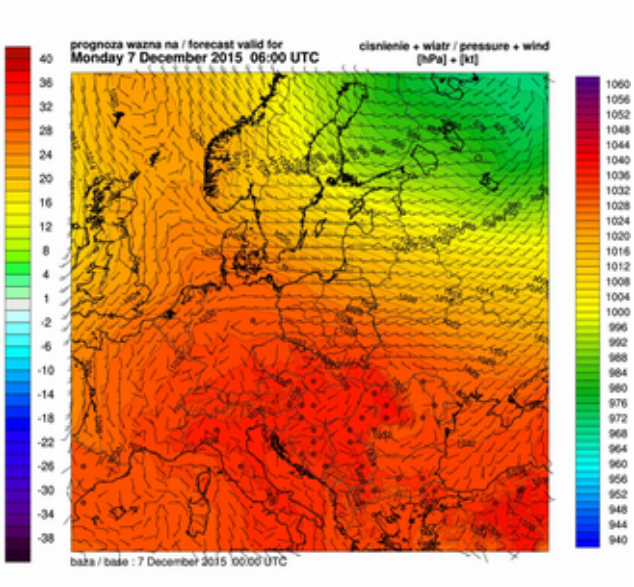

Figure 3: Forecast map for new domain – msl pressure and 10-m wind

Cooperation with Meteo France led to implementation of snow model CROCUS at IMGW. SURFEX OFFLINE code was downloaded and compiled on local cluster and as an input AROME forecast with 2.5 km resolution was applied. Various tests were done to validate snow model implementation. Winter season 2008/2009 was chosen to check results, as it shows big values of snow cover - even 3,5 m in Tatra Mountains. Additional validation was carried out for season 2014/2015. Example comparison of CROCUS forecast and SYNOP observations for Hala Gasiennicowa is shown at Figure 3.

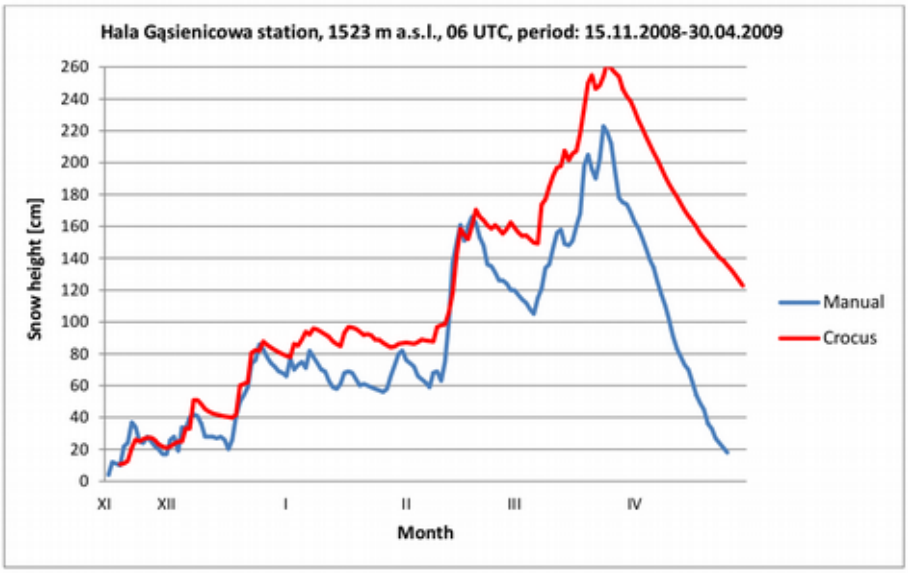

Figure 4: CROCUS model snow cover forecast for Hala Gasiennicowa

Comparison of CROCUS results with IMS3 image for snow cover over Poland is presented below – Figure 5. Further work was dedicated for testing CROCUS for hydrological applications, such as determining SWE for different rivers.

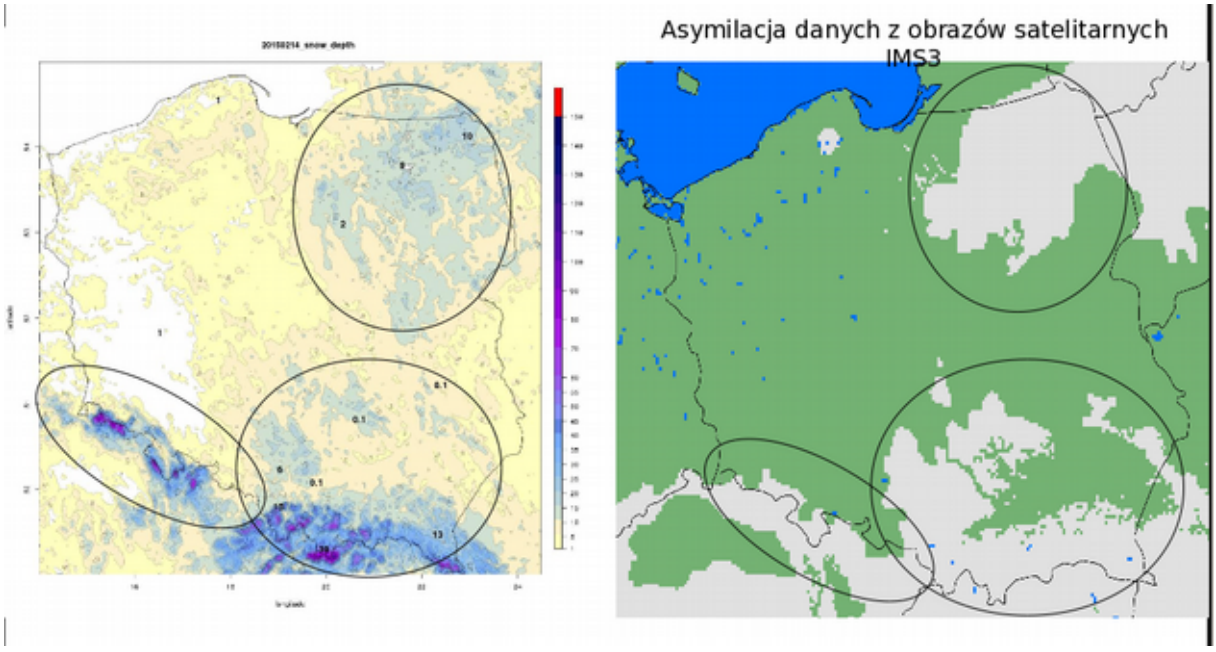

Figure 5: Comparison of CROCUS predicted snow cover with IMS3 product

Within an ISOK Project (Polish acronym of IT System for Country Protection against extreme hazards) ALADIN team cooperates with different departments of IMWM to develop a system of national protection, which includes protection against floods, identification and warning against extreme meteorological phenomena and technological (synergistic) events. Forecast charts, updated twice a day and constructed on the basis of a ALARO-1 model and developed algorithms provide

information on the current meteorological hazards (for the next 12, 24 and 48 hours). Meteorological hazard maps are combination of recent model forecast and historical maps of spatial diversity of extreme weather phenomena in Poland. Figure 6 shows an example of ISOK operational product.

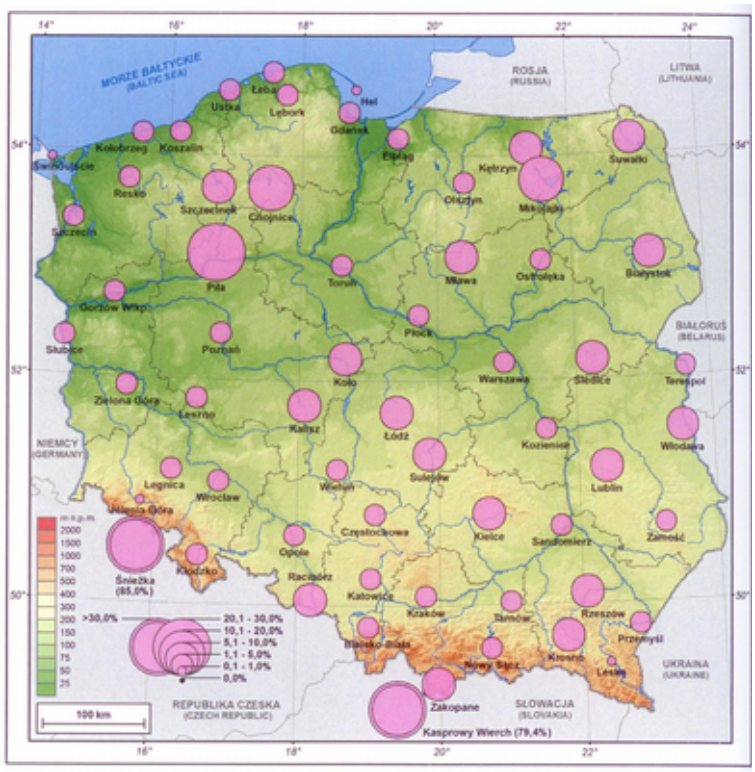

Figure 6: Occurrence probability of a day with rime ice in February

ALADIN Highlights for IPMA, I.P. (Portugal)

Maria Monteiro, João Rio, Vanda Costa, Manuel João Lopes, Lourdes Bugalho, Nuno Moreira

1 Introduction

As a continuity of the last report, effots have been focused into the three main aspects: in the first place, on the upgrade of the Portuguese Numerical Weather Prediction (NWP) operational system; secondly, on the support of internal and external customers of the NWP products; and finally, on the design and creation of a local data assimilation system. In this publication, we summarise the main achievements on these different aspects.

In section 2, details are given on the local NWP system progress. In section 3, some basic information is provided on NWP historical scores computed from the forecasts of three different locally available models: the (disseminated) global model from the European Center for Medium-range Weather Forecasts (ECMWF) and the local versions of ALADIN and AROME limited area models. Finally, in section 4, it is provided the status of a local surface data assimilation component of a future local data assimilation system.

2 Local NWP operational system evolution status

During 2015 several upgrades of the local NWP operational system have been accomplished taking advantage of the recent acquisition and installation (2014) of a new High Performance Computing (HPC) plataform, the IBM Power 7+ (8+1 nodes).

In April, a first step was successfully given, with the entrance into operations of a new cycle in all system configurations and geographical domains - the CY38T1_bf03. The main system configurations considered here were: 001 (model integration, for both hydrostatic and non-hydrostatic dynamics, with ALADIN and AROME physics, respectively) and 701 (standalone screen level parameters hourly analysis, using ALADIN background and SYNOP observational data).

As detailed information, it is worth mentioning three significative changes on the new system: the enlargement of the AROME-Portuguese Mainland domain, particularly eastward, the upgrade of the climatologies to CY38, and the implementation of a new AROME initialization by direct coupling of the ARPEGE model analysis (from Météo-France) instead of using ALADIN as an intermediate coupling model. Figure 1 gives an illustration of the actual local system geographical domains (see legend for detailed description). In particular, over the Portuguese mainland, three domains can be observed: 'PTG' is the designation for the frozen domain; 'PT2' represents the actual operational domain and 'IBE' is the domain under study.

As a very general comment we can say that the impact of moving to a new cycle was more positively noticeable on the forecast scores (at least for surface parameters) than just changing the coupling model. Furthermore, changing the coupling model in particular - ALADIN at 9 km horizontal resolution to ARPEGE at 18 km horizontal resolution - has had a strong negative impact on the wind (mostly) due to the increase of the model spin up (AROME horizontal resolution is 2,5 km).

Just after this step, by the end of June, a second changing moment has happened with the implementation of a new TELECOM files' dissemination. ARPEGE coupling fields are now received four times a day at 10 km

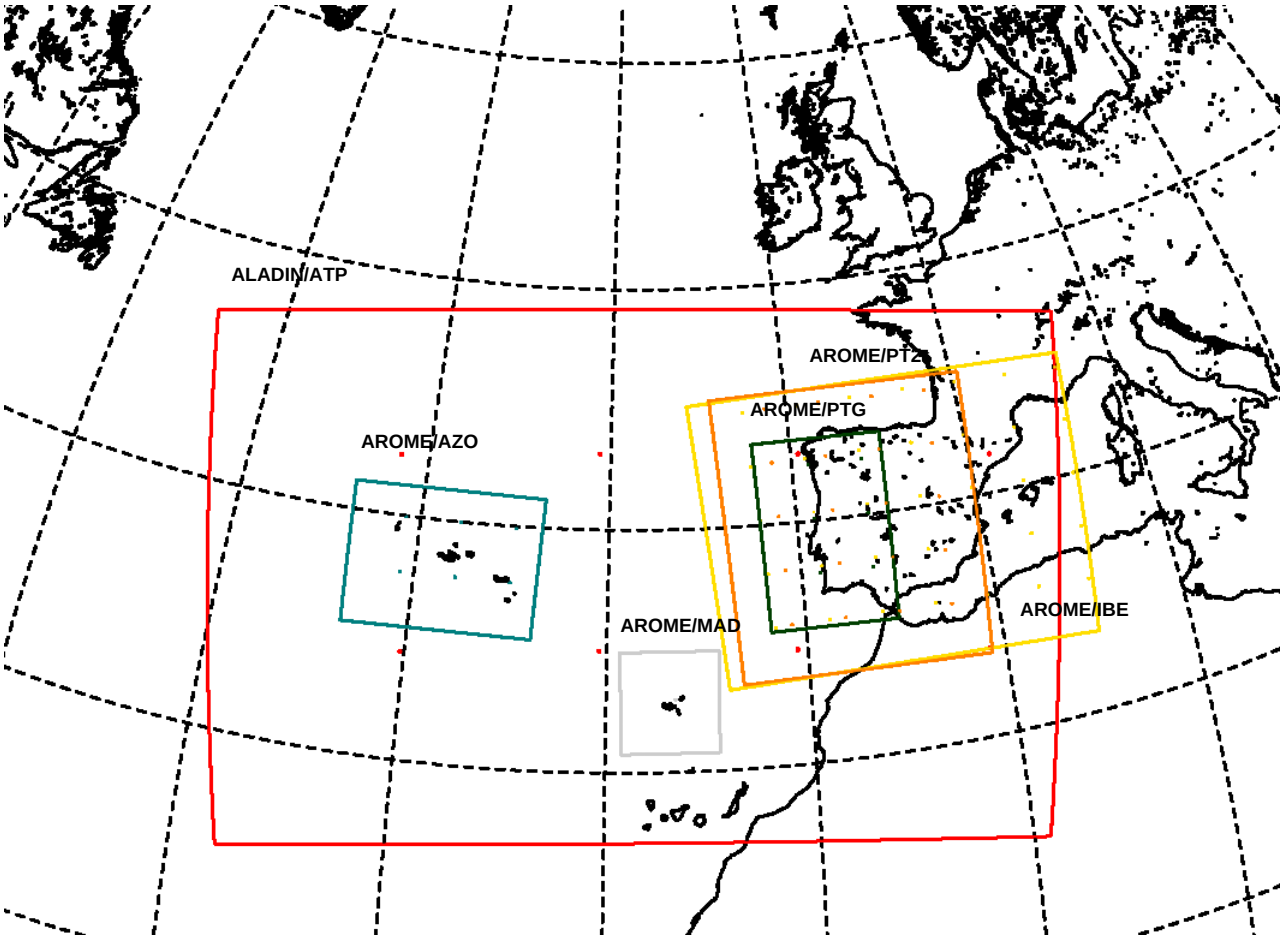

Figure 1: Geographical domains in use at the Portuguese NWP system: in red, the Portuguese Mainland and Adjacent Atlantic area, for the actual operational ALADIN/ATP (9 km) model integration; in green, the Azores archipelago, for the actual operational AROME/AZO (2,5 km); in grey, the Madeira Archipelago, for the actual operational AROME/MAD (2,5 km) model integration; in dark green, the Portuguese-Mainland, for the frozen AROME/PTG model integration; in orange, the extended Portuguese-Mainland, for the actual operational AROME/PT2 integration; and, in yellow, the future Iberian Peninsula, for the future AROME/IBE model integration.

horizontal resolution over the Portuguese Mainland plus Adjacent Atlantic area and on 60 vertical levels (using only 46 levels). Using these new facility, the AROME model is now coupled with ARPEGE at 10 km.

Foreseen upgrades on the local system include a new enlargement of the AROME-Portuguese Mainland domain in order to cover a wider geographical area of the Iberian Peninsula (the AROME/IBE) as well as the increase of the number of levels (to 60) and the increase of the model daily runs (to four times a day). At the same time, it is expected to freeze the ALADIN system configuration and to move its downstream applications to a direct AROME input. Taking into account the mentioned changes, a new pre-operational suite re-design has already taken place, which is only executed at 12UTC for validation purposes; meanwhile, an upgrade of the front-end and archiving machines is being expected to allow the execution of the pre-operational system in full, four times a day.

3 Historical scores over Portuguese mainland

The quality assessment of the local models is monitored on a daily basis, through the computation of simple statistic parameters which are plotted under several forms. In this way, historical scores using 21 synoptic observation stations (48 for precipitation) over mainland have been used to draw the quality tendency of the available surface fields used to forecast the weather conditions over Portuguese mainland territory. The chosen (surface) fields are: mean sea level pressure (at the rannge H+15), 2-meter temperature and relative humidity (at the range H+15), 2-meter maximum and minimum temperature (at the range D+2), 10-meter wind intensity (at the range H+15) and 24-accumulated precipitation (between the ranges H+06/H+30).

Plots for three models are available: ECMWF and ALADIN, since October 2007; and for AROME (2,5 km), since December 2010.

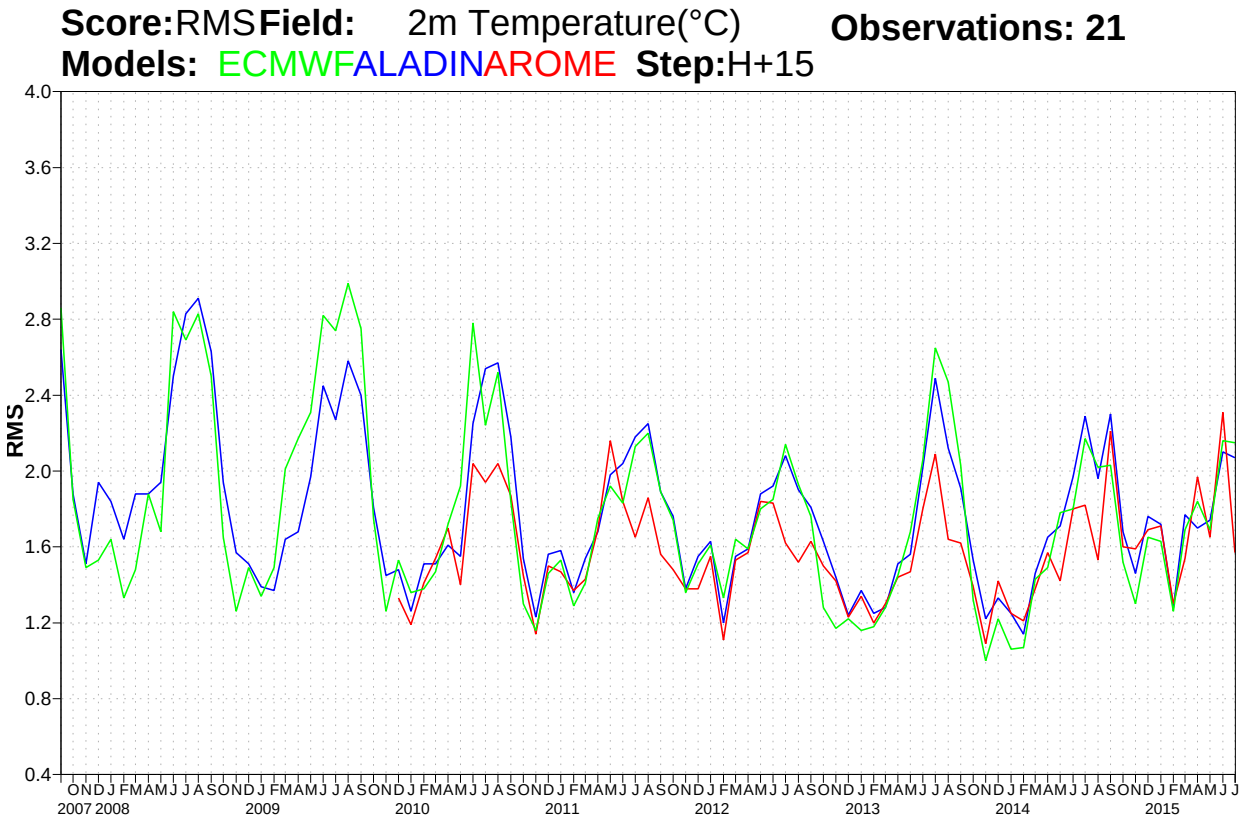

Figure 2: RMSE historical series for 2-meter temperature, using 21 observations over the Portuguese mainland, for the three different model forecasts: ECMWF (green line) and local versions of ALADIN (blue line) and AROME (red line).

As it is illustrated in Figure 2 for 2-meter temperature at the 15-hour range and as a general conclusion, we can say that a possible minimum threshold of the quality of those locally available fields has been achieved at the end of 2013. This means that (for the selected observation stations) there was a trend to decrease the RMSE in all the models up to this moment that has stabilized somehow after that. And this conclusion is common when we look to the fields forecasted by ECMWF, or by the local versions of ALADIN and AROME models. More detailed conclusions are moreover allowed from the end 2013 up to nowdays (not shown here): i) for 24-precipitation, the error is now roughly independent of the source of information, being close in all the models; ii) for the 10-meter wind intensity, the error is no longer clearly smaller if the information comes from the local

version of the ALADIN model. In fact, it seems that the local version of AROME is also a good source of information; iii) for minimum temperature, the error is smaller when the information is obtained from ECMWF forecasts; and iv) for the mean sea level pressure, the error is usualy smaller when the information source is the local version of the AROME model.

Further illustrations and conclusions can be found in ECMWF Annual Report 2015 :

(http://www.ecmwf.int/sites/default/files/elibrary/2015/10079-portugal.pdf).

4 Surface data assimilation

Along the year, a surface data assimilation scheme has been developed which is now running in test mode for validation purposes. The system has been developed in order to support the project Spanish-Portuguese Meteorological Information System, for Transboundary Operation in Forecast Fires (SPITFIRE), which has the objective to improve the information exchange on meteorology and forest fire risk in the border area of both countries, by the Civil Protection and Firefighters of both countries. The surface system analysis and forecats should be used to compute a local version of the Canadian Fire Risk Index (FWI).

Recent studies have shown that the FWI values (at the analysis time on a grid mesh) having AROME-Portuguese Mainland initial fields (H+00) at 2,5 km as input tend to provide (more) realistic results when compared with the FWI calculated from the observational data. In these studies, the AROME fields were obtained by dynamical adaptation from the ALADIN/Portugal model (CY36) at 9 km without the assimilation of surface observations. These fields are calculated by the CANOPY surface boundary layer scheme (Masson and Seity, 2009) from the AROME's surface model - SURFEX (SURface EXternalisée), taking into account the surface temperature and the lowest AROME atmospheric level (17 m) at its initial state.

At present, the local versions of the AROME-Portuguese Mainland model does not contains its own data assimilation system. In order to introduce localised observations information on the H+00 fields a surface data assimilation system was created by the OI_MAIN scheme (which uses the Optimum Interpolation scheme described in Giard and Bazile (2000) to produce the soil moisture and temperature fields needed to run SURFEX).

On the system that is already under test the surface conditions are updated each 6 hours taking into account the AROME atmospheric forcing. It produces a T2m, H2m (and V10m) analysis at each 6-hour cycle. The difference from the initial step on the FWI computation is that there is now a direct adjustment of the analysis and the model initialization to the surface conditions provided by the available in-situ observations.

Once validated, the system will be part of a more sofisticated data assimilation system of the local NWP system.

The Figure 3 illustrates a sequence of FWI daily charts valid at 12UTC, when using H+00 fields from the 12UTC daily integration of AROME-Portuguese Mainland model.

5 References

Giard, D., & Bazile, E. (2000): Implementation of a new assimilation scheme for soil and surface variables in a global NWP model. Monthly Weather Review, 128, 997-1015.

Masson, V., & Seity, Y. (2009): Including atmospheric layers in vegetation and urban offline surface schems. J. Appl. Meteor. Climatol., 48, 1377-1397.

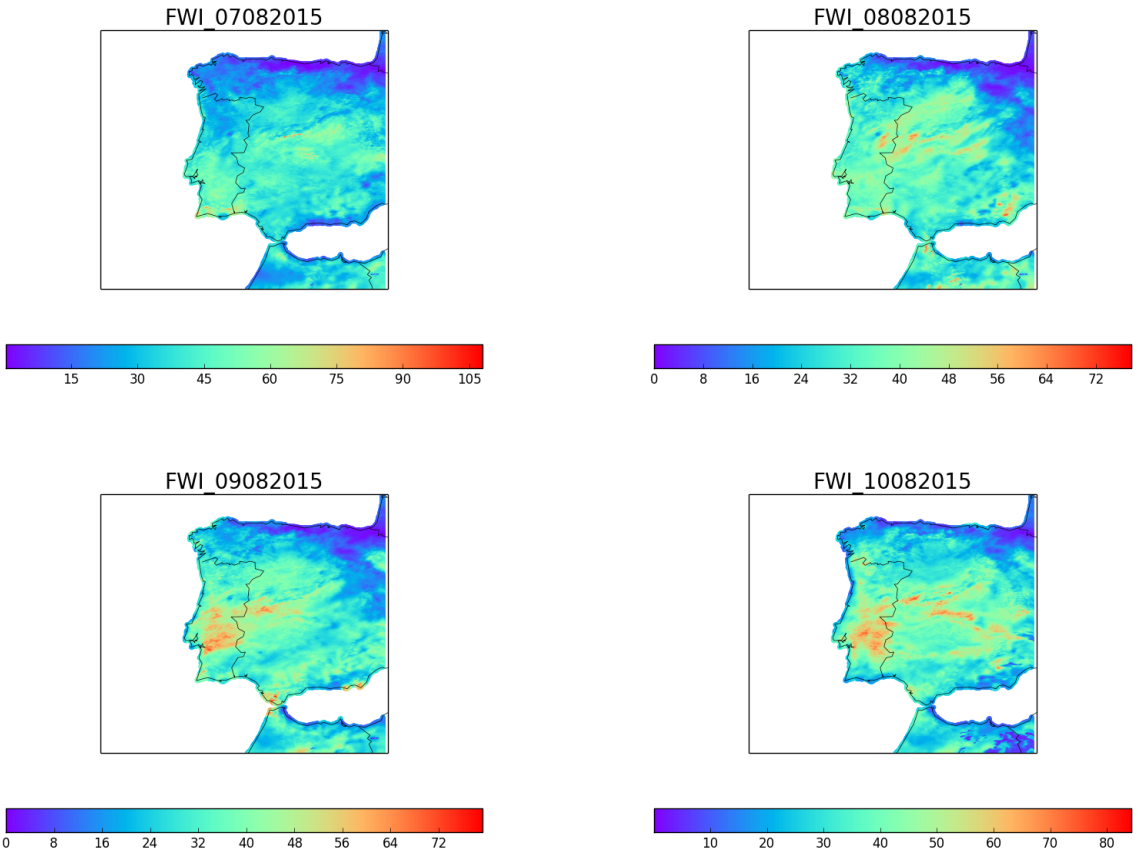

Figure 3: FWI computed on the AROME-Portuguese Mainland gridpoint mesh at 2,5 km resolution, using the model's H+00 screen level fields, post-processed by the CANOPY scheme, for the 12UTC on the sequence of days: 07, 08, 09 and 10 of August 2015.

Wind shear profile using SODAR data and ALARO model

Ana Denisa Urlea[1], Simona Taşcu[2], Mirela Pietrişi[2], Alexandra Crăciun[2], Simona Briceag[2]
[1]Romanian Air Traffic Services Administration, Romania
[2]National Meteorological Administration, Romania

1 Introduction

Analysis of the low level wind shear effects on aircraft flights, especially in the phases of take-off and landing aircraft, is an important topic for aviation. This phenomenon can be generated from several sources, for example: frontal surfaces, convection, breezes (either sea or mountain originated), strong surface wind coupled with local topography, mountain waves or low level temperature inversions.

Often, the Low Level Wind Shear can be caused by the presence of a Low Level Jet. Over Romania, the Low Level Jet can occur for different reasons, the most encountered synoptic situation being characterized by a Mediterranean Low in the South-Eastern part of Europe, mainly in winter, but sometimes also in the first days of spring or last days of autumn. This leads to Low Level Wind Shear in a layer up to 600 m above surface, affecting approaching, landing or take-off phases of an aircraft flight.

2 Statistical approach

The aim of this study is to assess the data collected at Otopeni airport site (44°34'16" N and 26°05'06" E), obtained from the SODAR (**SO**nic **D**etection **A**nd **R**anging system -PCS.2000- Metek) instrument (Figure 1). The validation was performed for a three months period (May – July 2014), using different height levels (between 60 m – 220 m, having 20 m space resolution). The SODAR data were analysed and compared in respect to the limited area model ALARO operationally integrated at the National Meteorological Administration of Romania, having 6.5km horizontal resolution and 60 vertical levels with a higher vertical resolution near the surface. For this comparison, the ALARO forecasts were post-proccessed at the same height levels for the same period.

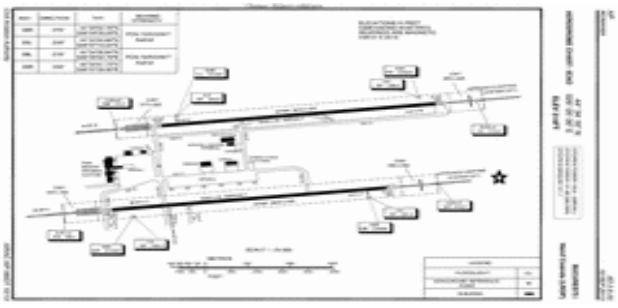

Figure 1. SODAR placement (represented by asterisk) at the Otopeni airport in Bucharest

In order to approximate the wind shear profile, the shear power law exponent (alpha) is computed as follows (Rareshide, 2009):

$$\frac{U_z}{U_{ref}} = \left(\frac{z}{z_{ref}}\right)^{\alpha}$$

where U_z is the wind speed at height z, U_{ref} is the wind speed at the reference height z_{ref} and α is the power law exponent. In our case, the reference height is 60 m.

The α power law exponent describes the shape of the wind shear profile, a low α indicates little shear (the wind speed does not drastically change) and a high α indicates large shear. Figure 2 shows the wind shear profile for SODAR and ALARO data. The α value for SODAR is 0.27292 and for ALARO forecasts is 0.22769. It can be noticed that ALARO model underestimates the wind shear, but it has a more logarithmic profile.

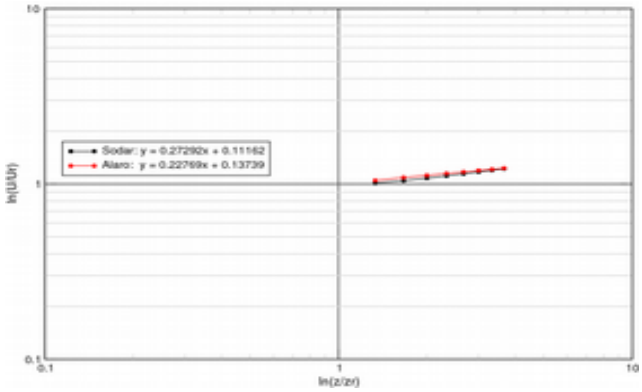

Figure 2. α power law exponent for SODAR (black) and ALARO (red) for Otopeni airport for May – July 2014

Another type of comparison was to calculate the mean of the SODAR and ALARO wind speed (Figure 3), for the whole period and for each month in part, at the same height levels as above (between 60 m - 220 m). It can be observed that the lowest error is for July, when the convective activity was intense.

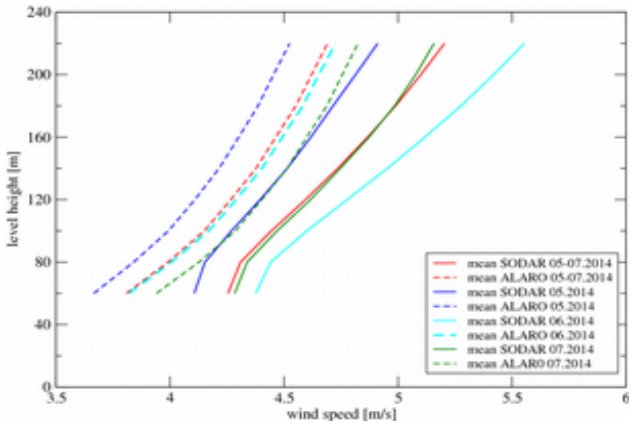

Figure 3. Average wind speed profile for: SODAR – solid lines and for ALARO – dashed lines (red – mean for May-July 2014, blue for May 2014, cyan for June 2014, green for July 2014)

Figure 4 shows the wind speed averaged over all height levels for each hour between 00 – 23 UTC, for SODAR and ALARO model. It can be noticed that they have a comparable diurnal cycle,

having similar values between 06 - 18 UTC. Therefore, the results show that ALARO model is able to capture the values of wind speed during daytime when the convective activities are more intense.

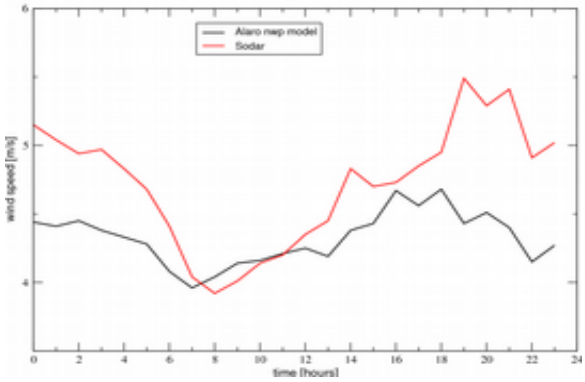

Figure 4. Hourly and level averaged wind speed for: SODAR – red line and for ALARO – black line, for Otopeni airport for May – July 2014

3 Case of 21st of June 2014

Furthermore, a case study from June 21, 2014 was analysed, when the Control Tower from Otopeni airport (AFR 081C) reported severe turbulence at 11:30 UTC and height 20 FT above ground level. The synoptic situation was characterized by a low pressure system and the presence of a upper trough over the East of Europe (Figure 5).

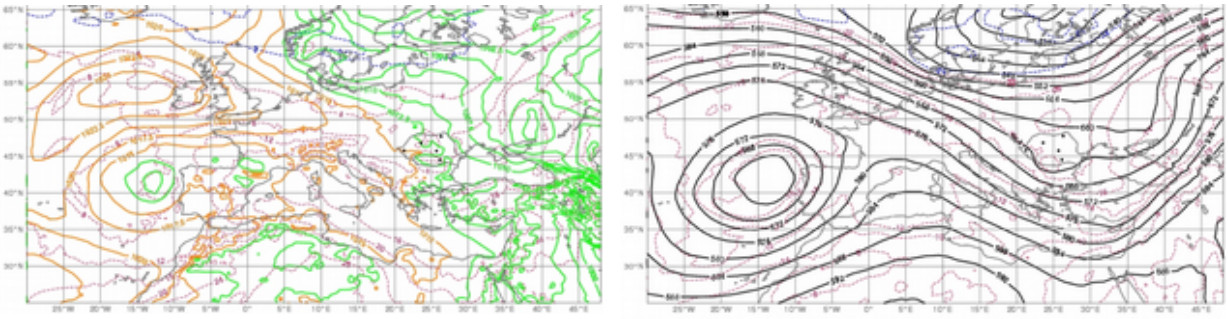

Figure 5: ARPEGE analysis 21.06.2014, 12 UTC: left – mean sea level pressure and temperature at 850 hPa and right - geopotential and temperature at 500 hPa

A nucleus of maximum vorticity, located in the South-Western part of Romania in the morning (Figure 6, left), moves to the South part of the country in the evening (Figure 6, right) providing favourable conditions for wind shear.

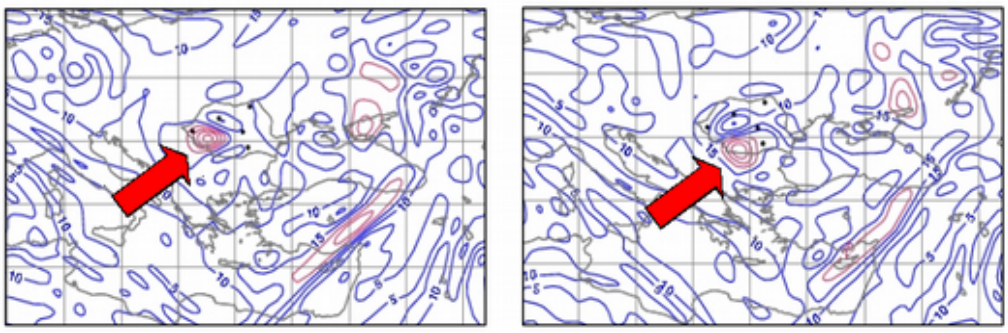

Figure 6: ARPEGE analysis 21.06.2014, absolute vortex at 500 hPa: left – 06 UTC and right – 12 UTC

The SODAR wind profile (Figure 7) shows an increase of the wind speed from 10 - 11 UTC, for height levels between 260 m – 500 m. Thus, the wind speed strengthens from 5-8 m/s up to 15 m/s, with a change in direction from 180 to 220-230 degrees North. For the following time interval 11 – 13 UTC, constant wind speed and direction (about 5 m/s and 210 degrees North) is observed for all vertical levels. After 13 UTC, the wind speed increases, with a change in direction from North up to the 300 m level and from West between 300 - 500 m. All these facts indicate the presence of the wind shear, the wind direction changing with 60 degrees and the wind speed varying from 22 knots to 40 knots (an increase of 8-10 m/s).

Although the wind speed is underestimated by the ALARO model, a wind speed increase and change in direction can also be observed in the meteogram plotted in Figure 8.

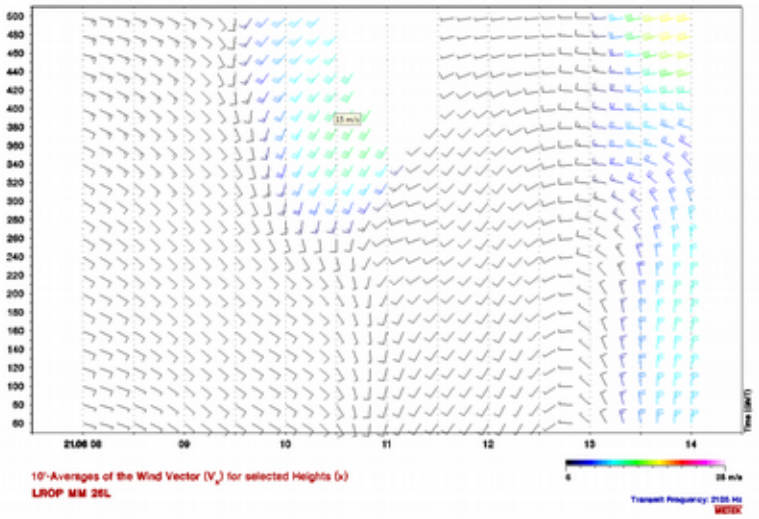

Figure 7: SODAR wind profile for Otopeni airport: 21.06.2014, 08 UTC – 14 UTC

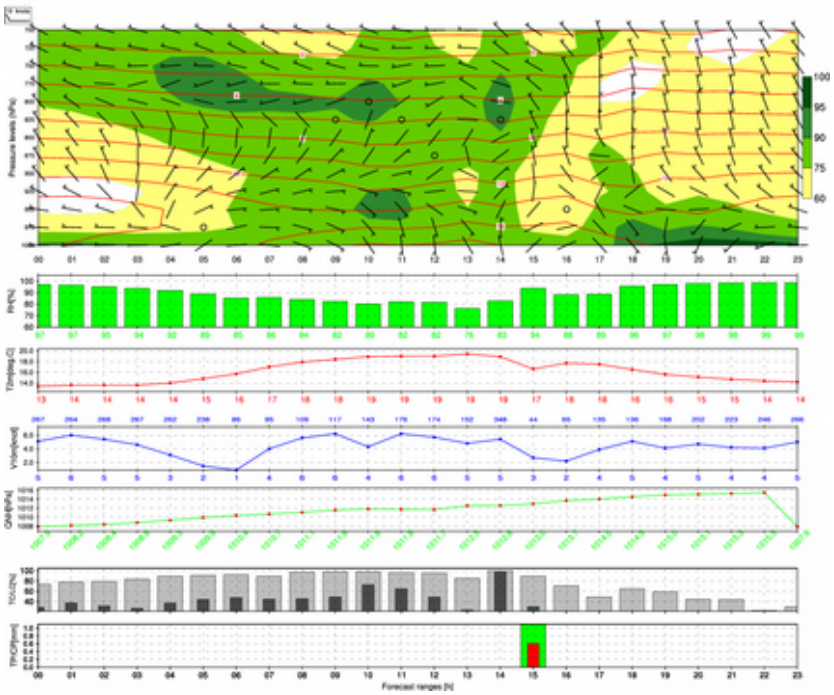

Figure 8: ALARO meteogram for Otopeni airport from 21.06.2014, 00 UTC

4 Conclusions

The results of this study indicate that the ALARO model has a more logarithmic profile compared to the SODAR, underestimating the wind shear at the low atmospheric levels for Otopeni airport (with a difference of 0.05 between the ALARO and SODAR alpha values). Also, the diurnal cycle for the wind speed is similar for the two systems, especially noticing the fact that the ALARO model simulates well the wind speed during the daytime, when the convective activity is more intense.

5 References

Rareshide E., A. Tindall, C. Johnson, A.M. Graves, E. Simpson and J. Bleeg, 2009: "Effects of complex wind regimes on turbine performance". Podium presentation at the AWEA WINDPOWER Conference. Chicago, US.

ALADIN related activities @SHMU (2015)

Mária Derková, Martin Belluš, Jozef Vivoda, Oldřich Španiel, Martin Dian, Viktor Tarjáni

1 Introduction

The summary of ALADIN related activities at Slovak Hydrometeorological Institute in 2015 is given. The setup of ALADIN operational system is described and some research and development activities are highlighted.

2 Operational ALADIN/SHMU NWP system

The ALADIN/SHMU system setup

The operational ALADIN/SHMU NWP system covers so-called LACE domain with 9km horizontal resolution and 37 vertical levels. It is running 4 times per day up to +72h. Current model version is based on CY36T1 with so-called ALARO+3MT physics and ISBA surface scheme, coupled to Arpege global model. The spectral blending by digital filter is applied for the upper-air pseudo-assimilation using Arpege analysis. For surface the CANARI data assimilation scheme using additional local observations is active. More ALADIN/SHMU details are given in Table 1. In addition, the high resolution e-suite is running since June 2014 with resolution of 4.5km in horizontal and 63 levels in vertical. It is based on CY38T1bf03_export version with ALARO-0 physics setup. The assimilation system is identical with the operational one.

Table 1: ***ALADIN/SHMU - operational & e-suite setup, HPC parameters***

Model version	ALADIN/ALARO, CY36T1_bf10	CY38T1bf03_export, ALARO
Resolution	9.0 km	4.5km
Levels	37	63
Area	2882 x 2594 km (320 x 288 points) [2.19; 33.99 SW, 39.06; 55.63 NE]	2812 x 2594 km (625 x 576 points) [2.31; 33.77 SW, 39.07; 55.88 NE]
Initial conditions	CANARI surface analysis & upper-air spectral blending by DFI 6 hours cycling	
Boundaries	ARPEGE, 3h coupling frequency	
Starting times	00, 06, 12, 18 UTC	00,06, 12, 18 UTC
Forecast length	+72h (+60h at 18UTC)	+78h/+36h/+72h/+36h
Physics	ALARO+3MT	ALARO-0 (CY38t1bf03)
Surface scheme	ISBA	
Dynamics	2TL SL hydrostatic; SLHD	
HPC	10 nodes of IBM Power 755: 4x Power7 8core CPUs, 256 GB RAM total: 320 CPUs, 2.5 TB RAM	
Management servers	2x IBM Power 750: 1x Power7 6core CPU (3.6 GHz), 64 GB RAM	
Software & file system	AIX 6 SE OS, IBM Load Leveler queueing system, 40 TB GPFS	

Activities in Y2015 and plans for Y2016

- The telecom climate and LBC files were upgraded in coordination with LACE (and ALADIN) Partners on 30/06/2015 to follow the Arpege resolution increase (8km, 105 levels).

- High resolution e-suite on CY38T1bf03_export was extended to four runs/day upon the request of aviation meteorology department. Outputs for 06 and 18UTC are available up to +36h. The 00UTC production was prolonged up to +78h.

- The ALARO-1 physics package has been implemented and tested in above-mentioned high resolution environment for CY38T1. Two periods of parallel suite were evaluated: 10 days in Feb/March 2015 and 14+12 days in July/August 2015 with mostly neutral results. Example of the scores is given on Figure 1.

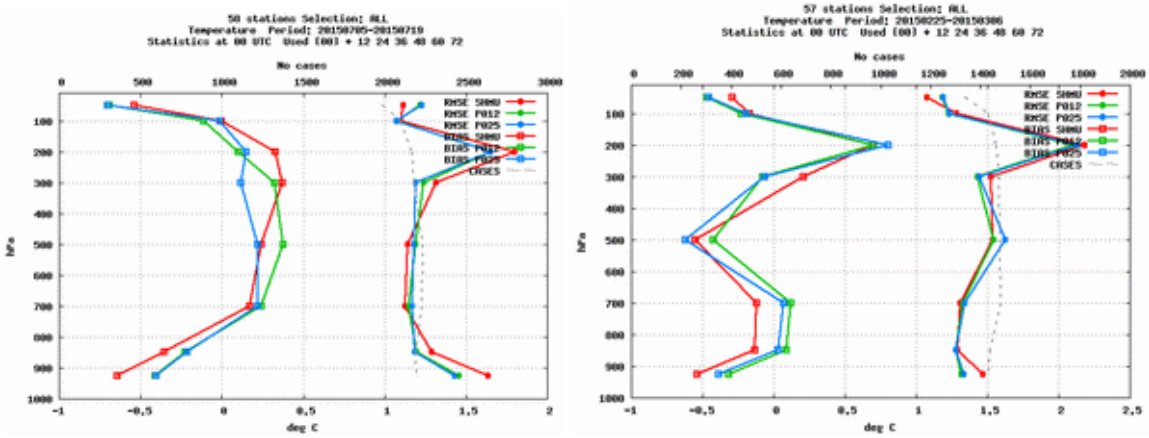

Figure 1: The verification scores of temperature against TEMP stations. Summer period (left) and winter one (right). Operational model in red, high resolution e-suite in green and high resolution suite with ALARO-1 physics in blue.

- The ALARO-1 setup was ported and technically validated on CY40T1.bf05_export version as well, but in a dynamical adaptation mode only, with plans to introduce it as a next operational cycle.

- New version of observation and measurement processing to obsoul format was implemented (obsoul_merge_v03.pl), allowing to join data within the defined time window; and fixing the bug in processing duplicated data. Moreover, it is now possible to merge more than 2 obsoul files.

- Series of tests were run to study quite poor performance of operational ALADIN system during extremely hot summer episodes, when the daily 2m temperature maxima were underestimated for about 3°C and the night minima were overestimated for about 2°C in average (see Figure 2). Operational runs were compared to downscaled dynamical adaptation runs; the vegetation thermal coefficient was retuned and ALARO-1 was tested. Slight improvement was reached with retuning of vegetation thermal coefficient as illustrated of Figure 3, but more investigations are needed.

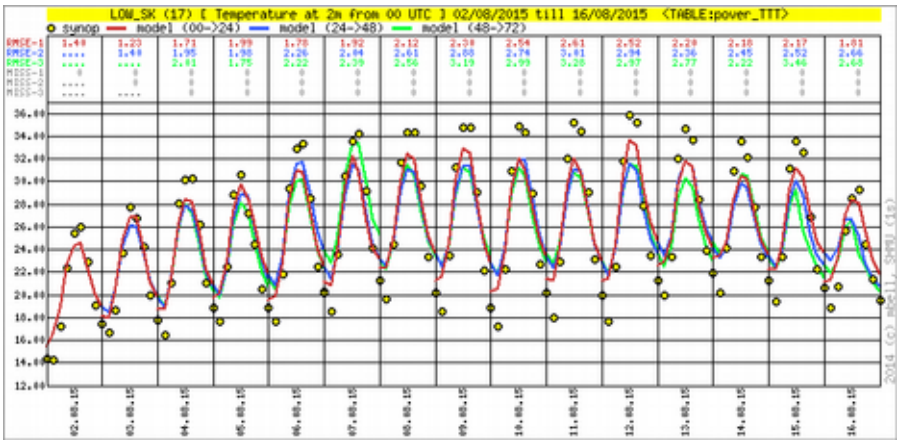

Figure 2: Comparison of ALADIN 2mT forecasts for the 1st (red), the 2nd (blue) and the 3rd (green) forecast day against observations (yellow circles) over lowland stations in Slovakia for two hot weeks in August 2015.

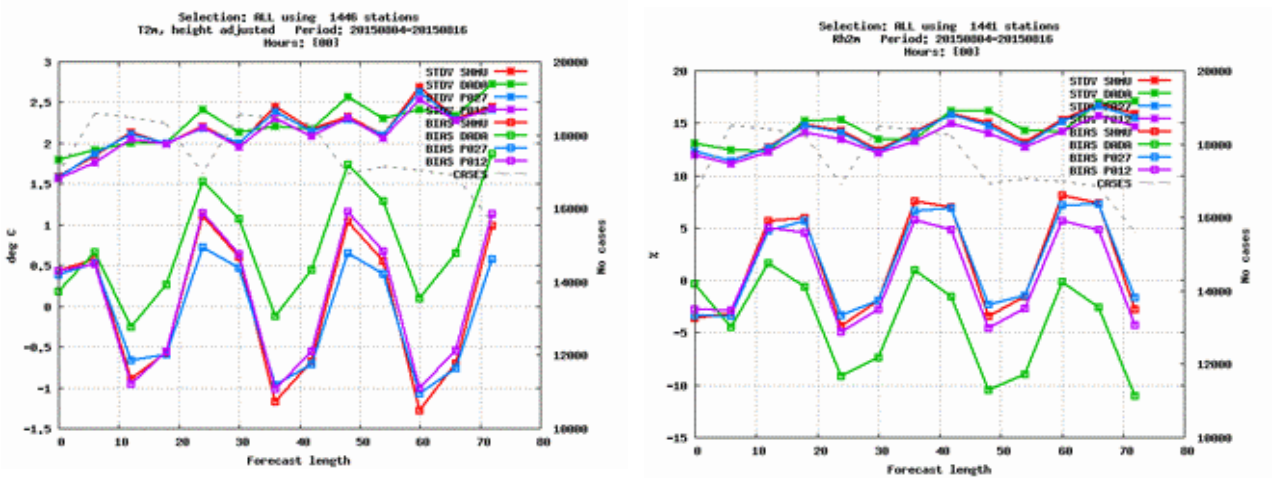

Figure 3: Verification results during hot summer of 2015 for 2m temperature (left) and 2m relative humidity (right). The operational suite is in red, the dynamical adaptation with operational resolution in green, the high resolution e-suite in violet, and the experiments with the retuned thermal vegetation coefficients in CANARI assimilation in blue.

Due to heavy delay in new HPC delivery it is planned to build new operational system on CY40T1.b05_export, with above mentioned high resolution (4.5km/63levs; ALARO-1 physics) by beginning of 2016. At the same time the surface data assimilation shall benefit from an upgraded network of surface automatic stations that happened in 2015 in frame of the POVAPSYS governmental project (Flood Warning and Forecasting System of the Slovak Republic).

3 Research and Development activities

Vertical finite element discretization in NH kernel of model system AAA (Jozef Vivoda)

Several issues were tackled in the area of the vertical finite element (VFE) discretization scheme. The backward compatibility of various R&D version of the VFE code was ensured by introduction of a new key LVFE_COMPATIBILITY. The code was consolidated, obsolete keys were cleaned. The known bug in splines orders different than four was investigated (more tests should be performed still). The work on the comparison of the vertical velocity on full levels within VFE scheme vs. on half levels with finite differences treatment has started. Further tests of fixed orders vs. fixed knots options has continued. The keys to control the spline fit of input function (operators with explicit vs. implicit boundary conditions) were implemented and the preliminary tests has started. The work on the draft of the VFE article for MWR has continued.
A complete report from the stay will be available on the RC LACE web pages (www.rclace.eu).

ALADIN-LAEF (Martin Bellus)

There are two different sources of uncertainties in NWP modelling. The first one is the uncertainty of the initial (IC) and boundary conditions and the second one is the uncertainty of the numerical models themselves. In ALADIN-LAEF several perturbation methods for IC and model uncertainty simulation have been implemented. Operational version comprises ensemble of CANARI surface assimilation where screen-level observations are randomly perturbed. Stochastic physics, for the perturbation of surface prognostic (SPPT) fields through their parameterized tendencies, was introduced into the ALADIN-LAEF R&D version last year. The impact of both perturbations - the initial one (denoted CANA and plotted in red on Figure 4) and the model one (SPPT in green) and their combined effect (CANASPPT - blue) on the regional ensemble system quality was assessed recently. ALADIN-LAEF system with combined perturbation techniques proved to be stable and reliable. The statistical scores have shown that the overall impact is clearly positive for all the monitored surface fields. Two examples of verification results are plotted on Figure 4 for 10m wind speed and surface temperature.
Moreover, the stochastic perturbation of physic tendencies for surface prognostic variables technique was upgraded in ALADIN-LAEF for CY40T1 and ALARO-1 physics.
More details to be found in the reports available on www.rclace.eu.

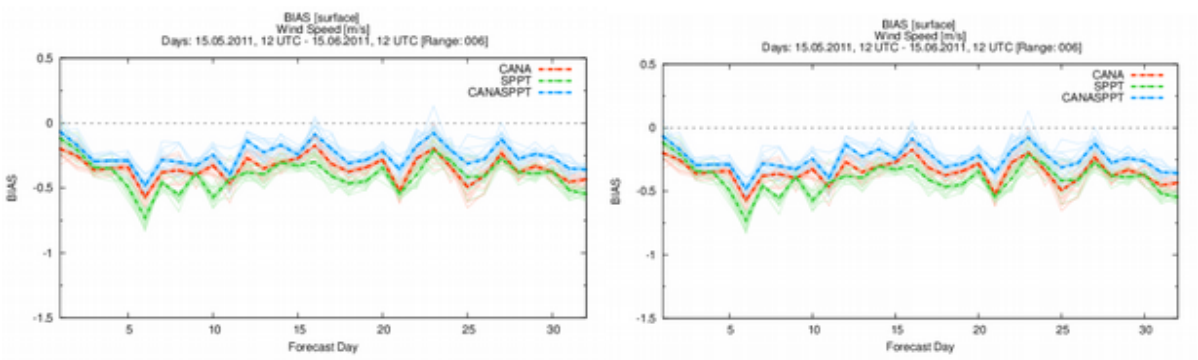

Figure 4: Verification scores for two types of perturbation techniques: on the initial fields (CANA, red), on the surface prognostic variables (SPPT, green) and their combined effect (CANASPPT, blue) for BIAS of 10m wind (left) and surface temperature (right).

Parametrization of orographic effects on surface radiation in AROME (Martin Dian)

New radiation parametrization in AROME including the effects of sky view factor, slope effects and local horizon (shadowing) – in total 34 new fields in .pdg file - was studied and tested. The parametrized fields were checked in 2.5km and 1.0km resolution in the area of Inn valley. Local horizon appeared to be the most important factor, influencing the global radiation and temperature values in the morning and evening hours. Results for selected case of 12/03/2014 +24h are presented

on Figure 5 for Schroecken station (real sky view factor 80%) for global radiation (left), and 2m temperature at 2.5km (middle) and 1km (right). More details can be found in the dedicated report, to be available on RC LACE web page soon.

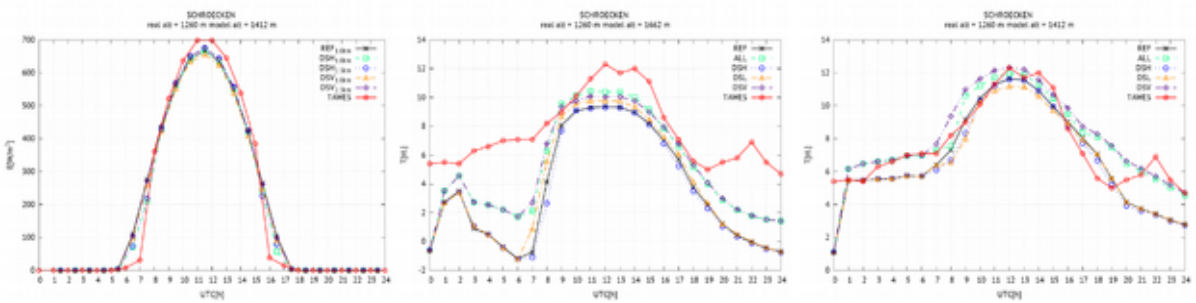

Figure 5: Global radiation (left), and 2m temperature at 2.5km (middle) and 1km (right) values for different experiments testing the orographic effects (see legend) vs. observed values (in red) for Schroecken station, 12/03/2014 +24h.

Surface assimilation using Extended Kalman-Filter (Viktor Tarjáni)

Extended Kalman Filter (EKF) surface assimilation study was continued at OMSZ during the RC LACE stay in Budapest. Validation was originally started with offline SURFEX version 6.0 and AROME cy36t1. Issues have been found with SURFEX offline runs with enabled town energy balance scheme (TEB). Unrealistic high 2m temperature values were detected over town tiles, as illustrated on Figure 6. Initial surface condition was first checked showing no indication of mentioned issue. However issue immediately appeared in the first offline SURFEX step and then remaining present in all subsequent steps. It was found that problem can be eliminated by enabling TOWN2ROCK switch in offline SURFEX. This however effectively eliminates TEB scheme for town tiles. Instead it was decided to use the original SURFEX setup (with TOWN2ROCK disabled) but with new offline SURFEX release and newer common cycle. Two latest offline SURFEX releases were tested (7.2 and 7.3) with AROME (cy38t1). Necessary namelist upgrades for 927 and 001 configurations for cy38t1 were also done. Preliminary tests indicated that mentioned issues has been successfully eliminated. Validation of the gridded observation procedure (CANARI) and the EKF analysis has been started as well. In the near future analysis increments of EKF method will be compared with those of OI_MAIN method. More comprehensive description will be addressed in a report soon available on www.rclace.eu.

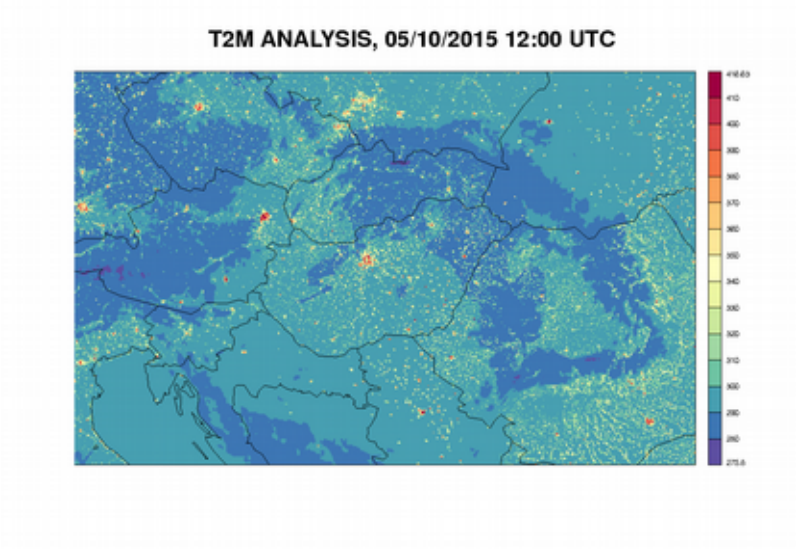

Figure 6: 2m air temperature at the end of the 6h assimilation window illustrating the problem of unrealistic high values over town tiles in offline SURFEX run.

HARMONIE system Working Week (Oldrich Spaniel, Maria Derkova)

The HARMONIE System Working Week (WW) has been organized in the week from Nov 9 to Nov 13, 2015 at Slovak Hydrometeorological Institute (SHMU) in Bratislava, Slovakia. Contrary to WW in 2014 that was devoted mostly to training of ALADIN colleagues to work with the HARMONIE system, this year it was true system Working Week. 9 colleagues from HIRLAM Consortia were participating, and 8 from ALADIN team (including ACNA and RC LACE ASC). Apart from HIRLAM-specific tasks (for more details see https://hirlam.org/trac/wiki/HarmonieWorkingWeek/System201511) SURFEX was defined as a common topic for ALADIN and HIRLAM people. Two SURFEX issues were tackled: SURFEX 7.3 coupled to ALARO (including TOUCANS) in CY40 and coupling of ARPEGE with SURFEX to ALADIN with ISBA. The reproducibility of ALARO and AROME configurations - as defined by the Toulouse code export version - within the HARMONIE system environment was also addressed. Further continuation of HIRLAM-ALADIN collaboration on the code and system aspect was discussed.

5 References

Belluš, M., 2015: Combination of IC and model uncertainties for the surface prognostic variables in ALADIN-LAEF system. Report on RC LACE stay at ZAMG, Vienna, Austria, 2015. Available on www.rclace.eu.

Belluš, M., 2015: Stochastic perturbation of physics tendencies in new CY40T1 with ALARO-1 physics. Report on RC LACE stay at ZAMG, Vienna, Austria, 2015. Soon available on www.rclace.eu.

Dian, M, 2015: Validation of orographic radiation parameterization. Report on RC LACE stay at ZAMG, Vienna, Austria, 2015. Soon available on www.rclace.eu.

Tarjáni, V., 2015: Surface assimilation using Extended Kalman-Filter. Report on RC LACE stay at OMSZ, Budapest, Hungary, 2015. Soon available on www.rclace.eu

Vivoda, J., 2015: Vertical finite element discretization in NH kernel of model system AAA. Report on stay at CHMI, Prague, 2015. Soon available on www.rclace.eu.

ALADIN highlights from Slovenia

Benedikt Strajnar, Neva Pristov, Jure Cedilnik, Jure Jerman,
Peter Smerkol, Matjaž Ličer, Anja Fettich

1 Introduction

After a significant upgrade of the operational ALADIN system in 2014 (see A-H Newsletter 4) it remained the same in 2015. Efforts have been invested into validation of the physical package ALARO-1vA and preparation of the environment for recomputing forecasts for the period 2011-2015. This data set will be used for model output statistics, as an input for historical runs of chemistry model and as a specialized data sets for end-users. Data assimilation (simple injection of snow cover into the model based on some simple rules) of 15 minute LandSAF snow cover has been designed and tested. Although some improvements have been noted, it turned out that the method is not useful for operational set-up as LandSAF snow at this frequency is not an operationally disseminated product.

In this contribution we present an overview of the two main developments in 2015. After the successful implementation and usage of Mode-S MRAR data we have started to explore Zenith Total Delay (ZTD) observations. A sample of data from Slovenian and E-GVAP network was obtained and used. The development and evaluation of 2-way coupling between ocean and atmosphere continued (see also contribution in A-H Newsletter 4). Additional fluxes (sensible and latent heat) are now passed from ALADIN to the ocean model.

2 Data assimilation of ZTD GNSS observations

Humidity is one of the most crucial variables for mesoscale and convective-scale limited area modeling, where convection and precipitation are among the most dominant weather processes.
The Global Navigation Satellite System (GNSS) ZTD measurements are becoming more and more used in Europe. Apart from the data provided by the EUMETNET's E-GVAP project, there is a network of additional 15 stations in Slovenia (plus some additional stations from their international exchange).

The data from both sources were validated and tested in ALADIN data assimilation. In order to use trustful data, white lists of GPS stations were first created. The selection process was based on July 2015, however, in order to obtain more objective results, we applied experiments on a different period, September 2015. Four experiments were conducted: the reference experiment included operational Slovenian suite parameters which does not include GPS data assimilation. A second experiment has been set up in order to assimilate E-GVAP data only. Then, to study also the Slovenian network data impact, a third experiment has been set including all the available observations. Finally, opposite to the other experiments which used a static bias correction approach, a fourth experiment based on variational bias correction method has been run including all the available GPS data.

As a first finding, the GPS data assimilation had a small but consistent beneficial impact especially on surface pressure, relative humidity and also cumulative rain and cloud cover. A bias reduction has been observed for these parameters. The variational bias correction method had positive impact as well compared to reference experiment and static bias correction method. On the other hand, no significant impact has been noticed for surface temperature and wind parameters.

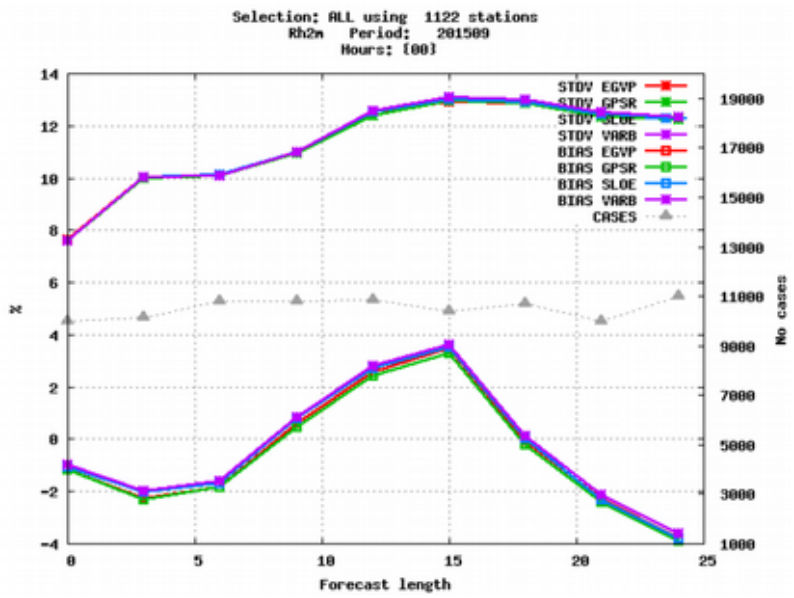

Figure 1: Verification of various experiments using GPS ZTD data against reference (green) for relative humidity over the operational domain for all network times.

3 Two-way atmosphere-ocean model coupling

Atmosphere and sea interact with each other through the sea surface. The influence of the ocean evolution on ALADIN model during the forecast was studied by online coupling with the Adriatic setup of Princeton Ocean Model (POM) run by Slovenian Environment Agency. As northern Adriatic Sea is a shallow sea its circulation is largely driven by the atmosphere and its sea surface temperature (SST) may change dramatically in the time scale of days.

The two models were coupled every time stamp of ALADIN integration using OASIS3-MCT model coupling toolkit. While heat fluxes, wind, precipitation and air pressure fields are passed to POM from ALADIN, the SST is returned back to ALADIN and is thus evolving over time (unlike in the standard uncoupled environment). In the sea areas within ALADIN domain which are not covered by the Adriatic POM, sea forecast fields of Mediterranean Forecasting System (MFS) were applied.

The experiments were designed as follows. The POM and ALADIN are initialized every 24 hours; in the two-way coupled system, POM takes its previous forecasts as initial condition while ALADIN is initialized from a separate precomputed data assimilation cycle (without atmosphere-sea coupling). In the one-way coupled experiment, the POM takes ALADIN fields hourly (as in the standard operational setup). In both experiments, POM uses fields of MFS as boundary conditions.

The performance of two- and one way coupled system was evaluated, with measurements from sea buoys as a reference. The testing period between January and March 2012 corresponded to a strong Bora wind event which led to extreme air-sea interactions. The coupled system simulated better the Bora induced cooling through the sensible heat loss. The impact on ALADIN 2 m temperature forecasts also positive in the downwind side of Adriatic sea, as detected by a comparison on meteorological stations located along the Italian coast.

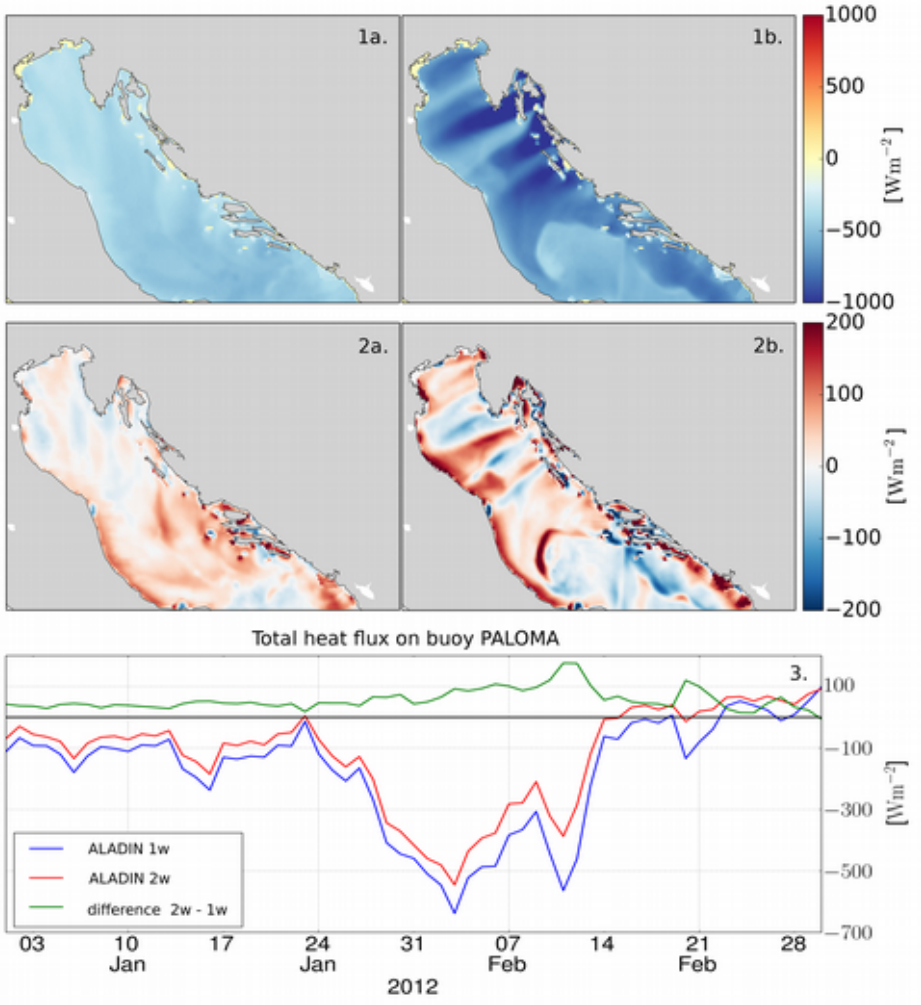

Figure 2: (1) Total heat flux from ALADIN to POM in two-way coupled experiment at 23:00 UTC: (1a) No Bora period (20.1.2012), (1b) Bora case (10.2.2012). Negative values mean that the flux is from ocean to atmosphere (ocean heat loss); (2) Difference between heat fluxes at 23:00; (3) Time series of heat flux on Paloma buoy (Paloma data courtesy of CNR-ISMAR Trieste, Italy) in January and February 2012. Red line denotes two-way, blue one-way coupled experiment and green line depicts their difference.

4 References

Ličer M., P. Smerkol, A. Fettich, M. Ravdas, A. Papapostolou, A. Mantziafou, B. Strajnar, J. Cedilnik, M. Jeromel, J. Jerman, S. Petan, V. Malačič, and S. Sofianos, 2015: Modeling ocean response to an extreme Bora event in Northern Adriatic using one-way and two-way atmosphere-ocean coupling, Ocean Sci. Discuss., 12, 1389-1431.

Sassy Z., 2015: Validation of RUC: Assimilation of GPS moisture information, RC-LACE stay report, Ljubljana, October 2015.

40 Years in Numerical Weather Prediction
Mariano Hortal interviewed by Angeles Hernandez

Angeles Hernandez [1], Mariano Hortal (AEMET)

Note: acronyms are listed at the end, as are references to most of the developments mentioned along the interview.

Mariano, you are retiring today, 5 January 2016, after a long career of almost 40 years in NWP, working mainly in numerical methods. It seems a good time to have a look at these years in numerical methods in NWP in Europe. But let's start at the beginning... How did you become interested in meteorology and NWP?

I had a job in experimental physics, in Universidad Autonoma de Madrid. Before that, I had done a degree in physics and then a PhD. Well... before that (laughter), when I was a teenager, I was very interested in electronics, and I enjoyed doing experiments at home. Whenever the electricity went off at home, my mum shouted "Mariano, what are you doing this time?" I enjoyed my job at the university, but contracts were on a one-year basis. I had started a family, so I was looking for a more stable position. At some point, my father told me that the Spanish NMS, called Servicio Meteorologico Nacional (SMN) at that time, had announced a few vacancies that might be of interest to me. My wife had a look, and decided that indeed I was interested, so I applied for the positions. I passed the exam, and then did a training course in meteorology; this was 1976. I heard from one of the course lecturers that there was the intention of creating an NWP unit in SMN, and I expressed my interest in it.

Then you started your work in SMN in the new NWP unit.

Well... not really. It took some time, during which I worked as operational forecaster in the Canary Islands. But when the NWP unit was created, I joined it, as did my good friend Jesus García Rendo, a mathematician who also worked at university, in applied mathematics. He was very keen on finite elements, and we decided to get started by implementing a quasi-geostrophic model published in the literature by Lennart Bengtsson, using finite elements. Eventually, we got it working on the IBM 360/40 available at the time.

So this was a model to get experience... What about the first operational NWP model in the Spanish NMS?

Around 1978, ECMWF had already prepared the first limited area version of its forecast model. We managed to get this version running in the IBM 360/40. Unfortunately, it took 24 hours to run a one-hour forecast, so clearly that was not the way to produce operational forecasts (laughter). We contacted again ECMWF, and David Burridge, head of the Research Department at the time, suggested that we waited for the semi-implicit version of the model, which was being developed at the time.

1 Corresponding e-mail address: ahernandezc at aemet.es

What else did you do in the meantime?

The following years were a time of growth in the NWP group in the Spanish NMS, which in 1978 had changed its name to Instituto Nacional de Meteorología (INM). New personnel joined the unit, and INM bought a new computer, a Fujitsu M-382. I was the head of the NWP group at the time, and together we built the first operational NWP suite in INM. The main components of this suite were the semi-implicit version of the ECMWF limited area forecast model, which indeed was much faster than the explicit version, and an assimilation system developed at SMHI, the Swedish NMS, kindly offered by Nils Gustafsson. If I remember rightly, it was 1985 when the first operational NWP forecast was produced in INM. However, by that time, ECMWF was already producing its global forecasts operationally, and our colleagues in operational weather forecasting preferred those to ours, partly because the visual representation of ECMWF forecast fields was more user-friendly. A large part of the work at that time was very technical, and during these years I got the base of my expertise in NWP and in computing in general.

When did you move to ECMWF? For how long were you at ECMWF?

In 1988 I had the opportunity to join the Numerical Aspects Section of ECMWF, and a new period started for me. I was very lucky that the head of the section was Adrian Simmons, not only because he is a great person and a great scientist, but because of his wide knowledge of NWP in general. I was working at ECMWF for eighteen years. One of the best things at ECMWF is that whenever you have a difficulty, you will find there is an expert around the corner that will help you. The opposite was true in INM: if you didn't have any problem, somebody around the corner would create one for you (laughter).

Well, I will let you get away with that only because you are retiring... Anyway, what were your main developments during this long period at ECMWF?

My first job in the section had to do with the Gaussian grid, the set of gridpoints associated to the specific spectral truncation used, and where part of the calculations are carried out. At the time, the Gaussian grid used in the ECMWF forecast model was regular in longitude and almost regular in latitude. My task was to develop a suitable reduced Gaussian grid, where the number of points along a parallel decreases as we get closer to the poles, with the aim of saving computing resources - mainly time, but also memory and storage. The task was relatively easy because ECMWF is such a supportive environment. In particular, it was important to use the Fast Fourier Transforms (FFT) developed by Clive Temperton, who was also in the Numerical Aspects Section, because his FFTs allowed a greater variety of points per row than previously possible with others.

What after the reduced Gaussian grid?

I joined the group that was developing a semi-Lagrangian version of the ECMWF forecast model. The idea was to implement a semi-Lagrangian treatment of advection instead of the traditional Eulerian, as it had already been done in some NWP centres. One of the main benefits of semi-Lagrangian schemes for the treatment of advection, compared with Eulerian, is that they allow larger time steps, which leads to considerable savings in computing time. The key person in that group was Hal Ritchie, from the Canadian NMS, who was already an expert in semi-Lagrangian methods. By the way, at that time the operational forecast model was called SPM (SPectral Model), and the IFS was being written.

When did the first semi-Lagrangian version of the ECMWF model become operational?

The first version became operational in 1991. It was fully interpolating in the vertical and the horizontal resolution was T213. These were interesting times, but there was a lot of stress too. The forecasts were often quite different from one day to the next, for the same verification time, and people were unhappy about this jumpiness. Some people thought the reasons were that T213 was a too

high resolution for the spectral method, and that the large timesteps allowed by the semi-Lagrangian scheme were actually too large. It took some time until we developed an alternative version more stable and understood the reasons for the jumpiness.

So they were some unwanted side effects. How did you overcome them?

First we tried alternatives, like a version of the semi-Lagrangian scheme non-interpolating in the vertical, but it was noisy in the stratosphere... Then Adrian came from a conference with new ideas from a presentation about quasi-monotone schemes (see Bermejo and Staniforth, 1992). Eventually, we implemented a quasi-monotone scheme, fully interpolating in the vertical, and without the jumpiness. We also understood that the reason for the problems we had had with our first semi-Lagrangian scheme were the overshootings and undershootings in the interpolation, which lead to an increase in the kinetic energy of the model as the forecast progressed. The quasi-monotone scheme did not have these problems.

What after the semi-Lagrangian version?

The next improvement actually came from the Canadians again. When the advection is Eulerian, there are large quadratic terms, and in order to represent them accurately, the Gaussian grid used needs to have a number of longitudes of at least 3N+1, where N is the truncation wavenumber in the spectral representation. Such a Gaussian grid is often called quadratic (see e.g. Wedi, 2014). In the first semi-Lagrangian version of the model, we were using a quadratic Gaussian grid, but that was mainly for historical reasons, as with the semi-Lagrangian advection it is enough a linear Gaussian grid (the number of longitudes must be greater or equal to 2N+1). The change from quadratic to linear grid allowed to increase the spectral resolution from T213 to T319 for the same set of gridpoints in grid space. However, with the T319 we noticed a clear noise problem. We had already seen it in the T213, but it became much more apparent in the T319. There was an instability associated to the two-time-level semi-Lagrangian scheme we were using (the first version was a three-time-level scheme). Talking with Agathe Untch, newly arrived at the section, about second-order accuracy in time, I got the idea of the SETTLS scheme. We tried it, and the new version was indeed more stable. This was the mid 1990s.

And what was next, after the linear Gaussian grid and SETTLS?

It was time to think about finite elements again, as a way of improving the accuracy of the vertical discretization. At that time, we were using centered finite differences, which would have been of second order for regularly distributed vertical levels, but it was in fact only of first order for our non-regular distribution of levels. There was clearly a need to improve the order of the vertical discretization and make it closer to that of the horizontal discretization. There had been a previous attempt of using finite elements for the vertical discretization at ECMWF, but it was numerically unstable; actually, it exploded just the day before its planned first day in operations. I started the new work with finite elements with something simple, from first principles, but it didn't work. The reason was that what we needed was the integral operator, not the derivative operator, and although in theory the integral operator is the inverse of the derivative operator, when you use finite elements this is not really the case – the inverse of the derivative operator is an integral operator which includes a lot of noise. Then I tried to develop an integral operator directly, using linear elements, and it was OK. However, Agathe Untch thought it would be better to use cubic elements instead of linear. I was concerned that this would be much more complicated, but she said "Don't worry, I will do it." So Agathe took over the implementation. It worked well, and has been operational since 2002.

In 2006 you retired from ECMWF, and went back to INM, part of the HIRLAM Consortium.

In the 1990s, while I was employed at ECMWF, INM had become a member of HIRLAM, a consortium of European NMSs, whose main aim was to develop and maintain a common state-of-the-

art limited area model suitable for operational use in its NMS members. A few months before my retirement from ECMWF, the vacancy of project leader for Dynamics and EPS was advertised, I applied for it, and the decision was taken to split it between Trond Iversen, an expert in EPS, and myself. Back in INM, the focus of my work was the dynamics and numerics of the HARMONIE model, essentially the same as those of IFS. Except for the developments related to model nesting, the type of work was very similar to what I had been doing for eighteen years. For instance, when the cubic Gaussian grid was proposed by ECMWF, I was able to implement it the next day in the HARMONIE model; as I had the experience of going from the quadratic to the linear grid, then the change to cubic grid was immediate.

Let's have a look now at how numerical methods in NWP have evolved during all these years. What have been the key milestones, in your view?

Without doubt, that would be the semi-Lagrangian advection. Well, of course, another milestone was the use of spectral methods, but that was in the 1970s, before I started working in NWP. If I had to choose a single great step forward, it would be the spectral method. Although some people in NWP expected it to become uncompetitive as the resolution increased, the truth is that it has been useful for many decades. In the estimations of scalability to many processors of different LAM models, the spectral method starts with an efficiency advantage of a factor of 100 over gridpoint methods due to the use of the semi-implicit scheme together with the semi-Lagrangian advection.

What are the current challenges in the area? What improvements can we expect to see in the next years?

It depends very much on how the computer market evolves. If the trend of increasing the number of processors continues, certainly the challenge is to find methods that provide an accuracy close to that of the spectral method but that are more local, to avoid the costs associated to the communication between processors, which is the bottleneck. Several groups, for instance ECMWF and ALADIN, are working in this direction. However, there are other trends in the computer market, like the use of GPUs; the challenge here is to use more efficiently the accelerators that appear in the market. In the future, quantum computers might have a very high computational power with very small processors; if this happens, computing in NWP will be completely different of what it is today.

Looking back at your career, what would you say has been your main achievement?

Well, it depends on how you look at it. From the point of view of challenging mathematics, certainly the most important development was the finite-element scheme for the vertical discretization of the ECMWF forecast model. But if you have computational efficiency in mind, perhaps the best was the upper boundary conditions implemented recently in the HARMONIE model. A very simple approach allowed to use the SETTLS scheme instead of the predictor-corrector scheme, and this has brought considerable savings in computing time.

And your main mistake? Is there something you remember in particular?

Yes, when we started working with semi-Lagrangian schemes at ECMWF... I did not expect it to work well, so I tried other methods, like a semi-analytical way of handling the advection part. After some time trying, I realized that the Eulerian way of treating advection was too far from linearity for semi-analytical methods to work.

So you took the scenic route to the semi-Lagrangian advection...

Well, yes, but then I became truly convinced of its value!

Any advice to people who start working in the area?

It is very difficult to give any advice, because the situation is completely different now. When I started, there was no NWP in the Spanish NMS, and ECMWF had just started. Nowadays the situation is very different, and my experience is not really applicable. The only advice I would give is not to trust conventional wisdom - always try it yourself!

Do you mean that things have a tendency to work in ways different from what one expects?

Yes, this is the always the case with numerical methods. Something that you believe is very clear at certain resolution turns not to be the case with another. As an example, when I started to work in HIRLAM, one of the first things I did was to explore whether a limited area model with a horizontal resolution of 2.5 km could be nested directly in a global model with a horizontal resolution of 32 km (the resolution of the operational ECMWF model at the time). From 32 km to 2.5 km there is a factor of more than 10, and according to conventional wisdom, an intermediate resolution model would have been the right choice. However, the tests we did showed that the use of an intermediate resolution was actually detrimental. Progress in research often goes against conventional wisdom.

I wonder if there any wisdom in conventional wisdom. Isn't it more like intellectual extrapolation?

That's right, and extrapolations are always unstable (laughter). When ECMWF started using the spectral method with the T106, some people said that the method would not last long, because the cost of the Legendre transforms increases with the cube of the resolution instead of quadratically. However, the method has stayed alive and well despite the increasingly finer resolution, thanks to technical improvements with massive parallel computers that allow to keep the Fourier and Legendre transforms between spectral space and grid space affordable.

What is next for you? Do you plan to be involved in NWP in any way after your retirement?

No, I do not have any plans to stay involved in NWP, but there are very few people working in dynamics in HIRLAM, and I will offer them my support. If they need my advice, I will be available, and I might be a bit involved... while I can still recognize the code. Nowadays the IFS is changing so quickly that after a couple of cycles you have a look and you don't recognize anything (laughter).

One more question to end, more personal: what plans do you have for all that free time?

I plan to play golf, which I enjoy very much. I'd also like to start playing music again, and the first thing I need to do for that is to tune the piano. I have already an oscillator at home, and I will connect it to the hi-fi to help me with the tuning. In general, I'm quite interested in domotics. For instance, I'd like to develop a mobile phone application so that when the mobile alarm rings, the window blinds get open automatically, controlled by the computer. Things like that. Enjoying myself.

Thank you for the interview, Mariano, and best wishes for a long, happy and fruitful retirement.

Acronyms

AEMET - Agencial Estatal de METeorología (name of the Spanish NMS from 2008)
ECMWF - European Centre for Medium-range Weather Forecasts
EPS - Ensemble Prediction System
FFT - Fast Fourier Transform
GPU - Graphics Processing Unit
HIRLAM - HIgh Resolution Limited Area Model
INM - Instituto Nacional de Meteorología (name of the Spanish NMS between 1978 and 2008)
LAM - Limited Area Model
NMS - National Meteorological Service
NWP - Numerical Weather Prediction
SETTLS - Stable Extrapolation Two Time Level Scheme
SMHI - Swedish Meteorological and Hydrological Institute
SMN - Servicio Meteorológico Nacional (name of the Spanish NMS until 1978)

References

Bermejo, R., and A. Staniforth, 1992: The Conversion of Semi-Lagrangian Advection Schemes to Quasi-Monotone Schemes. *Mon. Wea. Rev*., 120, 2622–2632.

Hortal, M., and A. Simmons, 1991: Use of Reduced Gaussian Grids in Spectral Models. *Mon. Wea. Rev*., 119, 1057-1074.

Hortal, M., 2002: The development and testing of a new two-time-level semi-Lagrangian scheme (SETTLS) in the ECMWF forecast model. *Q. J. R. Meteorol. Soc*., 128, 1671-1687.

Ritchie, H., C. Temperton, A. Simmons, M. Hortal, T. Davies, D. Dent, and M. Hamrud, 1995: Implementation of the Semi-Lagrangian Method in a High-Resolution Version of the ECMWF Forecast Model. *Mon. Wea. Rev.*, 123, 489-514.

Temperton, C., 1991: On Scalar and Vector Transform Methods for Global Spectral Models. *Mon. Wea. Rev*., 119, 1303-1307.

Temperton, C., M. Hortal, and A. Simmons, 2001: A two-time-level semi-Lagrangian global spectral model. *Q. J. R. Meteorol. Soc*., 127, 111-127.

Untch, A., and M. Hortal, 2004: A finite-element scheme for the vertical discretization of the semi-Lagrangian version of the ECMWF forecast model. *Q. J. R. Meteorol. Soc*., 130, 1505-1530.

Wedi, N., 2014: Increasing horizontal resolution in in numerical weather prediction and climate simulations: illusion or panacea? *Phil. Trans. R. Soc. A*, 372, 20130289.

ALADIN-HIRLAM Newsletter contribution

INM, Tunisia

1 Introduction

This contribution summarizes recent ongoing development works in INM including operational activities (Parallel Suites and verification system) and models intercomparison for convective systems.

2 Parallel Suites

New model versions have been implemented on HP machine (Recently installed at INM). The HP machine characteristics are described in the following table:

Table 1: HP machine characteristics

Model	HP proliant DI560 Gen8
Processors	4 CPUs (6,42GHZ), 40 cores, 80 threads
RAM	256 Go
Storage	16 To
Operating System	Redhat Linex 6.5

Parallel suite model versions:

The following models are being tested on pre-operational mode on the HP server.

Table 2: Parallel suite models

Model	ALADIN	AROME	HARMONIE
Model Version	CY38T1_bf.03	CY38T1op2	CY38T1_bf.03
Spatial Resolution	7.5 km	2.5 km	2.5 km
Vertical Levels	70	60	65
Boundaries	ARPEGE	ARPEGE	ALADIN
Time Step	450s	45s	65s

In addition, the porting of the 1.3 km AROME-Tunisia prototype and the testing of CY40T1_bf.05 are in progress.

3 Developments to NWFVS system:

After the pre-operational implementation of the Numerical Weather Forecast Verification System, more scores were introduced.
Further spatial verification scores are under development especially for precipitations.

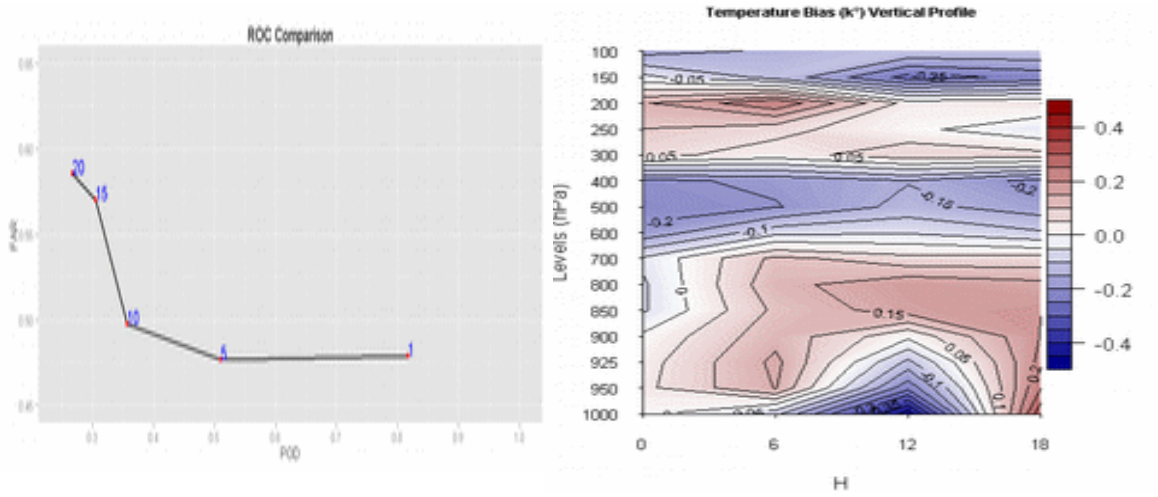

Figure 1: Examples of verification products

4 Models Intercomparison: Study of the September 19th, 2013 Convective System

A special interest was accorded to the prediction of convective rain systems since Tunisia is characterized by a high frequency of convective situations, which may generate flash-floods especially in the inter-season periods, as was the case of September 19th 2013 floods. Therefore, different numerical models were applied in order to investigate their performance on such situation.

The actual case study was based on the comparison of simulated 24h accumulated precipitation (from 06H to 06H) against observation data which was collected from more than 300 pluviometric stations.
Four numerical models were considered during this case study; Operational ALADIN-Tunisia suite (12.5km), ALADIN-Tunisia (7.5km with SURFEX), AROME-Tunisia (2.5km) and HARMONIE-Tunisia (2.5km).

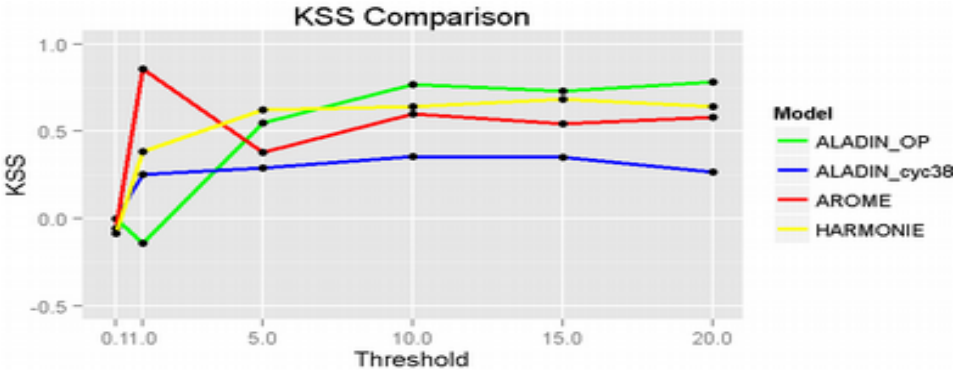

Figure 2: 24H accumulated precipitation KSS score for 0.1mm, 1mm, 5mm, 10mm, 15mm and 20mm thresholds

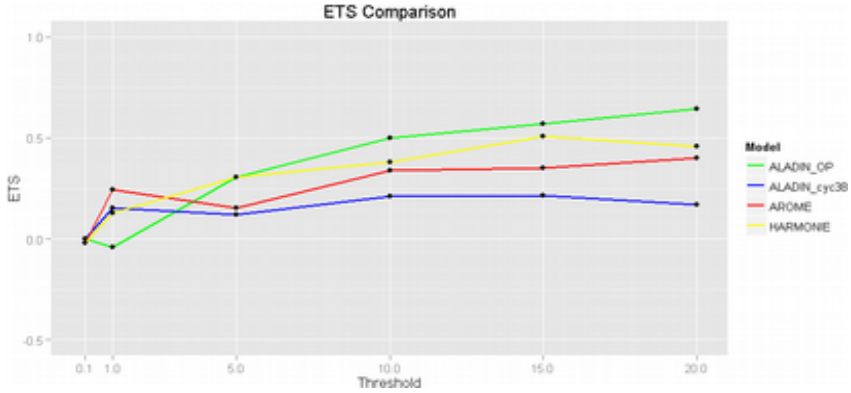

Figure 3: 24H accumulated precipitation ETS score for 0.1mm, 1mm, 5mm, 10mm, 15mm and 20mm thresholds

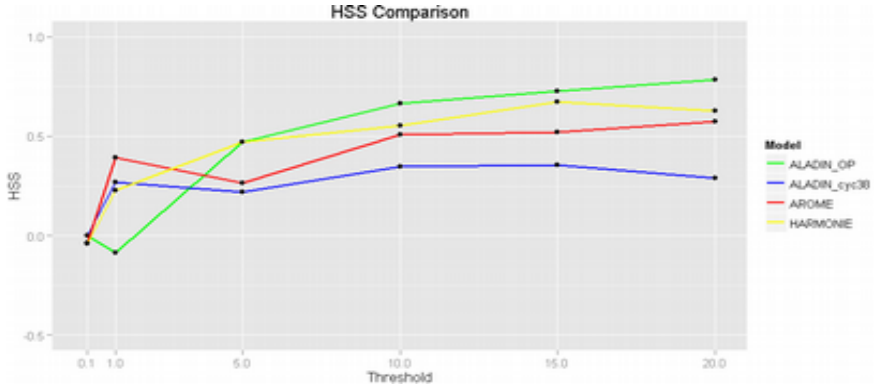

Figure 4: 24H accumulated precipitation HSS score for 0.1mm, 1mm, 5mm, 10mm, 15mm and 20mm thresholds

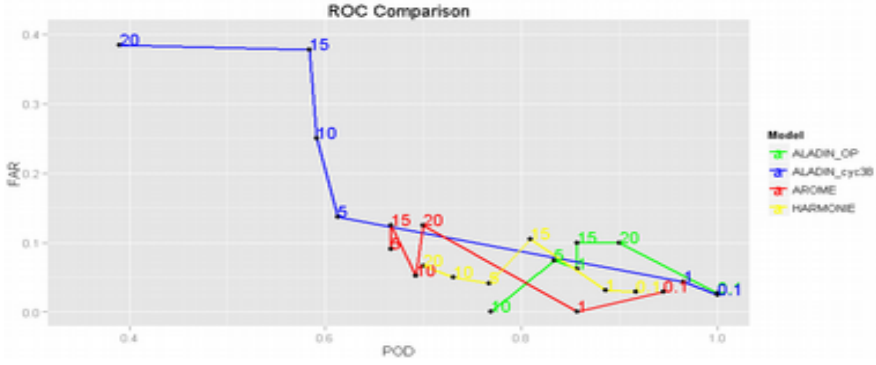

Figure 5: 24H accumulated precipitation ROC score

Interactive SkewT-LogP Diagram Application

Unal TOKA, Yelis CENGIZ, Duygu AKTAS
(Turkish State Met. Service)

Introduction

Interactive SkewT – LogP Project, which enables the user to plot the Temp diagram of any given point when clicked on google based map. The diagrams are produced based on WRF and ALARO models. In the project, open source codes and softwares were used and code improvements were done by Turkish Aladiners.

User-friendly SkewT diagrams are produced for the given point instead of generating this diagram for every point in the map and user can make alteration on the diagram. In this context, the computer resources are used more efficiently. Therefore, it was a necessity to switch to interactive applications.

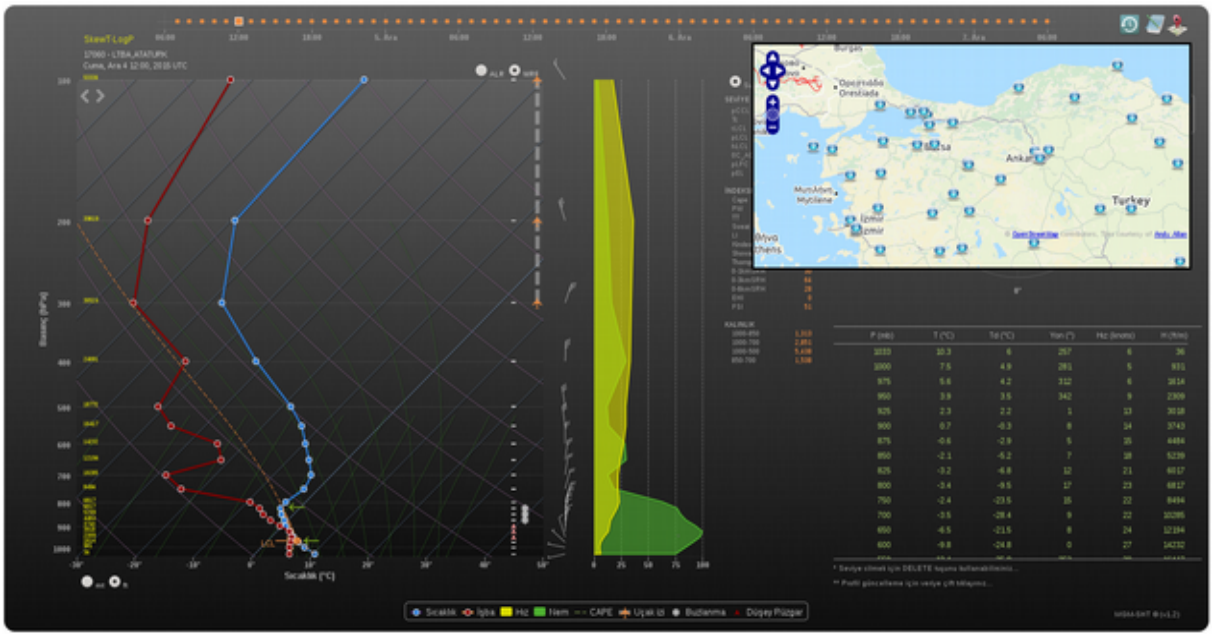

Figure 1: SkewT-LogP Diagram and airport/point selection
(http://212.175.180.126/skewt/index.html)

Features of SkewT-LogP Diagram

WRF and ALARO models are updated 4 times a day. When the models are updated, “Interactive SkewT- LogP” application is able to use the lastest model outputs. The airports in Turkey are also indicated in the map (Fig. 1).

This application generates the following parameters: Temperature, Dew-Point, Velocity, Humidity, CAPE, Contrail, Icing, Vertical Wind, Instability Indices, Thickness. The parameters such as, icing, contrail and vertical wind are calculated to be used for aviation purpose. “Surface CAPE” and “Parcel CAPE” identify the CAPE values calculated by different calculation methods.

For each pressure level, temperature, dew-point temperature, wind speed and direction and the height of the pressure level are shown in a table. The application allows the user to make changes in values and atmospheric profile. After the modifications, all instability indices are recalculated.

In addition, the application has hodograph feature. Wind shear is plotted in 0-1, 0-3, 0-6, 0-16 km height ranges on the hodograph.

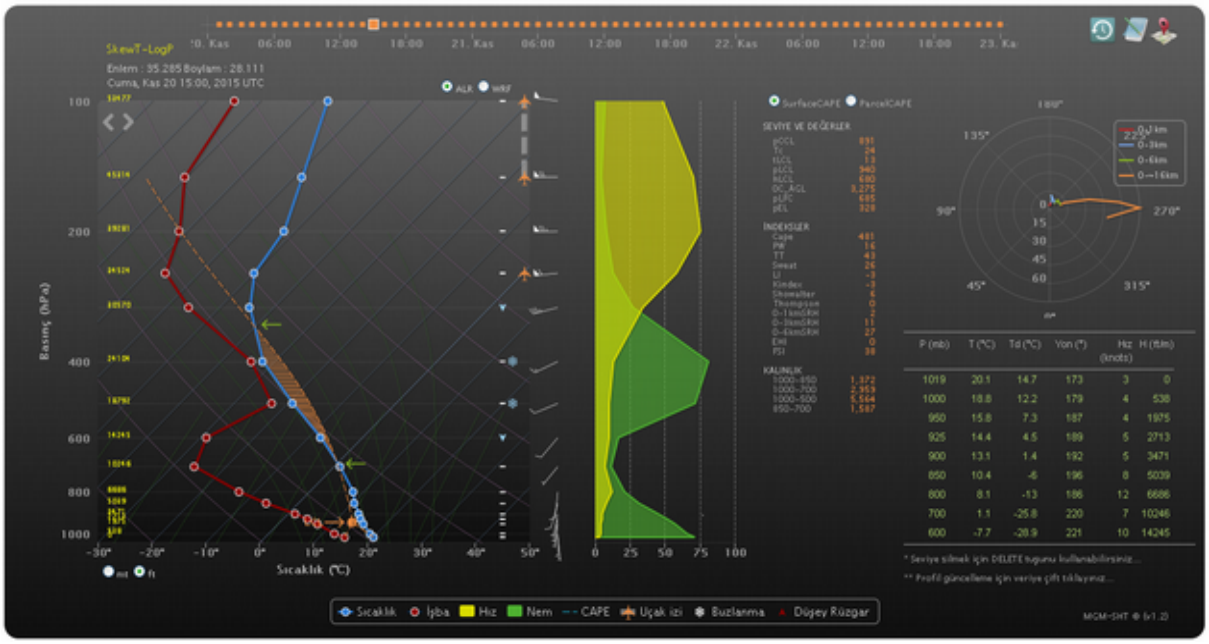

Figure 2: Interactive SkewT-LogP Diagram

Overview of the operational configurations

Patricia Pottier

1 Introduction

Our 26 NMSs run deterministic LAM 42 configurations. The table below gives their main fictures. More details about the configurations and more maps can be found on the operational page on the ALADIN website.

Operational configurations	Horiz resol (km)	Size (grid-point)	Vertic levels	Version	Coupled with	Computer	Configu-ration	DA	DA (details)
1. Algeria: ALADIN-ALGE	12.00	300 x300	70	CY38T1	ARPEGE	MF (BULL)	ALADIN	NO	
2. Austria: ALARO5	4.82	540 x600	60	CY36T1	IFS	SGI ICE-X	ALARO	YES	CANARI
3. Austria: AROME-Au	2.50	432 x600	90	CY37T1	IFS	SGI ICE-X	AROME	YES	3DVAR + OI Main
4. Belgium: ALARO-7km	6.97	240 x240	46	CY38T1.bf03	ARPEGE	SGI Altix 4700	ALARO	NO	
5. Belgium: ALARO-4km	4.01	181 x181	46	CY38T1.bf03	ARPEGE	SGI Altix 4700	ALARO	NO	
6. Bulgaria: ALADIN-Bg	7.00	144 x180	70	CY38T1.bf03	ARPEGE	Linux cluster	ALADIN	NO	
7. Croatia: ALARO-88	8.00	216 x240	37	CY38T1.bf03	IFS	SGI UV 2000	ALARO	YES	3DVAR + CANARI
8. Croatia: ALARO-22	2.00	450 x450	37	CY36T1.bf08	ALARO-88	SGI Altix	ALARO	NO	
9. Czech Rep: ALARO-Cz	4.71	432 x540	87	38T1.bf03 + local dev ALARO1	ARPEGE	NEC SX-9	ALARO	YES	3DVAR + CANARI+ DFI_blending
10. Denmark: AROME-DKA	2.50	600 x800	65	CY38H1.2 + local adapt.	IFS	Cray-XT5	AROME	YES	3DVAR+CANARI,OI,SODA for SURFEX
11. Denmark: AROME-GLB (SWGreenl)	2.00	800 x400	65	CY38H1.2 + local adapt.	IFS	Cray-XT5	AROME	YES	BLENDING+CANARI,OI, SODA for SURFEX
12. Finland: AROME-FMI	2.50	800 x720	65	CY38H1.2 + local adapt.	IFS	Cray XC30	AROME	YES	3DVAR + CANARI OI, SODA for SURFEX
13. France: AROME-France	1.30	1440x 1536	90	CY41_T1	ARPEGE	BULLx B710 DLC	AROME	YES	3DVAR + OI Main
14. Hungary: ALARO-HU-determinist	7.96	320 x360	49	CY38T1	IFS	IBM iDataPlex Clust.	ALARO	YES	3DVAR + CANARI

Operational configurations	Horiz resol (km)	Size (grid-point)	Vertic levels	Version	Coupled with	Computer	Configu-ration	DA	DA (details)
15. Hungary: AROME-HU	2.50	320 x500	60	CY38T1	IFS	IBM iDataPlex Clust.	AROME	YES	3DVAR + OI Main
16. Iceland: AROME-IMO	2.50	500 x480	65	CY38H1.2 + local adapt.	IFS	ECMWF (cca/ccb)	AROME	YES	CANARI OI, SODA for SURFEX
17. Ireland: AROME-IRELAND25	2.50	500 x540	65	CY37H1.1	IFS	SGI ICE X	AROME	YES	CANARI OI + SURFEX OI
18. Lithuania: AROME-LHMS	2.50	432 x432	60	CY37H1.2	IFS		AROME	YES	Upper air blending +CANARI, OI_Main for SURFEX
19. Morocco: ALADIN-Mo1	18.00	324 x540	70	CY36T1 / CY38T1.bf03	ARPEGE	IBM HPC	ALADIN	Y/N	DA (3DVAR + CANARI) in CY36T1 version only
20. Morocco: ALADIN-Mo2	10.00	320 x320	70	CY38T1.bf03 with SURFEX	ARPEGE	IBM HPC	ALADIN	NO	3DVAR+Canari is ongoing for CY40t1
21. Morocco: AROME Maroc	2.50	800 x800	60	CY38T1.bf03	ALADIN -Mo2	IBM HPC	AROME	NO	
22. Netherlands: AROME-KNMI	2.50	800 x800	60	CY36H1.4	HIRLAM	BULL	AROME	YES	3DVAR + CANARI OI, OI_MAIN for SURFEX
23. No&Se: AROME-MetCoOp	2.50	960 x750	65	CY38H1.2 + local adapt.	IFS	SGI, Intel Sandy Br.	AROME	YES	3DVAR + CANARI OI, SODA for SURFEX
24. Norway: AROME-Arctic	2.50	960 x750	65	CY38H1.2 + local adapt.	IFS	SGI, Intel Sandy Br.	AROME	YES	3DVAR + CANARI OI, SODA for SURFEX
25. Poland: ALARO-E040	4.00	800 x800	60	CY40T1.bf5	ARPEGE	Linux cluster	ALARO	NO	
26. Poland: AROME-P025	2.55	648 x648	60	CY40T1.bf5	ALARO-E040	Linux cluster	AROME	NO	
27. Portugal: ALADIN-ATP	9.00	288 x450	46	CY38T1	ARPEGE	IBM POWER7+	ALADIN	NO	
28. Portugal: AROME-PT2	2.50	540 x480	46	CY38T1	ARPEGE	IBM POWER7+	AROME	NO	
29. Portugal: AROME-Madeira	2.50	200 x192	46	CY38T1	ARPEGE	IBM POWER7+	AROME	NO	
30. Portugal: AROME-Azores	2.50	270 x360	46	CY38T1	ARPEGE	IBM POWER7+	AROME	NO	
31. Romania: ALARO-Ro2	6.50	240 x240	60	CY36T1	ARPEGE	cluster IBM BLADE	ALARO	NO	
32. Slovakia: ALARO-Sk	9.01	288 x320	37	CY36T1.bf10	ARPEGE	IBM Power7	ALARO	YES	CANARI+ DFI_blending
33. Slovenia: ALARO-Si	4.40	432 x432	87	38T1	IFS	SGI ALTIX ICE 8200	ALARO	YES	3DVAR + CANARI

Operational configurations	Horiz resol (km)	Size (grid-point)	Vertic levels	Version	Coupled with	Computer	Configu-ration	DA	DA (details)
34. Spain: AROME-IBERIA	2.50	800 x648	65	CY38H1.2 + local adapt.	IFS	ECMWF (cca/ccb)	AROME	YES	3DVAR + CANARI OI, SODA for SURFEX
35. Spain: AROME-CANARIAS	2.50	576 x480	65	CY38H1.2 + local adapt.	IFS	ECMWF (cca/ccb)	AROME	YES	Blending + CANARI OI, SODA for SURFEX
36. Tunisia: ALADIN-Tn	12.50	162 x128	60	CY29T1	ARPEGE	IBM PS690	ALADIN	NO	
37. Turkey: ALARO-Tk	4.50	450 x720	60	CY38T1.bf03	ARPEGE	Altix 4700	ALARO	NO	
38. Turkey: AROME-Tk	2.50	512 x1000	60	CY38T1.bf03	ARPEGE	SGI UV2000	AROME	NO	
39. France: ALADIN-Ant-Guyana	8.00	512 x450	70	CY41_T1	IFS	BULLx B710 DLC	ALADIN	YES	3DVAR + OI Main ; Wind bogus for trop. cyclones ; SURFEX V7
40. France: ALADIN-Caledonia	8.00	360 x288	70	CY41_T1	IFS	BULLx B710 DLC	ALADIN	YES	3DVAR + OI Main ; Wind bogus for trop. cyclones ; SURFEX V7
41. France: ALADIN-Polynesia	8.00	486 x540	70	CY41_T1	IFS	BULLx B710 DLC	ALADIN	YES	3DVAR + OI Main ; Wind bogus for trop. cyclones ; SURFEX V7
42. France: ALADIN-Reunion	8.00	500 x810	70	CY41_T1	ARPEGE	BULLx B710 DLC	ALADIN	YES	3DVAR + OI Main ; Wind bogus for trop. cyclones ; SURFEX V7

2 All over the world …

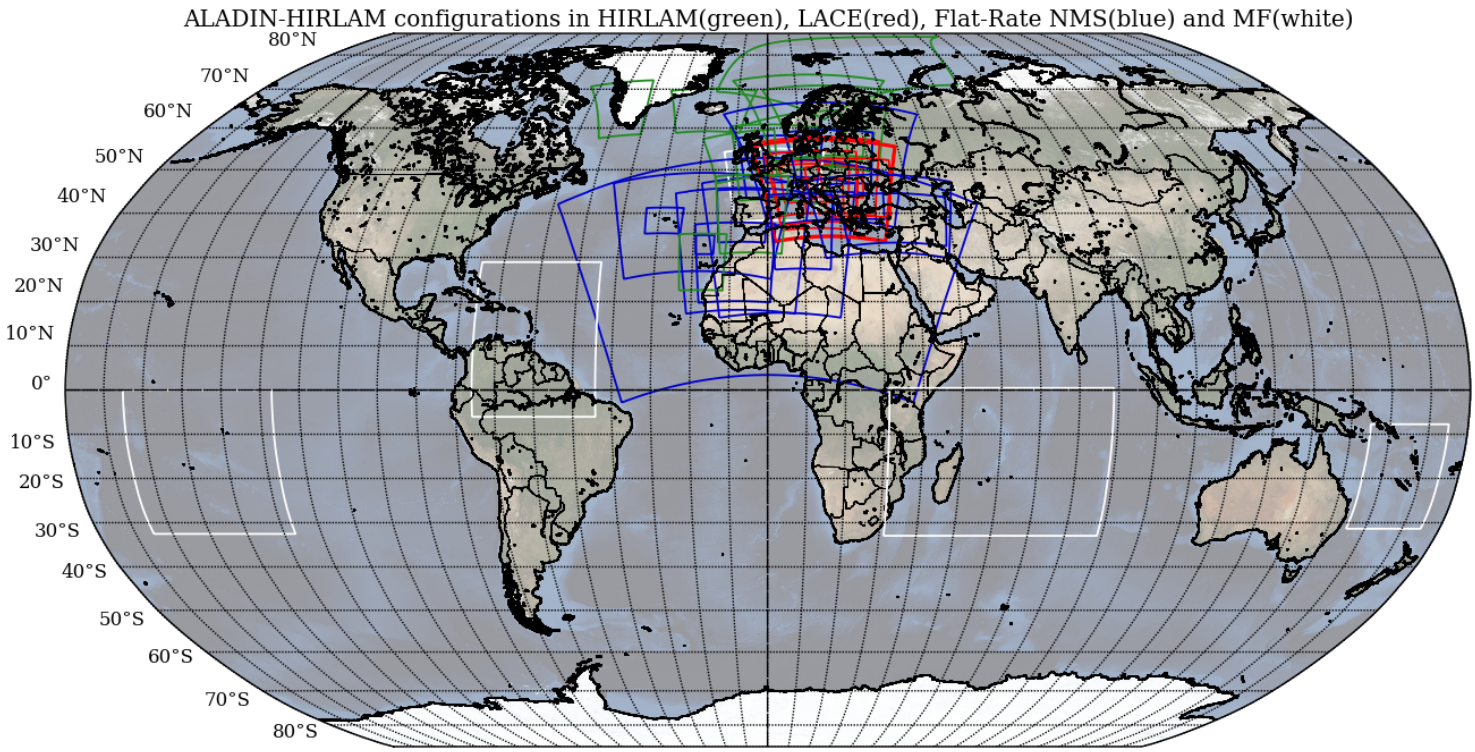

3 The 42 configurations

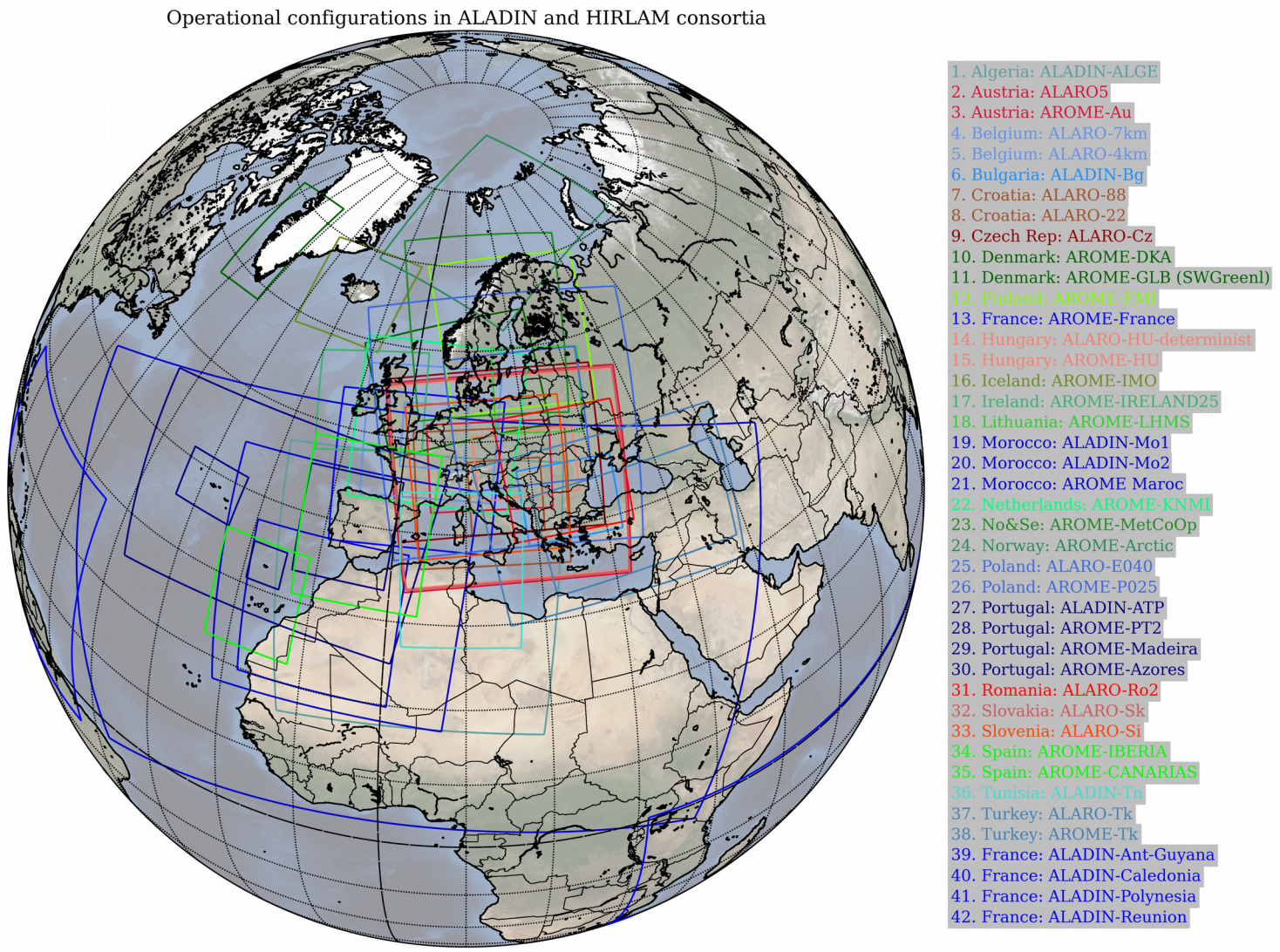

4 AROME, ALARO, ALADIN configurations

ALADIN-HIRLAM model configurations : AROME (red) ALARO (green) ALADIN (blue)

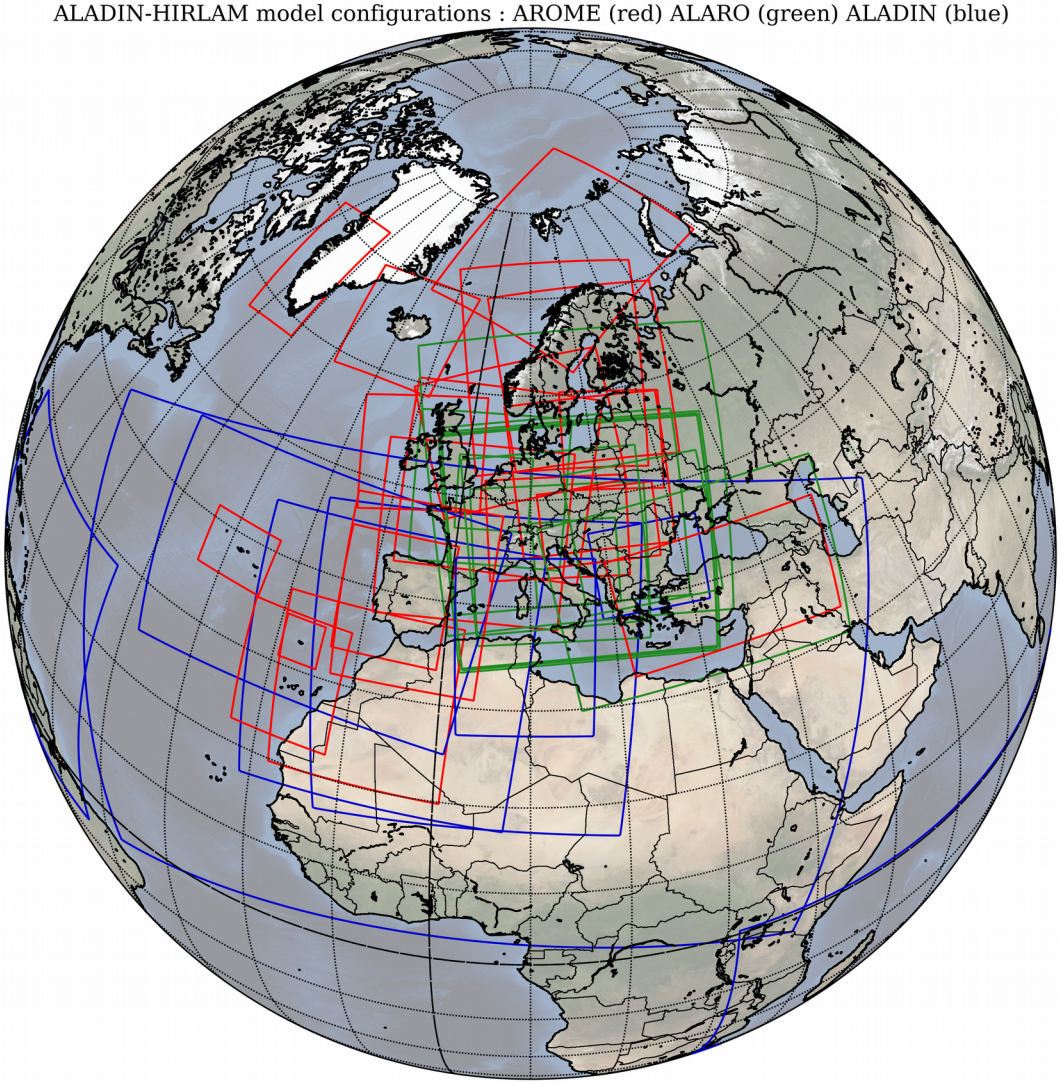

1. Algeria: ALADIN-ALGE
2. Austria: ALARO5
3. Austria: AROME-Au
4. Belgium: ALARO-7km
5. Belgium: ALARO-4km
6. Bulgaria: ALADIN-Bg
7. Croatia: ALARO-88
8. Croatia: ALARO-22
9. Czech Rep: ALARO-Cz
10. Denmark: AROME-DKA
11. Denmark: AROME-GLB (SWGreenl)
12. Finland: AROME-FMI
13. France: AROME-France
14. Hungary: ALARO-HU-determinist
15. Hungary: AROME-HU
16. Iceland: AROME-IMO
17. Ireland: AROME-IRELAND25
18. Lithuania: AROME-LHMS
19. Morocco: ALADIN-Mo1
20. Morocco: ALADIN-Mo2
21. Morocco: AROME Maroc
22. Netherlands: AROME-KNMI
23. No&Se: AROME-MetCoOp
24. Norway: AROME-Arctic
25. Poland: ALARO-E040
26. Poland: AROME-P025
27. Portugal: ALADIN-ATP
28. Portugal: AROME-PT2
29. Portugal: AROME-Madeira
30. Portugal: AROME-Azores
31. Romania: ALARO-Ro2
32. Slovakia: ALARO-Sk
33. Slovenia: ALARO-Si
34. Spain: AROME-IBERIA
35. Spain: AROME-CANARIAS
36. Tunisia: ALADIN-Tn
37. Turkey: ALARO-Tk
38. Turkey: AROME-Tk
39. France: ALADIN-Ant-Guyana
40. France: ALADIN-Caledonia
41. France: ALADIN-Polynesia
42. France: ALADIN-Reunion

5 Configurations with / without Data Assimilation

ALADIN-HIRLAM configurations with DA (blue) and without (red)

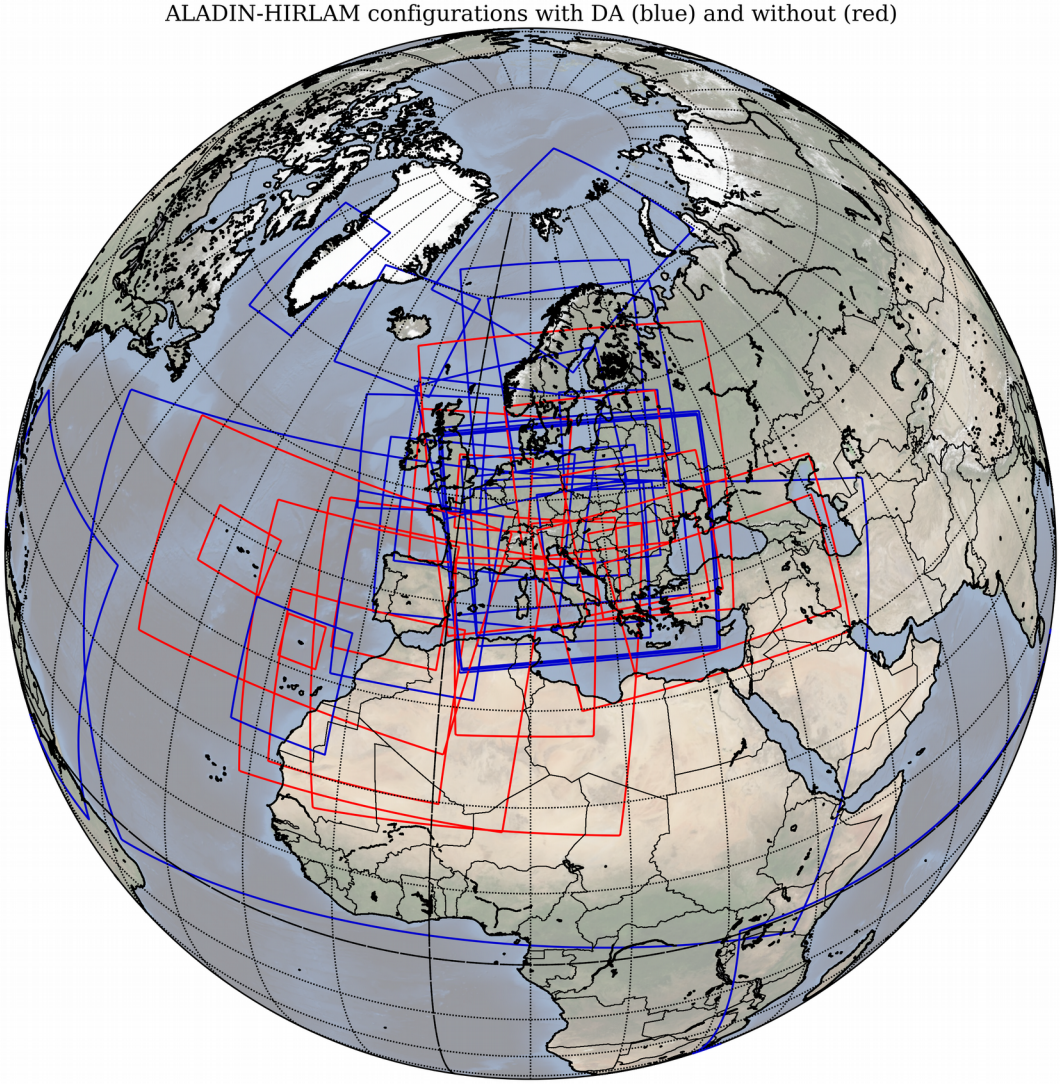

1. Algeria: ALADIN-ALGE
2. Austria: ALARO5
3. Austria: AROME-Au
4. Belgium: ALARO-7km
5. Belgium: ALARO-4km
6. Bulgaria: ALADIN-Bg
7. Croatia: ALARO-88
8. Croatia: ALARO-22
9. Czech Rep: ALARO-Cz
10. Denmark: AROME-DKA
11. Denmark: AROME-GLB (SWGreenl)
12. Finland: AROME-FMI
13. France: AROME-France
14. Hungary: ALARO-HU-determinist
15. Hungary: AROME-HU
16. Iceland: AROME-IMO
17. Ireland: AROME-IRELAND25
18. Lithuania: AROME-LHMS
19. Morocco: ALADIN-Mo1
20. Morocco: ALADIN-Mo2
21. Morocco: AROME Maroc
22. Netherlands: AROME-KNMI
23. No&Se: AROME-MetCoOp
24. Norway: AROME-Arctic
25. Poland: ALARO-E040
26. Poland: AROME-P025
27. Portugal: ALADIN-ATP
28. Portugal: AROME-PT2
29. Portugal: AROME-Madeira
30. Portugal: AROME-Azores
31. Romania: ALARO-Ro2
32. Slovakia: ALARO-Sk
33. Slovenia: ALARO-Si
34. Spain: AROME-IBERIA
35. Spain: AROME-CANARIAS
36. Tunisia: ALADIN-Tn
37. Turkey: ALARO-Tk
38. Turkey: AROME-Tk
39. France: ALADIN-Ant-Guyana
40. France: ALADIN-Caledonia
41. France: ALADIN-Polynesia
42. France: ALADIN-Reunion

ALADIN and HIRLAM organisational charts

Patricia Pottier

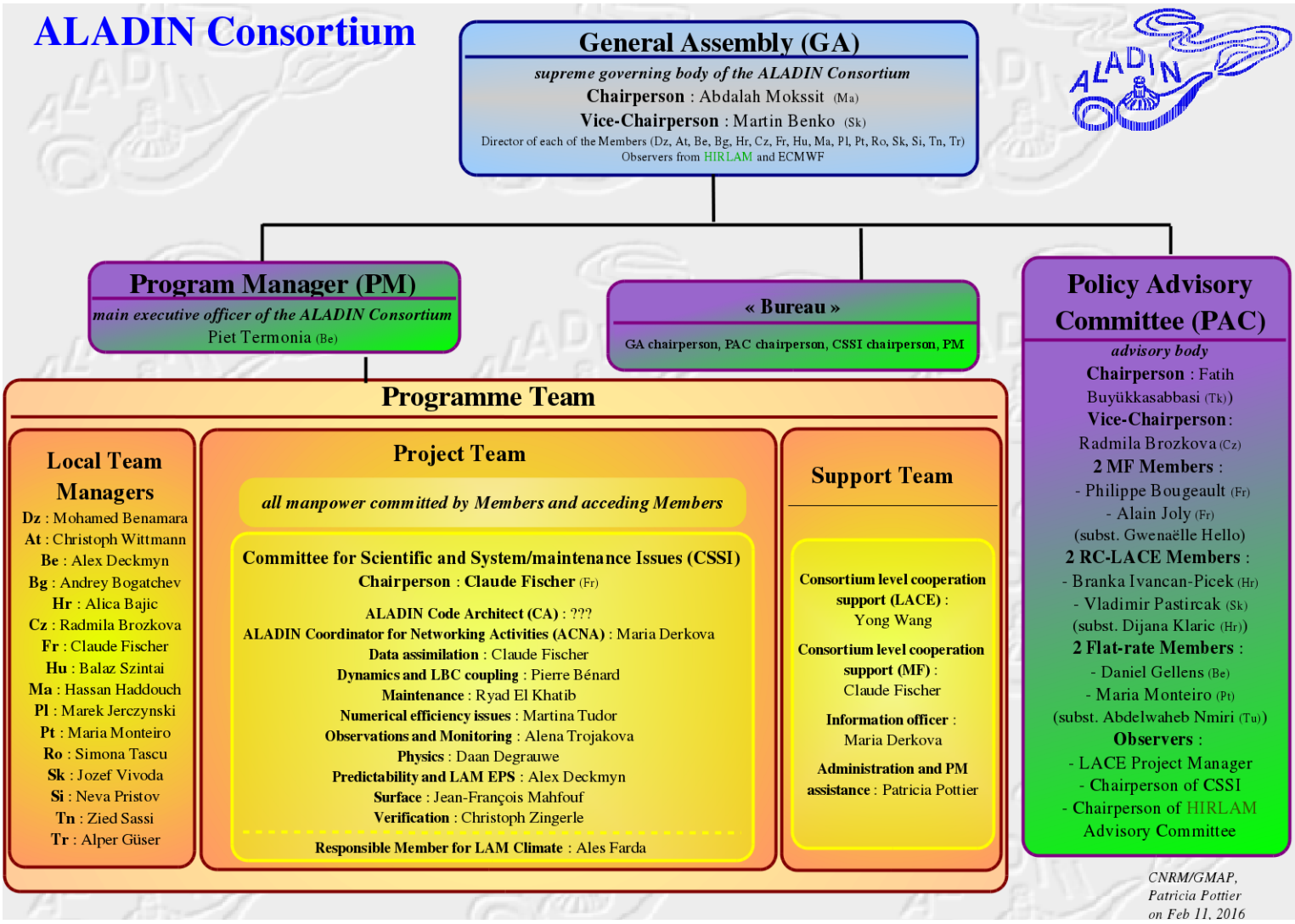

HIRLAM Consortium

Updated on 11 Feb 2016

HIRLAM Council

Overall authority for the HIRLAM Programme
Chairperson : Liam Campbell (Ie)
Vice-chairperson : Marianne Thyrring (Dk)
Directors of Dk, Es, Fi, Fr, Is, Ie, Lt, Nl, No, Sp, Se
(Observers from other organisations on a case-by-case basis)

HIRLAM Advisory Committee (HAC)

Chairperson : Heiner Kornich (Se)
Vice-chairperson : Jorn Kristiansen (No)

Dk : Rossella Ferretti
Es : Aarne Mannik
Fi : Carl Fortelius
Fr : Eric Bazile
Is : Theodor F. Hervarsson
Ie : Ray McGrath
Lt : ???
Nl : Jan Barkmeijer
No : Jorn Kristiansen
Sp : Javier Calvo
Se : Heiner Kornich
Observers :
- ALADIN PM
- ECMWF rep.
- EUMETNET/C-SRNWP PM

Programme Team

Heads of research
of the NMSs

Core Staff

Dk : 1 F.T.E.
Fi : 1 F.T.E.
Ie : 1 F.T.E.
Nl : 1 F.T.E.
No : 1 F.T.E.
Sp : 1 F.T.E.
Se : 1 F.T.E.

HIRLAM Management Group (HMG)

Program Manager (PM)
Jeanette Onvlee (Nl)

Project Leader for Quality Assurance : Bent Hansen Sass (Dk)
Project Leader for System : Daniel Santos (Sp)
Project Leader for Surface analysis and modelling: Patrick Samuelsson (Se)
Project Leader for Forecast model : Lisa Bengtsson (Se)
Project Leader for Probabilistic forecasting : Inger-Lise Frogner (No)
Project Leader for Upper air data assimilation : Roger Randriamampianina (No)

Regular Staff
all other manpower committed by Members and acceding Members

Support PM

Scientific secretary
????